From: Davila, Kenan D <kenan.d.davila@sargentlundy.com>
Sent: Friday, April 12, 2024 11:53
To: Comentarios <comentarios@jrsp.pr.gov>
Subject: Fwd: Negociado de Energía

INCREASING HOSTING CAPACITY OF DISTRIBUTION FEEDERS THROUGH ENERGY STORAGE AND SMART INVERTER FUNCTIONS

by

Anny Huaman Rivera

A thesis submitted in partial fulfillment of the requirements for the degree of

MASTER OF SCIENCE
in
ELECTRICAL ENGINEERING

UNIVERSITY OF PUERTO RICO
MAYAGÜEZ CAMPUS
2022

Approved by:

Agustin A. Irizarry Rivera, Ph.D. President, Graduate Committee	Date
Efrain O'Neill Carrillo, Ph.D. Member, Graduate Committee	Date
Fabio Andrade Rengifo, Ph.D. Member, Graduate Committee	Date
FirstName I. LastName, Ph.D. Representative of Graduate Studies	Date
Leyda V. Leon Colon, Ph.D. Director of ECE Department	Date

ABSTRACT

Electric power systems have been in constant transformation, specifically distribution systems, as the penetration of photovoltaic (PV) distributed energy resources (DER) has increased in recent years. However, PV DERs can lead to an increase in reverse power flows, causing voltage and thermal violations. For this reason, it is necessary to calculate the maximum allowable hosting capacity (HC) of PV penetration connected to low voltage networks to guarantee adequate distribution system operation.

This thesis focuses on studying a feeder's maximum accommodation capacity, evaluating the effects of increasing PV penetration, and mitigating these adverse effects through residential energy storage systems (RESS) and smart inverter functions, specifically Volt-VAR.

OpenDSS was used, along with MATLAB, to model distribution systems under different levels of PV penetration.

Results show that the most limiting factors for the HC are voltage violations and thermal violations. The simulations were able to successfully identify feeder nodes where voltage and thermal violations occur. The study demonstrates that RESS and the Volt-Var function implementation increases a feeder's HC, guaranteeing distribution system operation.

RESUMEN

Los sistemas de energía eléctrica han estado en constante transformación, específicamente los sistemas de distribución, ya que la penetración de los recursos energéticos distribuidos (DER) fotovoltaicos (FV) ha aumentado en los últimos años. Sin embargo, los DER fotovoltaicos pueden provocar un aumento de los flujos inversos de potencia, causando violaciones de tensión y térmicas. Por este motivo, es necesario calcular la capacidad de acogida (HC) máxima permitida de la penetración FV conectada a las redes de baja tensión para garantizar un funcionamiento adecuado del sistema de distribución.

Esta tesis se centra en el estudio de la capacidad máxima de alojamiento de un alimentador, la evaluación de los efectos del aumento de la penetración FV, y la mitigación de estos efectos adversos a través de los sistemas de almacenamiento de energía residencial (RESS) y las funciones del inversor inteligente, específicamente Volt-VAR.

Se utilizó OpenDSS, junto con MATLAB, para modelar los sistemas de distribución bajo diferentes niveles de penetración FV.

Los resultados muestran que los factores más limitantes para la HC son las violaciones de tensión y las violaciones térmicas. Las simulaciones permitieron identificar con éxito los nodos de los alimentadores en los que se producen violaciones de tensión y térmicas. El estudio demuestra que la implementación de RESS y de la función Volt-Var aumenta la HC de un alimentador, garantizando el funcionamiento del sistema de distribución.

To my family, fiance and teachers who accompanied and supported me throughout the whole process

ACKNOWLEDGMENTS

First of all, I want to thank God for always guiding my steps, and for allowing me to have a wonderful family. To my parents, thank you, Fortunato Huaman Chiclla, and Maria Lourde Rivera Santa Rosa, for your support and unconditional support in this process; I owe many of my achievements to you, including this one. To my brothers and sisters for always being there for me, and encouraging me. Thanks to my fiance Ricardo for being my partner in this journey, and for giving me advice and comfort at times when I felt faint.

Without downplaying its importance, I want to thank Dr. Agustin Irizarry Rivera who trusted in my abilities and allowed me to work with him. I will never forget the consideration and patience he had along the way. He has been a model for me not only as a professional but also as a human being. Also, I would like to thank Dr. Fabio Andrade Rengifo and Dr. Efrain O'Neill Carrillo for being part of my graduate committee and for their support and help throughout this journey.

A special thanks to Sandy, for being there in difficult times, and providing emotional support when needed. I would like to thank Dr. Lauro Enciso Rodas for advising me and by his example motivating me to pursue this master's degree outside of Peru. Thanks to all my friends and family who were there during this process and shared with me the good and bad moments.

Thanks to the University of Puerto Rico for the opportunity to study and complete a master's degree in the field of electrical engineering.

Contents

List of Figures

List of Tables

List of Acronyms

BESS	Battery Power Storage System
DoD	Depth Of Discharge
DER	Distributed Energy Resources
DESS	Distributed Energy Storage System
DG	Distributed Generation
DRIVE	Distribution Resource Integration and Value Estimation
EPRI	Electric Power Research Institute
ESS	Energy Storage Systems
HV	High Voltage
HC	Hosting Capacity
Li-Ion	Lithium
LV	Low Voltage
MV	Medium Voltage
OpenDSS	Open Source Distribution System Simulator
PV	Photovoltaic
PnP	Plug-and-play
PHES	Pumped Hy- Droelectric Storage
PVLV	PV Penetration Level
LTCs	Regulators And Load Tap Changers
RESS	Residential Energy Storage Systems

NaS	Sodium Sulphur
TES	Thermal Energy Storage
UPS	Uninterruptible Power Supply
VVC	Volt-VAR Control

List of Appendices

Chapter 1

Introduction

1.1 Overview

In recent years, a growing matter of concern is to curb the emission of greenhouse gases to avoid increasing climate change. The above has caused several countries to promote policies to contribute to the care of the environment especially in the electricity sector. For this reason, this sector is looking for more environmentally friendly and economic solutions, putting the eyes on small-scale generation, known as distributed generation (DG). Located close to consumers, this type of generation has a great capacity for growth and presents great benefits for the system.

The definition of distributed generation encompasses the concept of DER. DER are a variety of small modular renewable generation or electricity storage technologies that can be aggregated into distribution systems to provide the energy needed to meet regular demand. Generation with renewable resources, including photovoltaics, has recently experienced high growth due to the large availability of space for installation on residential rooftops.

However, the integration of photovoltaic solar energy due to its variable behavior and the lack of control over the availability of the resource increases the level of complexity of the operation of the power systems. Additionally, if the integration of this technology is performed at high penetration levels it generates negative impacts on power quality. Among these impacts, are: voltage variations, voltage unbalance, overvoltages and reverse power flow. The magnitude of these impacts depends on three fundamental parameters: penetration level, generation distribution, and distribution circuit conditions[1].

From all the above it can be stated that solar photovoltaic technology will become an important part of the distribution systems, with a high level of penetration, but this can cause negative impacts on the network in which it is connected. To avoid these effects it is important to promote research studies to determine the accommodation capacity of the distribution networks of photovoltaic systems without causing negative effects on the electrical system and seek solutions to allow greater penetration of photovoltaic systems.

Consequently, this thesis will focus on the analysis of the HC of distributed photovoltaic systems in a typical urban distribution system in Puerto Rico. It will also evaluate the effects of increasing PV penetration and how to mitigate these adverse effects with RESS and Volt-VAR fusion of smart inverters. All simulations and hosting capacity analysis were performed using Open Source Distribution System Simulator (OpenDSS) interfaced with Matlab and GridPV toolbox.

1.2 Justification

Based on the issues presented previously, regarding HC with DERs, this thesis will address the following questions:

1. How to determine the HC of a feeder?
2. How much PV system penetration can a typical feeder support without affecting power quality?
3. What types of problems are caused by high penetration of distributed PV systems on a feeder?
4. How to increase the HC?
5. How can I mitigate voltage or thermal violations caused by increased PV system penetration?
6. Which points on the feeder are mainly affected by increased PV system penetration?

1.3 Objectives and Contributions of the Thesis

The main objectives of this thesis are:

1. To analyze the HC of distributed PV systems in typical urban feede.
2. To increase this HC using RESS and the Volt-VAR function of smart inverte.
3. To propose solutions that maximize feeder the HC.

The specific objectives of this work are the following:

- Identify a typical representative urban feeder for the study.
- Determine the analysis methodology and simulation software to be used for the analysis of HC.
- Adequately model the feeder to be studied, in order to obtain realistic scenarios.
- Implement different scenarios of distributed photovoltaic system penetration into the simulation.
- Perform the HC analysis of a typical feeder, using the different penetration scenarios of distributed photovoltaic systems.
- Study the impact of residential energy storage systems on the feeder's HC.
- Study the impact of integrating Volt-VAR function of smart inverters on the feeder's HC .

1.4 Thesis Outline

The contents of this thesis are organized as follows:

Chapter 2: Literature Review

Chapter 3: Distribution System to be Modeled

Chapter 4: Research Methodology

Chapter 5: Results

Chapter 6: Conclusions and Future Work

Chapter 2

Literature Review

2.1 Distribution System

2.1.1 Introduction

Electrical power systems contain all the equipment necessary to supply electrical energy to users, such as generators, transformers, transmission lines, distribution lines, conductors, protection systems, etc. Power systems are mainly divided into three parts(Figure 2.1).

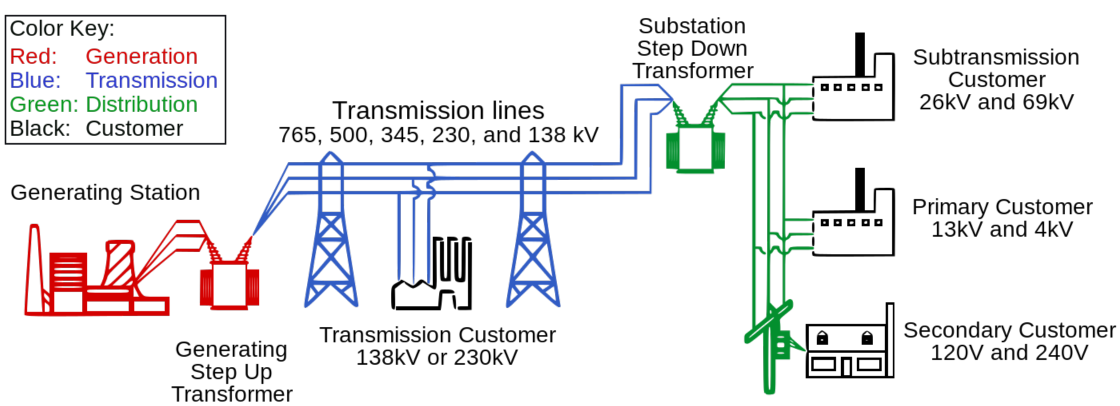

Figure 2.1: Electricity supply system. (Source [2])

- The first part is the generation system, which consists of the power plants. The energy is at the generation voltage level. The voltage is increased by power transformers to transmit the energy over long distances under the most economical conditions.

- The second part is the transmission system, which is responsible for carrying the energy from the generation centers to the load centers, through cables or overhead transmission lines, at high voltage(HV).

- The third part is the distribution system, where the high transmission voltage levels are reduced at the substation to medium voltage (MV) levels. The power is transmitted through distribution lines to local substations (distribution transformers) where the voltage is reduced to the consumers' level or low voltage (LV). The local utility or distribution company's power lines carry the electricity to homes or commercial establishments [3].

  North American and European are the two most common distribution system voltage levels around the world. The primary and secondary voltages (MV and LV, respectively) are given in Table 2.1 for both systems. The voltage choice depends on the type of load (residential, commercial, industrial), load size, and the distance at which the load is located [3].

Table 2.1: Distribution voltages for North American and European Systems. (Source [3])

Type of Voltage	North American System	European System
Primary distribution voltage (line to line)	From 4 to 35kV	From 6.6 to 33kV
Tree-phase secondary voltage (line to line)	208, 480, or 600V	380, 400, or 416V
Single-phase secondary voltage (line to neutral)	120/240, 277, or 347V	220, 230, or 240V

2.1.2 Primary Distribution

The primary distribution system is that portion of the power network between the distribution substation and the utilization transformers. The primary distribution system consists of circuits, referred to as primary or distribution feeders, that originate at the secondary bus of the distribution substation. The distribution substation is usually the delivery point of electric power in large industrial or commercial applications [4].

Primary distribution system voltages range from 2,400 V to 69,000 V. Some of the standard nominal system voltages are:

Table 2.2: Primary distribution system voltages range. (Source [4])

Volts	Phase	Wire
4,160Y/2,400	Three	Four
4,160	Three	Three
6,900	Three	Three
12,470Y/7,200	Three	Four
12,470	Three	Three
13,200Y/7,620	Three	Four
13,200	Three	Three
13,800Y/7,970	Three	Four
13,800	Three	Three
24,940Y/14,400	Three	Four
34,500	Three	Three
69,000	Three	Three

There are two fundamental types of primary distribution systems; radial and network. Simply defined, a radial system has a single simultaneous path of power flow to the load. A network has more than one simultaneous path. Each of the two types of systems has a number of variations. Figure 2.2 illustrates four primary feeder arrangements showing loop, radial, tie, and parallel feeders [4].

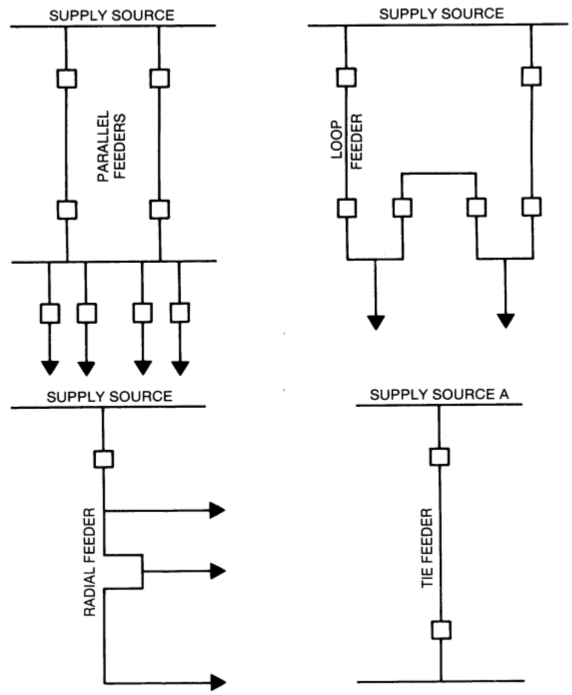

Figure 2.2: Four primary feeder arrangements. (Source [4])

2.1.3 Secondary Distribution

The secondary distribution system is that portion of the network between the primary feeders and utilization equipment. The secondary system consists of step down transformers and secondary circuits at utilization voltage levels. Residential secondary systems are predominantly single-phase, but commercial and industrial systems generally use three-phase power [4].

The voltage levels for a particular secondary system are determined by the loads to be served. The utilization voltages are generally in the range of 120 to 600 V. Standard nominal system voltages are:

Table 2.3: Secondary distribution system voltages range. (Source [4])

Volts	Phase	Wire
120	Single	2
120/240	Single	3
208Y/120	Three	4
240	Three	3
480Y/277	Three	4
480	Three	3
600	Three	3

In residential and rural areas the nominal supply is a 120/240 V, single-phase, three-wire grounded system. If three-phase power is required in these areas, the systems are normally 208Y/120 V or less commonly 240/120 V. In commercial or industrial areas, where motor loads are predominant, the common three-phase system voltages are 208Y/120V and 480Y/277V [4].

Various circuit arrangements are available for secondary power distribution. The basic circuits are: simple radial system, primary loop system, primary selective system, expanded radial system, secondary spot network, and secondary selective system.

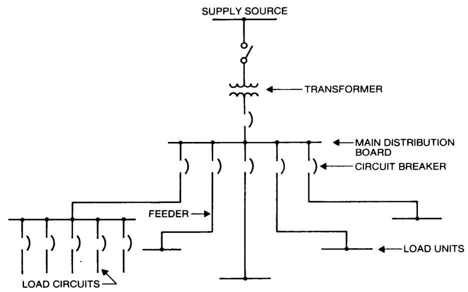

(a) Conventional simple - radial distribution system.

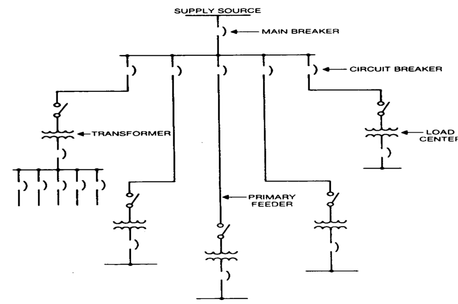

(b) Expanded radial distribution system.

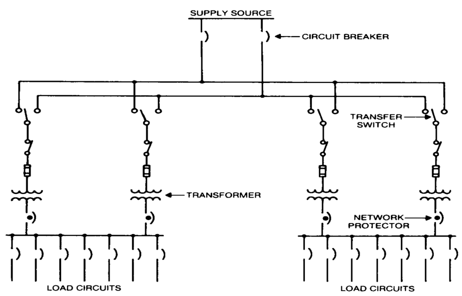

(c) Primary selective distribution system.

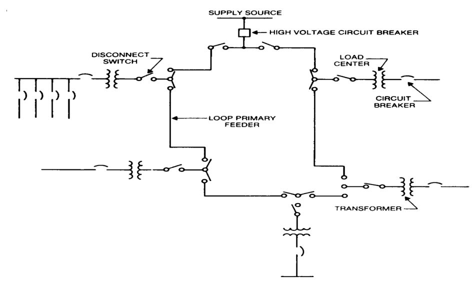

(d) Loop primary - radial distribution system.

Figure 2.3: Types of secondary distribution systems. (Source [4])

2.2 Hosting Capacity

2.2.1 Introduction

We use HC analysis to evaluate the number of DER which can be added to a specific feeder without generating technical problems or requiring major changes to the grid infrastructure. The amount of distributed generation resource integration has numerous benefits as well as some disadvantages, which we will detail below. To securely integrate DER into a distribution network, it is necessary to study the effect of DER on the study network.

2.2.2 Limiting Factors

The increase in DER can cause problems on power quality . As DER penetration increases, one begins to see certain violations of system operating standards. The main violations of operating standards, also known as limiting factors for HC calculation, are voltage and thermal violations.

2.2.2.1 Voltage Violations

Voltage analysis considers overvoltages and undervoltages (primary and secondary), voltage regulation, switched capacitor banks), changes to equipment operation (regulators and load tap changers (LTCs)[5].

All system voltages are verified against the ANSI C84.1 standard Range A standard[6]. As shown in Figure 2.4, all voltages in the simulations are also broken into the two service voltage categories using the 600 V threshold. For the steady-state simulations, the acceptable voltage range is 0.975-1.05 pu on the primary and 0.95-1.05 pu on the secondary. Anything above this range is considered an over-voltage violation, and any voltage below is an undervoltage violation. ANSI Range A is used for the steady-state simulations because the tension-regulating equipment has operated, and any violations would probably persist through the ANSI 10-minute tension averaging. The voltage analysis is applied per phase for every bus on the feeder. For the standard 3-phase 4-wire feeder, the voltages are measured as line-to-ground or line-to-neutral voltages. For 3-wire feeders without a neutral conductor, the ANSI range is applied to the line-to-line voltages [7].

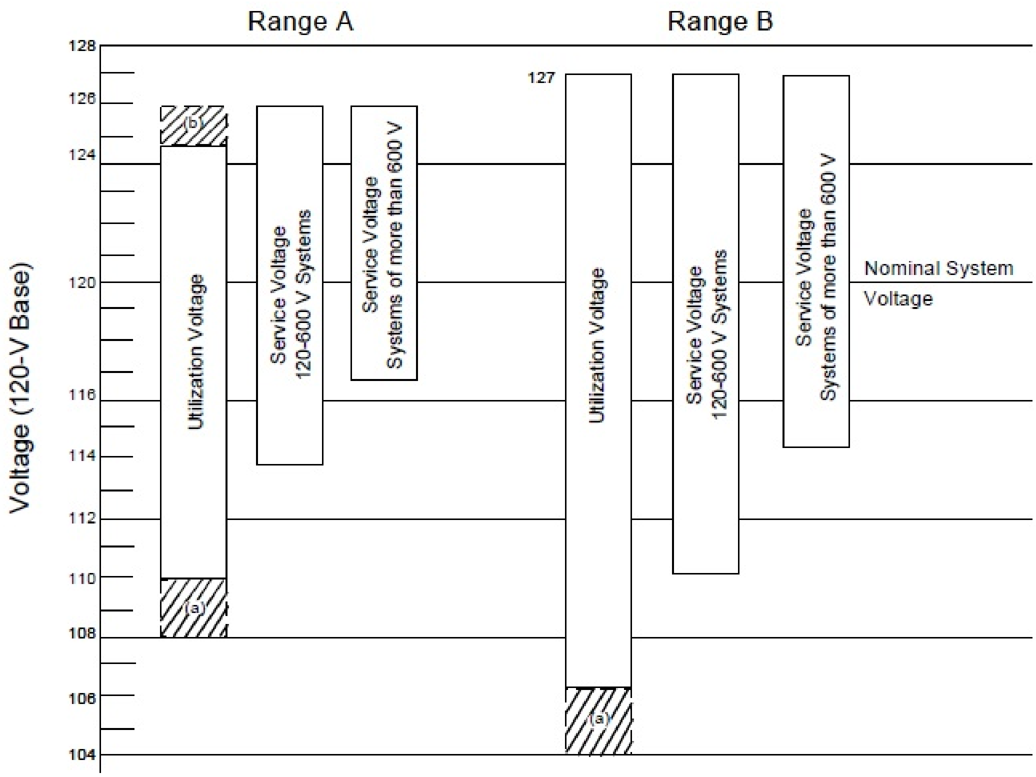

Figure 2.4: ANSI C84.1 voltage range. (Source [7])

ANSI C84.1, Notes to the figure:

a) The highlighted portions of the ranges do not cover circuits serving illumination loads.

b) The highlighted portion of the range does not cover 120 V - 600 V systems.

c) The difference between the minimum service and operating voltages is meant to permit the voltage drop in the customer's wiring system. This difference is bigger for service over 600 volts to permit the added voltage drop in the transformations between the service voltage and the utilization equipment.

For 120 V - 600 V Systems				
Nominal Voltage (V)	Service Voltage (V)			
	Range A		Range B	
	Max	Min	Max	Min
120	126	114	127	110
240	252	228	254	220
480	504	456	508	440

Figure 2.5: ANSI C84.1 service voltage range. (Source [7])

2.2.2.2 Thermal Violations

Overage power generated by DER devices during low consumption and high generation runs through distribution transformers and distribution lines back to the power plants. The transformers and the lines have nominal current capacity that can be adjusted. Surpassing this limit causes these components to overheat, giving rise to several operational failures [8].

2.2.2.3 Protection

Protection devices installed in distribution networks (radial systems) operate in a directional way. This signifies that they are engineered to disconnect and operate a section of the network when a given amount of power is flowing in the opposite way. The reverse flow of power resulting from the integration of DERs can lead to malfunction or unnecessary operation of these protective devices, resulting in the interruption of power to the systems [8].

It has been shown that PV generation can impact the fault current seen by protection devices (PDs). This can adversely affect the protection zone of a PD as well as the time dependent coordination between PDs. The scope of protection analysis is limited to steady-state analysis of distribution networks under fault conditions, so any issues that require the dynamic or time-domain simulation of the PV system in the distribution network are not considered. The four possible protection violations arising from steady-state PV fault current injection are: protection under-reach, PD coordination loss, nuisance tripping, and sympathetic tripping [9].

2.2.2.4 Power Quality

Power quality refers to the interaction between its customers and the utility. Current and voltage disturbances are regarded as disturbances of the pure sinusoidal waveform that will therefore affect both the customer and the grid. Voltage quality relates to the delivery of supply voltage to the client in reasonable limits. Over penetration of DG can cause many power quality disturbances such as voltage dips, flickers and power system harmonics.

2.2.3 Hosting Capacity Analysis Method

There are different methodologies for hosting capacity analysis that have been developed in recent times and others that are still in development. Three main methods of hosting capacity analysis have been identified, generally known as streamlined, iterative and stochastic.

There is a close similarity among all the methods, which is the application of power flow analysis to determine the values of currents and voltages in distribution networks.

2.2.3.1 The Streamlined Method

The streamlined method applies a set of simplified algorithms for each power system limitation (typically: safety/reliability, thermal, protection, and power quality/ voltage) to approximate the capacity limit of DERs at distribution circuit nodes [9].

This method can be considered an enhancement of the stochastic method, where instead of simulation of many scenarios, a few numbers of other scenarios are simulated to derive an estimation of the HC of a specific feeder. The streamlined method is a heuristic approach that was developed by the Electric Power Research Institute (EPRI) to find an estimate of the HC of a feeder's DER.The application of the streamlined method is limited to only a few studies, because the software algorithm has not been open-sourced, but is commercially accessible as a tool under the title "Distribution Resource Integration and Value Estimation (DRIVE)" [9].

2.2.3.2 The Iterative Method

The iterative method models DERs in the distribution network directly to identify host capacity constraints. A power flow simulation is executed iteratively at each node in the distribution network until a violation of one of the four power network constraints is identified. The iterative method is also sometimes called the detailed method [9].
The iterative method implies the estimation of the HC with known parameters of load consumption and DER generation. In the iterative method, there is no randomness in the computation and load consumption. Location information and DER generation are established before starting the HC computation [9].

2.2.3.3 The Stochastic Method

The stochastic method starts with a model of the existing distribution system, then new solar PV (or other DERs) of varying sizes are added to a feeder at randomly selected locations and the feeder is evaluated for any adverse effects that arise from this random allocation. The results are a hosting capacity range [9].
There are several methods for generating random scenarios. The most popular is Monte Carlo simulation. Other methods include random unfolding of DERs, dispersed network technique, and quasi Monte Carlo. Given that many unknown variables are present in the integration of DERs, holding some of these variables constant, while varying others

using stochastic techniques makes sense [8].

2.3 Energy Storage Systems

2.3.1 Introduction

Energy storage systems allow a certain amount of energy to be conserved and used when required. Efficient energy storage is a key pillar for the energy transition as it makes renewable energy production more flexible and ensures its integration into the electric system.

The continuous increase in the integration of photovoltaic systems can impact the correct functioning of the power grid, causing problems like harmonic distortions, thermal violations and voltage deviations, leading to protection systems and power quality issues [10]. In principle, all these issues can be addressed with the use of appropriately designed grid-connected storage systems along the distribution network, as shown in Figure 2.6. Storage can be sized in the kW range up to thousands of MW [11].

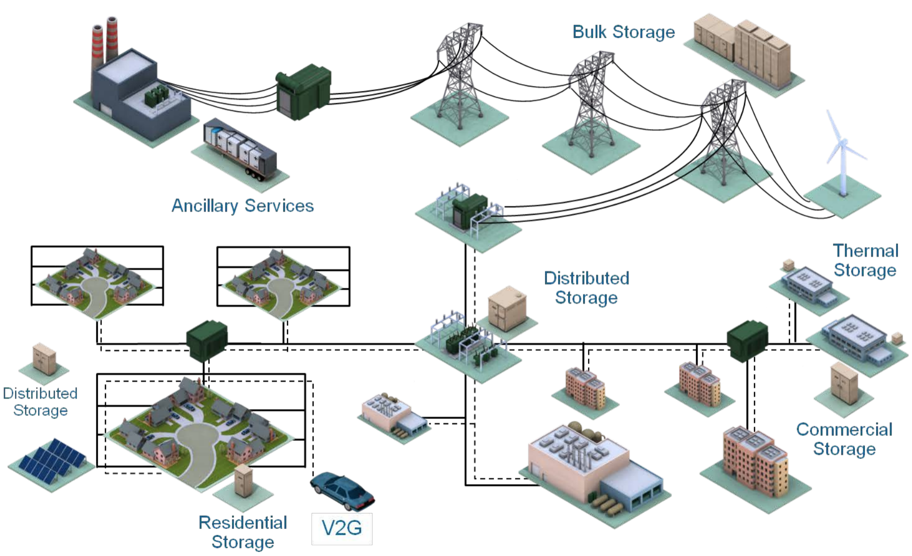

Figure 2.6: Energy storage applications. (Source [11])

Storage systems can be classified in different forms according to type, size, location, and uses, among others. We can classify them as large-scale and distributed energy storage systems. This classification is done according to its size and location.

2.3.2 Types of Storage Systems

Growing energy demand, rising fossil fuel prices, and greenhouse gas reduction policies, the number of renewable energy projects has increased. This change has been seen more in the energy distribution networks where the integration of DERs continues to grow at an accelerated pace. As more DER integration is considered, such as distributed photovoltaic systems, there is a need to better understand how these types of variable resources affect the existing distribution system through HC studies. Various methods are being studied to increase HC, such as the use of storage systems in networks with high penetration of DERs.

2.3.2.1 Distributed Energy Storage System(DESS)

DESSs are projected to play an important role as the penetration of variable solar resources grows. Energy storage is receiving increased attention from utility engineers and regulators for its potential to solve a wide number of technical challenges in the management of electric power. Storage can proactively lower active power variations and shift peak PV output to align with peak load demand and alleviate major operational challenges for utilities created by peak demand and non-dispatchable renewable resources [12].

The DESS are based on the battery power storage system (BESS), this technology has evolved and developed rapidly in recent years as it can provide power reliably, safely and easily.

BESSs function through reversible electrochemical responses, in which two electrodes (anode and cathode)are contained within a vessel full of a certain electrolyte. In the process of loading, the electrical energy is converted for storage into chemical energy, and during periods of demand, this energy is converted into electrical energy. There are various types of batteries appropriate for short-term, medium-term, and long-term use, each with different power, response time, and energy characteristics [13].

The technologies most commonly used in projects all around the world are flow batteries, sodium sulphur (NaS), lithium (Li-Ion) and lead acid, which are described in greater depth below:

- **Lithium-Ion Batteries**

  Lithium-ion batteries consist of lithium metal oxides at the positive electrode, while lithium and carbon ions arebe stored at the negative electrode. The electrolyte employed is lithium salts dissolved in organic carbonates. Lithium-ion batteries work by conducting a two-phase transfer of lithium ions. During charge, the lithium ions move from the positive to the negative electrode, while the contrary occurs during discharge. The high popularity of lithium-ion batteries is a result of their reliability and accessibility. Lithium-ion batteries offer good operating features, are highly versatile and scalable. These features ensure a wide variety of potential applications for this type of batteries, such as:

  Lithium-ion batteries offer good operating features, are highly versatile and scalable. These features ensure a wide variety of potential applications for this type of batteries, such as:

  - Distribution networks: Voltage, contingency and capacity support for smart grids
  - Commercial and residential buildings: Self-consumption and time-shifting of local photovoltaic generation

  - Renewable generation: Shaping and smoothing services, related to frequency and voltage support, to guarantee a better connection of large-capacity renewable installations to the power system
  - Transmission networks: Auxiliary services, for example, frequency regulation [13].

- **Lead-Acid Batteries**

  The lead-acid battery is composed of two electrodes immersed in a sulfuric acid electrolyte. The positive electrode consists of metallic grains of lead oxide, while the negative electrode is connected to a metallic lead grid.

  At present, lead-acid batteries are used extensively in automotive starting battery services, in mobile power equipment applications like forklifts, and uninterruptible power supply (UPS) units. Other important application of this battery is in connection with small photovoltaic systems. Nevertheless, in bigger scale renewable energy storage systems, the number of lead-acid installations is less than lithium-ion and sodium sulfide, because of their lower energy density, extended charging times, and short life cycles. Other drawbacks are that they do not work well at cold temperatures and cannot operate in the discharge cycle for a prolonged periods before breaking down [13].

- **Sodium Sulphur Batteries (NaS)**

  Sodium-sulfur batteries are based on molten salt technology, in which molten sulfur and molten sodium are utilized as the positive and negative electrodes. Solid sodium alumina acts as the electrolyte, dividing the two electrodes. Electricity is generated so that during discharge, the metallic sodium atoms liberate electrons, which result in sodium ions that travel to the positive electrode through the electrolyte.

From a technical standpoint, they have excellent energy density features, great efficiency (75-85%), fast response, and long-life cycles. They can also provide services such as peak shaving, stabilization and time shift for solar generation plants and wind farms. However, NaS downsides may include the need to operate at elevated temperatures, an elevated price, and limited applicability due to sodium polysulfide corrosion [13].

- **Vanadium Redox Flow Batteries** Vanadium redox flow batteries consist of two liquid electrolytes:, one positively charged, and the other negatively charged. The electrolytes are segregated by an ion-selective membrane which, when discharged and charged, permits the selective flow of ions, producing a chemical reaction. The electrolytes are stored in containers and, when needed, are transferred to the battery [13].

  These batteries have a high cycle life (around 10,000 cycles), are adequate for medium-term storage, have good power/energy flexibility and high energy capacity. These batteries are being considered a viable technology to bridge the gap between medium and long-term storage. An attractive feature of this battery is that energy and power are separated, where the power (kW) depending on the number of combined modules and the energy (kWh) on the volume of the electrolyte (container size). Nevertheless, this kind of battery is quite costly because it needs a large surface [13].

2.3.2.2 Large Scale Energy Storage System

Since most of the low-carbon electricity generation resources (e.g., solar, nuclear, and wind) are not able to flexibly adjust their output to match fluctuations in energy demand, there is a growing requirement for large-scale electricity storage because of the growing adoption of renewables.

Large-scale energy storage systems have become the ideal solution to ensure reliable electricity supply to the world population and are used where GW scales are involved. The main large-scale storage technologies are:

- **Pumped Hydroelectric Storage Systems** The most established technology for utility-scale electricity storage is pumped hydroelectric storage (PHES) and has been deployed commercially around the world since the 1890s. Since the 2000s, there has been renewed interest in developing PHES facilities around the world.

  Hydroelectric storage is a process that converts electrical energy into potential energy through pumping water to a high altitude and then releasing it to pass through hydraulic turbines and generate electrical energy [14]. Energy storage systems (PHES) have been the classic form of energy storage [15].

- **Thermal Energy Storage** In thermal energy storage (TES), a material acquires energy as its temperature rises and loses energy as its temperature falls. Exploiting this characteristic makes it possible to use several materials with different thermal characteristics that can lead to different thermal energy storage uses.

2.4 Smart Inverters

2.4.1 Introduction

With the rapid increase in GD from renewable sources, the power network has become more complex and vulnerable. Hence, distributed energy resource systems must be controlled with flexibility and reliability to eliminate these vulnerabilities.
Due to the increasing complexity of the grid, inverters must be smarter to provide better service to consumers. Smart inverters must adapt their functions to the demands of the grid as well as the needs of the users.

Using new advanced technologies, smart inverters will be able to withstand future requirements of the modern grid. As smart inverters operate autonomously, it has positive impact on adaptation, depending on the scenario. Therefore, smart inverters can be changed to minimize cost of maintenance and follow the system by increasing flexibility [16].

Smart inverters enable bidirectional communication with utility control centers. Moreover, advanced capabilities, such as voltage and frequency sensors, enable smart inverters to detect anomalies in the grid and send the information to utility operators. Figure 2.7 shows a general block diagram of smart PV inverter system [17].

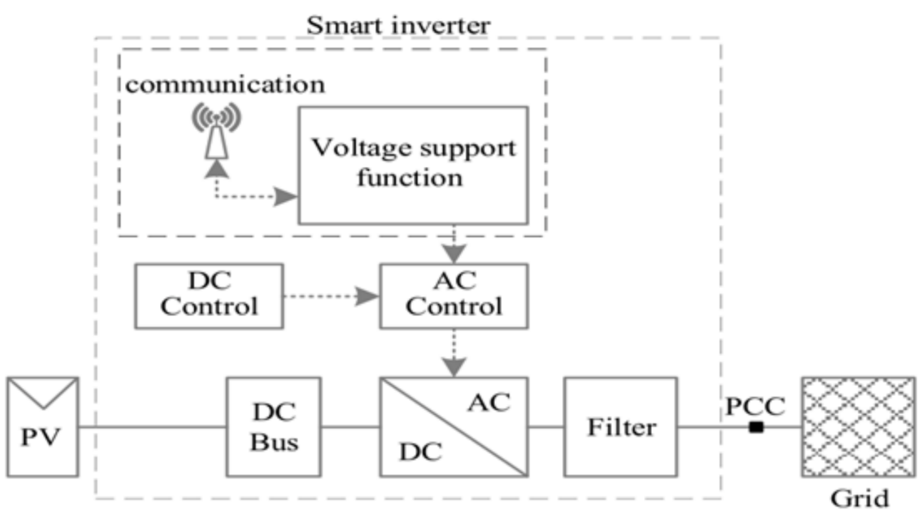

Figure 2.7: General block diagram of smart PV inverter. (Source [17])

2.4.2 IEEE 1547 Standard on Smart Inverters

From the series of standards, the IEEE Standard 1547 (2003) was the first regarding DER interconnection. Likewise, the standard requirements are applicable to interconnect performance, procedure, safety considerations, testing and maintenance [16, 17]. The IEEE 1547 discusses several aspects needed for interconnection of DER, including synchronous and induction machines, and power inverters and converters. IEEE 1547.8 addresses advanced controls and communications for gridsupporting inverters and the best practices focusing on distributed inverters and microgrids. It also provides information for DER behavior and interactions with grid devices (both operational and safetyassociated, including inadvertent isolation) and interconnection system reaction to unusual circumstances [17].

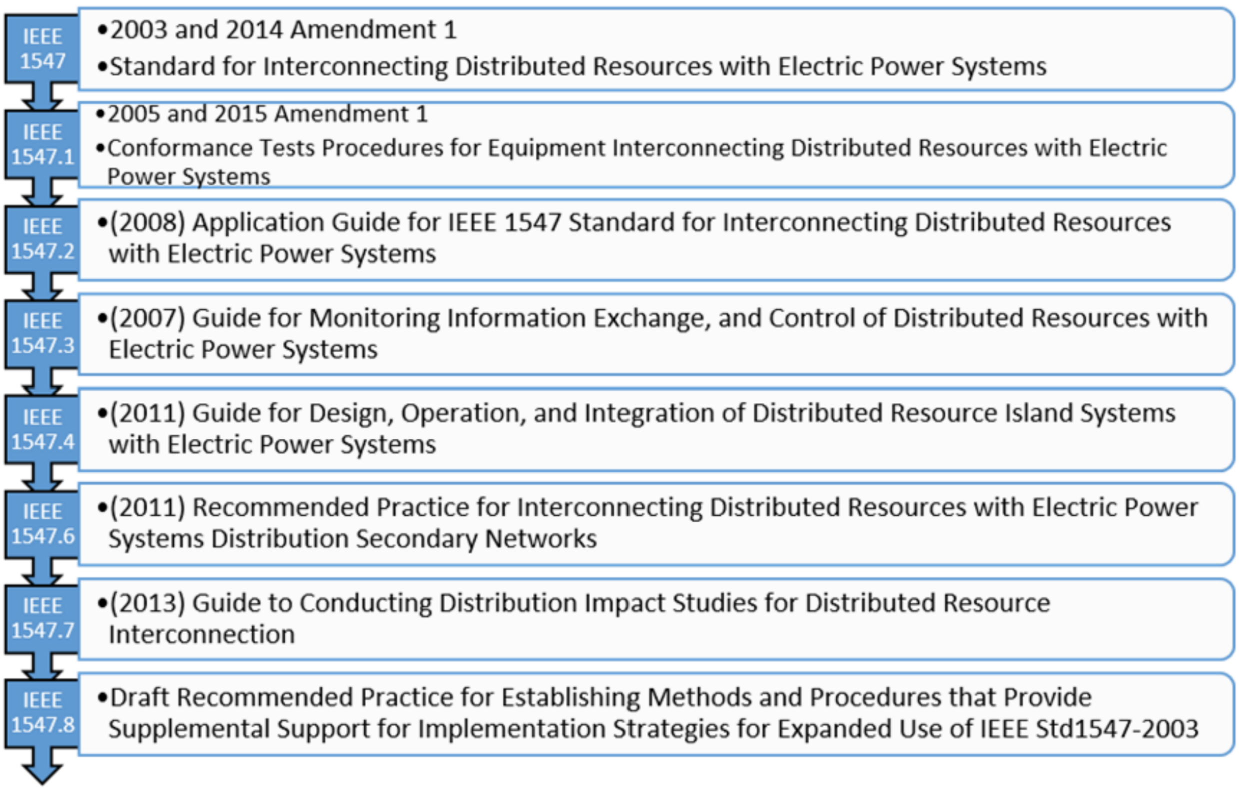

Figure 2.8: IEEE 1547 series of standards. (Source [17])

2.4.3 Functions Of Smart Inverters

Smart inverter functions and requirements considered to fulfill common problems include functions for power system stabilization and communication-based functions to improve the user friendliness. Figure 2.8 shows the sub functions of both categories [17].

2.4.3.1 Functions for Power System Stabilization

For smart inverters to provide greater stability, reliability, and efficiency to the network and to improve control algorithms, they require [16, 17].

- **Connect/Disconnect From Grid**

  This function provides two options for an inverter to cease operation and disconnect from the grid. The first is to set the power output to zero. This is also known as a virtual disconnect. The second is the physical operation of a switch to isolate the inverter from the grid, referred to as a physical disconnect [17].

  This function is not related to intentional islanding nor separating a customer from the grid. It refers to the management of a switch, or virtual switch that separates at the DER from the grid while maintaing customers connected to the grid. In reference to the example diagram in Figure 7, this function relates to the operation of the “Local DER Switch,” not the “Grid Switch” [18].

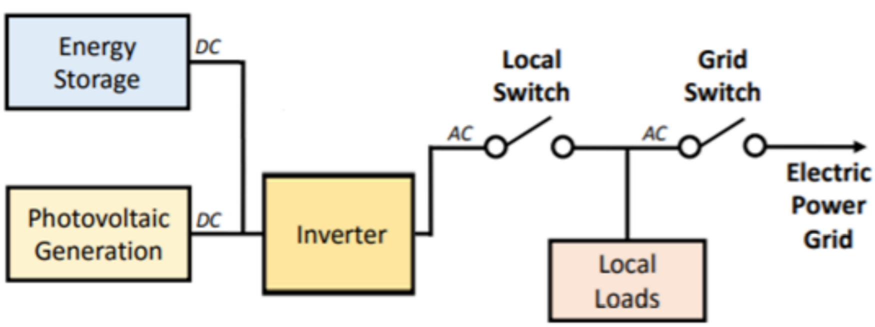

Figure 2.9: Connect/ disconnect mechanism. (Source [17])

- **Power Output Adjustment**

  This specification is meant to provide a flexible mechanism whereby energy input to or output from a distributed energy resource can be self-limiting. This covers the generations of a photovoltaic system or the discharging and charging of an energy storage system [18].

Grid frequency increases as a result of excessive generation and or insufficient load. Therefore, its active power output is changed relative to grid frequency. The desired response of the inverter is to reduce active power output when the frequency is high. Likewise, it is desired for the inverter to increase active power output as frequency decreases. PV inverters typically have a maximum commanded power limit and are only able to provide an over-voltage response if the inverter is already at full active power output. The inverter must have the ability to provide voltage support to the grid by adjusting the inverter's active power output, which varies the voltage of the grid [17].

- **VAR Management**

  Three control modes are used in active and reactive management: unity power factor, variable power factor and Volt-VAR. unity power factor with Q = 0 mode. These inverters can operate with unity power factor, with fractions or without re-injection of reactive power to the grid. Then, inverters in fixed power factor mode operate with a moderately outstanding power factor. They provide regulation to minimize voltage deviations that can be attributed to variations in output active power. Variable power factor mode. This mode allows the inverter to return reactive power to the grid by operating with a variable power factor. Volt-VAR control mode. Using this method, the inverter will be able to respond with a modified var response, proposed by the local utility, by monitoring its own terminal voltage [16].

- **Storage Management**

  The main component of this function is charging and discharging management.

Energy storage has been suggested as the solution to the power imbalance issue of power generation and load demand in view of the emergence of power grids with irregular renewable energy sources. In unlike the conventional control of power inverters connected to the grid to inject power into the grid, the storage management control scheme gives high priority to grid stability while maintaining its normal bi-directional power flow functions [17].

- **Event/History Logging**

  This function indicates a high priority on the need for a common method for event logging and reporting. For a system, it is important to monitor inverter behavior and to record abnormal conditions and events. All event log entries will contain the following five 5 fields: date and time stamp, data reference, value, event code, and optional text field [17, 18].

- **Status Reporting/Reading**

  This function makes the operating mode, status, and set points available to verify operation. The smart inverter architecture must be enhanced to monitor the local system status to identify attacks and hazards at the physical device layer. Therefore, the cyber hazards can be sensed at an early stage. Also, they can estimate the local voltage and current to sense system variances. In this function, the directories of power quality, unbalanced voltages/currents, and other parameters, will be intended to detect the cyber-attacks [17].

- **Time Adjustment**

  The ability to set the time in the DER device is considered a main requirement to support the scheduling of functions, and the time-stamping and logging of events. Research indicates that time-adjustment is generally supported by the specific communication protocols. Therefore, as a recommended method for distributed smart inverter time-adjustment is to apply the native time adjustment mechanism of the specific communication protocol being applied. As examples, the “DNP3” and the “ZigBee Smart Energy Profile 1.0” protocols have defined time-setting mechanisms that can be used for synchronizing smart inverter devices [17, 18].

2.4.3.2 Communication-Based Functions to Improve User Friendliness

When comparing components in a grid system, one of the most important objectives is the control of power inverters. These inverters implement interfaces between the DGs and the grid bus. In smart inverter development, an explanation of “smartness” states to minimizing the requirement of communication. At the same time, being equipped with communication protocols also indicates “smartness” since the necessity of communication cannot be neglected. Despite these advantages, there is a main disadvantage regarding security that can affect the communication and monitoring improvements. Mainly, privacy issues arise with these developments. A “smart inverter” should provide [16, 17].

- **Plug and Play**

  Plug-and-play (PnP) is the capacity of a smart inverter to be added to a power system and function independently without a separate technical setup. PnP operation guarantees the advantages of system scalability, interoperability, reliability, and resilience. PnP can be implemented at the power converters with flexible hardware structures, or at the smart inverters for distributing frequency/voltage regulation. Plug and play means that a distributed power supply can access to the grid directly without control and de-fend units. Management technology will be needed when distributed power with the function of “plug and play” accesses the grid [17].

- **Self-Awareness**

  Self-awareness becomes a particularly relevant function for decentralized systems to achieve autonomous performance at advanced levels. In the case of smart inverters, self-awareness intends to improve lifetime prediction and operational reliability. This allows for maintenance or fail-safe actions to effec-tively avoid accidents in power electronics systems. In addition, future smart inverters are expected to possess some degree of intelligence, such as knowledge of their role or status within their environment and the likely effect of potential future actions [17].

- **Adaptability**

  Adaptability is another critical characteristic of a smart inverter. A smart inverter must be able to adapt to system variations in operating conditions. This means it must have the capability to evaluate the parameters, mostly the impedance of the grid, and synchronization in terms of frequency. Unintentional islanding is one of the most significant performance problems of the network sys-tem. This happens mainly due to grid failure, and inverters must include islanding recognition algorithms to self-adapt depending on the situation. Fault tolerance and islanding detection are also classified in this category [16, 17].

- **Autonomy**

  This function consists of the intelligent system deciding its own mode of functioning. Autonomous operation is an elementary feature for a distributed system. Furthermore, a smart inverter with autonomous functioning may be required if communication is limited or non-existent, or if reliability is desired. A common situation is autonomous load power sharing using droop methods when several inverters are operated in parallel. For autonomous functioning, smart inverters must accomplish skills, such as dynamic grid creation, dynamic grid feeding, uninterruptible power transfer, power quality improvement, and black start [17].

- **Cooperativeness**

  The his function provides an inverter the ability to operate cooperatively with other inverters in a grid. All the inverters are essential to regulate and rectify the unbalances and conflicts in the system. Their process should be in alignment with other neighboring components when they are in operation, so further disturbances are not introduced into the system. Furthermore, cooperativeness helps with aspects, such as ramp rate control for renewable energy sources, reactive power and harmonic current sharing, and soft start capability [16, 17].

2.5 Previous Related Studies

In [8], a research review on hosting capacity analysis is presented. The authors classify papers according to the tools and methods used to calculate the hosting capacity of distribution networks. They also describe the limiting factors, performance indices, and impact factors, since they describe the distribution system characteristics that are impacted by DER connection.

In [7], the authors conduct PV hosting capacity analysis of different feeders, investigating all feeder regions where PV systems can be interconnected. The impact of PV system interconnection is used to determine the maximum hosting capacity of individual zones of the feeder, and in turn, determine the PV system risk impact, such as voltage and thermal violations. This report analyzes innovative methods for photovoltaic interconnections with advanced simulation methods.

In [19], the authors emphasize the study of hosting capacity on the secondary side of the distribution transformer. The paper provides the initial steps to determine the hosting capacity on three actual North American residential systems. In ad-dition, the impact of individual customer load variability and split-phase transformer unbalance is studied.

In [20] and [21], the authors develop methodologies for the sizing and location of renewable energy sources that determine the hosting capacity of solar pho-tovoltaic energy in a distribution network, considering the effect between MV and LV network interactions at distinct voltage levels. Performance parameters such as transmission capacity and voltage level are calculated, and the impact of different penetration scenarios is evaluated.

In [22] and [23], the authors propose efficient control of distributed electrical energy storage systems to increase the hosting capacity. They propose control approaches based on voltage analysis andreverse active power derating to prevent overvoltage and increase the PV hosting capacity of LV networks.

In [24] and [25], the authors investigate how the implementation of reactive power control in the PV inverter affects the PV hosting capacity in distribution networks. They use a local Volt-VAR droop control and simulations are performed in OpenDSS and MATLAB. They conclude that the control greatly improves the hosting capacity of feeders as well as the location hosting capacity of the majority of buses limited by voltage violations.

Chapter 3

Distribution System to be Modeled

3.1 Introduction

Puerto Rico's electrical system is typically made up of radial type feeders. For this thesis, we selected a representative feeder. The feeder used for modeling and simulation is a typical urban feeder, located in the south of Puerto Rico. The feeder is simulated in OpenDSS, for this purpose, technical data was collected from QGIS plans obtained from the open database of the Puerto Rico Electric Power Authority. Additionally this information was compared with Capstom reports on this feeder. Sections 3.2 to 3.4 describe in detail the sources, technical data and calculations performed to simulate this feeder in a more realistic way, and how this data was compared. In addition, the environmental conditions of peak sun hours, temperature, and irradiance in this part of the island were studied in section 3.2.

3.2 Solar Resource and Temperature

Temperature and irradiance data were collected from NASA's POWER database, which provides historical temperature and irradiance data for the entire planet. Temperature and irradiance averages were taken for each hour of the day, the result of which can be seen in Figure 3.1 . The sample taken to obtain the average temperature and irradiance per hour of the day is from January 1, 2020 to December 31, 2020; that is, a sample of 8766 hours.

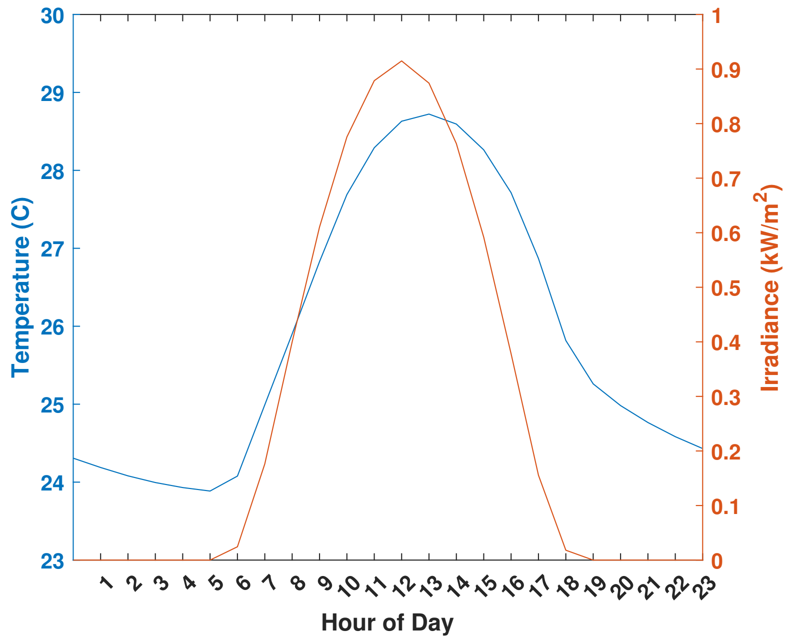

Figure 3.1: Load shape temperature and irradiance.

It is observed in the figure that the point of maximum solar availability occurs at noon, this is the period of maximum PV generation, coinciding with the point of low demand for electricity (shown in section 3.2). Therefore, it is a critical point for the maximum allowable generation capacity in the feeder, since under that condition of feeder operation, the voltage level will increase in greater proportion compared to the other hours of the day.

The generation efficiency of the solar panels is affected by the operating temperature of the panels, for the purpose of the research developed the impact of this variable is considered when modeling photovoltaic systems in OpenDSS.

Another significant parameter to consider in the modeling and photovoltaic systems are the hours of peak sunshine per day, the area where the feeder of study is located has 5 kWh/m2. We can see in Figure 3.2 the different values of peak sunshine hours for Puerto Rico [26].

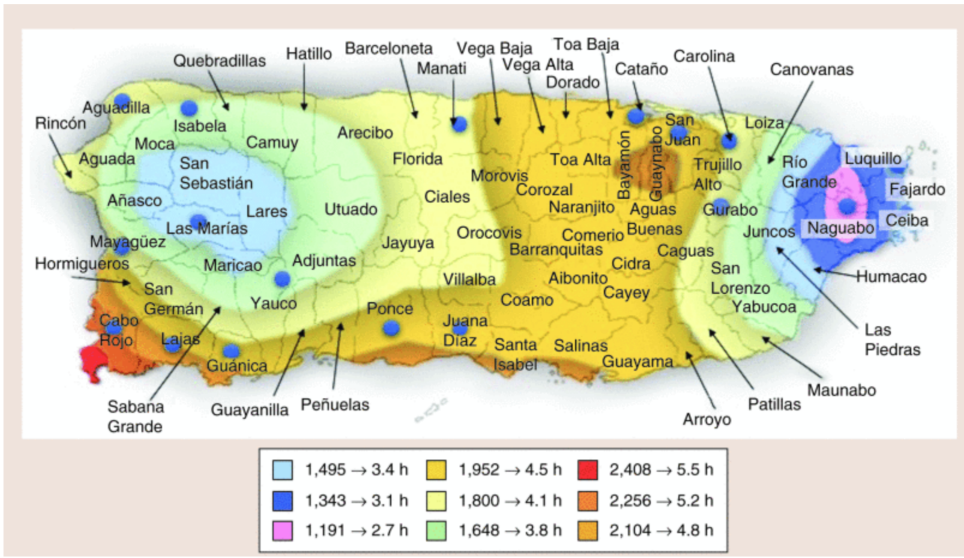

Figure 3.2: The annual average isolation in kWh/m2 and peak sun hours. (Source [26])

3.3 Demand Profiles

The demand profiles are an important part of feeder modeling. The demand profile is the representation of the energy consumption of the users of an electrical system. The daily demand variation represents a significant impact on the behavior of the electrical system. In this way the demand of a feeder is directly related to the maximum allowed capacity of solar PV penetration, since a higher value of PV penetration is obtained with a lower generation and a higher load. Therefore, it is important to adequately estimate the different load profiles of the feeder users to evaluate the impact on the feeder and its maximum capacity of PV penetration.

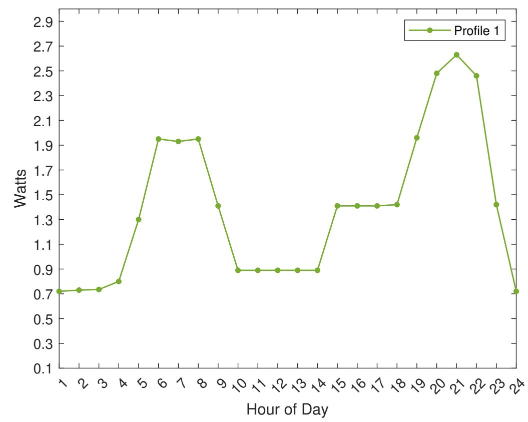

(a) Demand Profile 1 (33 kWh/day)

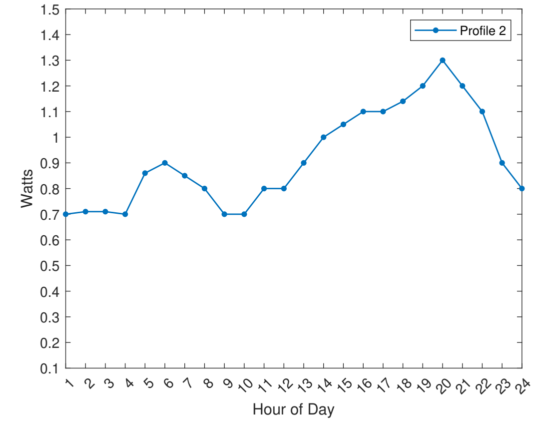

(b) Demand Profile 2 (22 kWh/day)

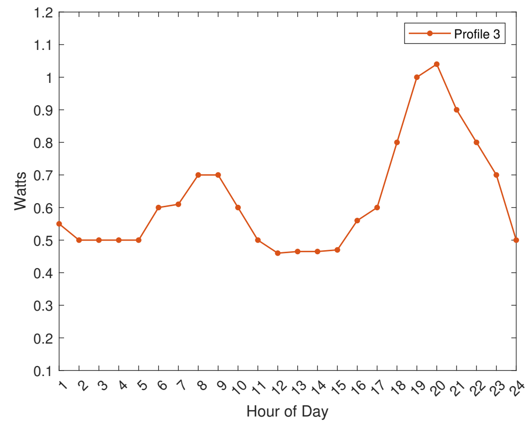

(c) Demand Profile 3 (15 kWh/day)

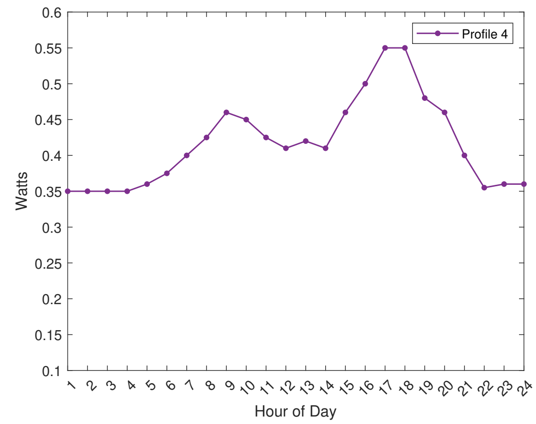

(d) Demand Profile 4 (10 kWh/day)

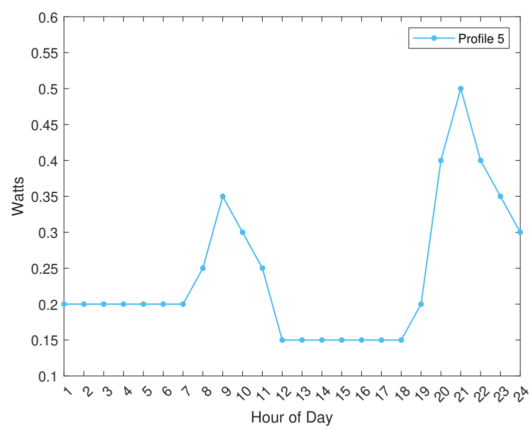

(e) Demand Profile 5 (5.755 kWh/day)

Figure 3.3: Types of demand profile.

The average daily demand profiles shown in Figure 3.3, are the result of the collection of electric bills of the feeder users. The curves were produced assuming the typical daily behavior of the loads. These five demand profiles were previously elaborated in capstone projects [27–29]. To design these demand profiles, we considered the number of inhabitants per dwelling. Profile 1 represents the daily energy consumption of a family of 6 people. This profile considers that parents and children work and study respectively throughout the morning, arrive at the house in the afternoon, and that an elderly adult always stays in the house. Table 3.1 shows the demand of households according to their consumption and family members [27].

Table 3.1: Demand profiles per energy consumption. (Source [27])

Demand Profile	Family Members	Daily Energy Demand(kWh)	Profile Description
1	6	33	Family of 6: Parents working during the day, children arrive from school in the afternoon, and the elderly person at home
2	5	22	Family of 5: Parents working during the day, children arrive from school in the afternoon
3	4	15	Family of 4: All family members arrive at home by 4:00pm
4	2	10	Family of 2: A couple that spent most time at home
5	1	5.75	A person that lives alone; At home during the day and work at afternoon

The feeder under study provides electricity to 708 homes, each home classified by type of demand profile. For the analysis, census population data from 2012 to 2016 was used to build household profiles by feeder location, as shown in Table 3.2. As a result of analyzing the distribution between these years, the total number of households was 10,809. When analyzing the percentage distribution of this total, 72% of the total households are family households, 24.2% represents households with a person living alone, and 10.8% represents households with persons aged 65 and over [27].

Table 3.2: 2012-2016 Census of Salinas by household type. (Source [27])

Subject	**Salinas Municipio, Puerto Rico**			
	Estimate	**Margin of Error**	**Percent**	**Percent Margin of Error**
Households by type				
Total households	10,809	+/-360	10,809	(X)
Family households (families)	7,781	+/-417	72.0%	+/-2.8
With own children of the householder under 18 years	3,393	+/-310	31.4%	+/-2.4
Married-couple family	4,117	+/-419	38.1%	+/-3.6
With own children of the householder under 18 years	1,338	+/-251	12.4%	+/-2.2
Male householder, no wife present, family	1,083	+/-223	10.0%	+/-2.0
With own children of the householder under 18 years	692	+/-187	6.4%	+/-1.7
Female householder, no husband present, family	2,581	+/-342	23.9%	+/-3.1
With own children of the householder under 18 years	1,363	+/-269	12.6%	+/-2.4
Nonfamily households	3,028	+/-305	28.0%	+/-2.8
Householder living alone	2,616	+/-323	24.2%	+/-2.9
65 years and over	1,162	+/-196	10.8%	+/-1.8

For these data, a distribution of the demand profiles was made by considering and matching the description of the existing demand profiles and the census data. As a result of this analysis, Table 3.3 was generated [27, 28].

Table 3.3: Distributed number of households by demand profile.

Demand Profile	**Family Members**	**House Energy Demand(kWh)**	**Household Distributed Percent(%)**	**Number of Households**
1	6	33	8.62%	61
2	5	22	29.52%	209
3	4	15	28.25%	200
4	2	10	9.89%	70
5	1	5.75	23.73%	168
			100.00%	708

After processing the data, the household profile distribution on a feeder distribution transformer was made. This is important because it will be useful for more accurate calculations for the design of PV systems. From this data, we can calculate the photovoltaic generation capacity in each feeder branch. Table 6.1 shows a summary of each distribution transformer with its respective number of households classified by their demand profile [28].

3.4 Technical Data

This section describes the technical data of the feeder used for the case study, starting from the substation to the distribution transformers. To determine the effect of high PV penetration on the feeder, it is necessary to detail and consider all the circuits connected to this feeder. Figure 6.2 details the topology of the feeder, which is composed of 56 distribution transformers. The feeder under study is a three-phase radial network of medium voltage at 4.16, with low voltage loads at 120/240.

3.4.1 Substation

The substation is where power is distributed at lower voltage. In Puerto Rico, the distribution substation transforms the voltage from 38 kV sub-transmission lines to distribution voltages of 13 kV, 8 kV or 4 kV. In the system modeled, the substation transformer transforms the 38 kV voltage to 4.16 kV. Additional substation parameters are detailed in Table 3.4.

Table 3.4: Substation Data.

Characteristics	**Substation Transformer**
Primary voltage	38 Kv
Secondary voltage	4.16 Kv
Capacity	2 MVA
Connexion	delta - star

Even though three feeders derive from the substation, as shown in 3.4, only one of the feeders is considered for the study.

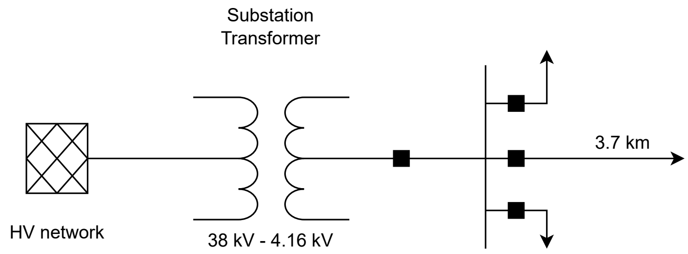

Figure 3.4: Single-line diagram of the substation.

3.4.2 Distribution Transformers

The distribution transformer is responsible for reducing the primary voltage of the electrical distribution system to customer service voltages. Distribution transformers are static devices composed of two or more windings. The most widely used transformers in Puerto Rico are single-phase overhead transformers, installed either to provide single-phase service or in a transformer bank to provide three-phase service.

The transformers that make up the feeder under study are 3-winding single-phase overhead transformers, which provide a voltage level of 120/240 (see Figure 3.5).

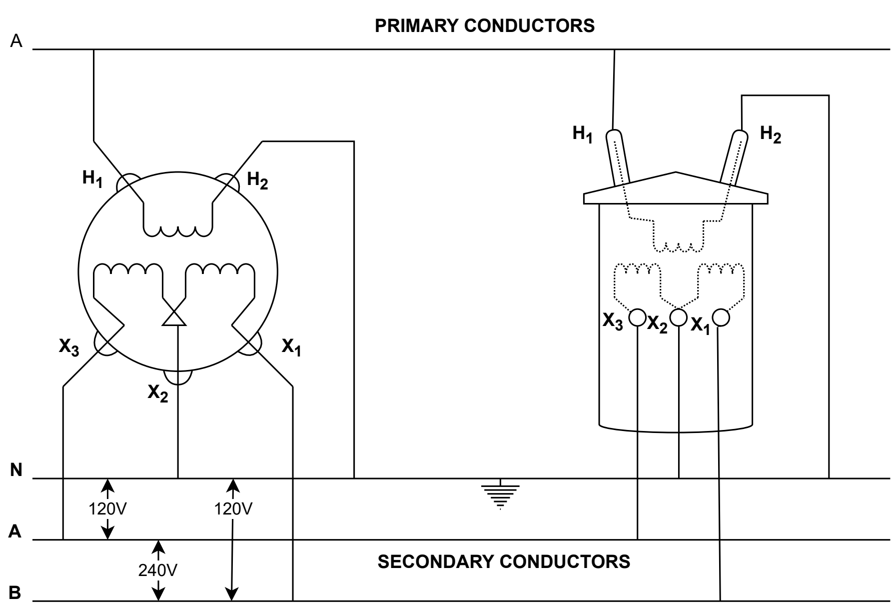

Figure 3.5: Transformer connection at 120/240V single phase service.

Table 3.5 describes the different distribution transformer parameters that are necessary for the modeling of distribution transformers. The values assigned for reactance and resistance were obtained from [30]. Since OpenDSS recommends using the example values in [30], if the reactance and resistance values of a typical distribution transformer are unknown. The feeder under analysis has 56 distribution transformers with capacity values of 25, 50 and 75.

Table 3.5: Distribution transformer design parameters.

Ratings (KVA)	Percent reactance high-to-low (XHL or X12)	Percent reactance low-to-tertiary (XLT or X23)	Percent reactance high-to-tertiary (XHT or X13)	Percent resistances for windings (%RS)	Connection
25	2.04	1.36	2.04	[0.6 1.2 1.2]	Y - Y
50	2.04	1.36	2.04	[0.6 1.2 1.2]	Y - Y
75	2.04	1.36	2.04	[0.6 1.2 1.2]	Y - Y

3.4.3 Overhead Line Spacings

The overhead line spacing refers to the height and arrangement of the distribution conductors. The height of the primary distribution poles and the spacing of the conductors were obtained from the Puerto Rico Electric Power Authority's manual of overhead distribution construction patterns [31]. In addition, the technical communiqués were verified.In particular, technical communiqué 12-02 of 2012 modifies the minimum vertical clearance height for power lines (figure 3.6) [32].

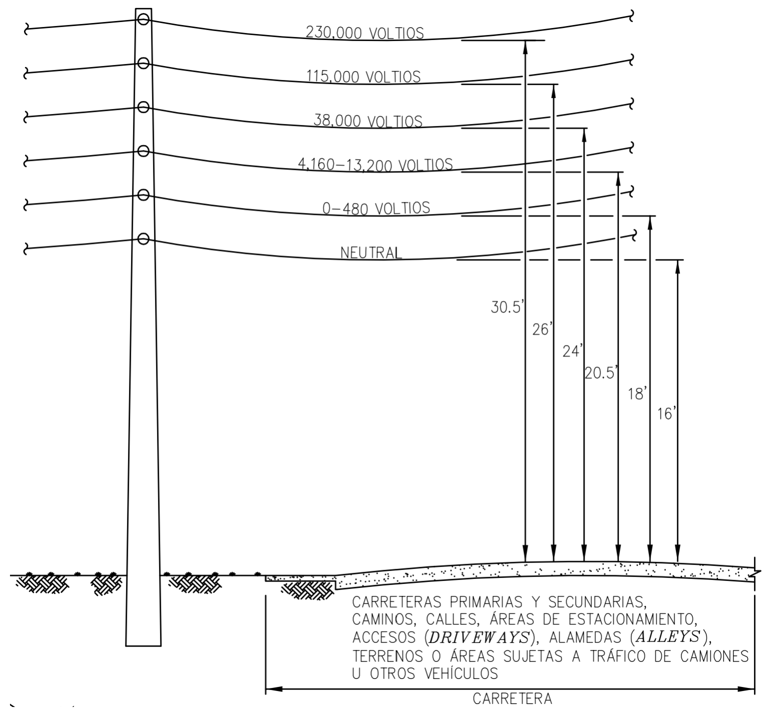

Figure 3.6: Minimum vertical clearances of power lines recommended by PREPA.

Figures 3.7 describes the structure of concrete poles without crossarm of one phase, two phase, and three phase, respectively, for voltage levels 4.16 kV, 8.32kV or 13.2 kV.

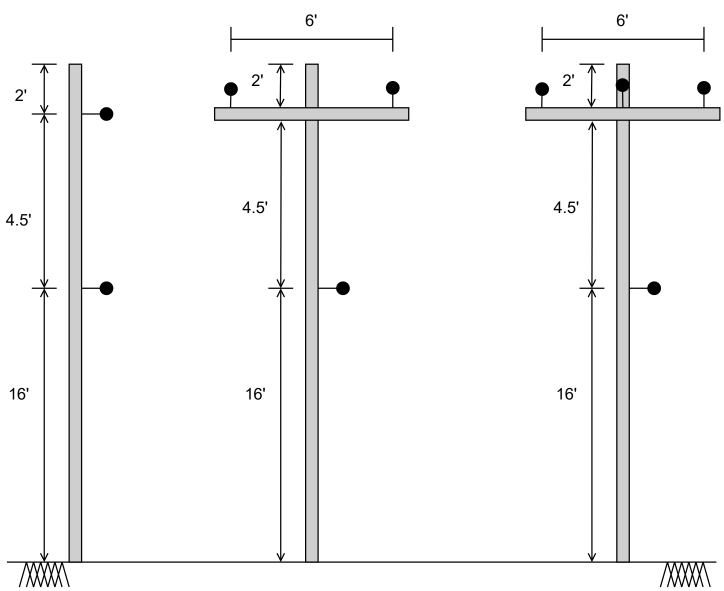

Figure 3.7: Schematic of verhead line spacings.

3.4.4 Conductors

The Puerto Rico Electric Power Authority uses ACSR type wires in its overhead lines, according to communiqué 95-09 [33].

In circular communication 91-04, AEE informs that the aerial neutral conductor (ground wire) can be of the following types shown in table 3.6 [33].

Table 3.6: Used neutral conductor AEE.

Wire	Tension under hurricane winds	Initial or installation tension
1/0 ACSR(Raven)	1000 lbs	160 lbs
2/0 ACSR(Quail)	1150 lbs	200 lbs

Table 3.7 shows the different types of conductors found in the feeder under study with their respective parameters.

Table 3.7: Conductor data.

Size	Material	Diameter(in.)	GMR(in)	Resistance(kΩ/ft)
266,800	ACSR	0.642	0.260	0.073
3/0	ACSR	0.502	0.072	0.129
1/0	ACSR	0.398	0.054	0.212

3.4.5 Secondary Circuit

Secondary circuits are always of the radial type. Figure 3.8) shows two common types of residential secondary circuit topology: ”Home Run” and ”Shared Service”. In the ”Home Run” configuration, residential customers are connected to the distribution transformer by means of an individual conductor for each customer, while the ”Shared Service” configuration supplies several customers with a conductor from the distribution transformer [19].

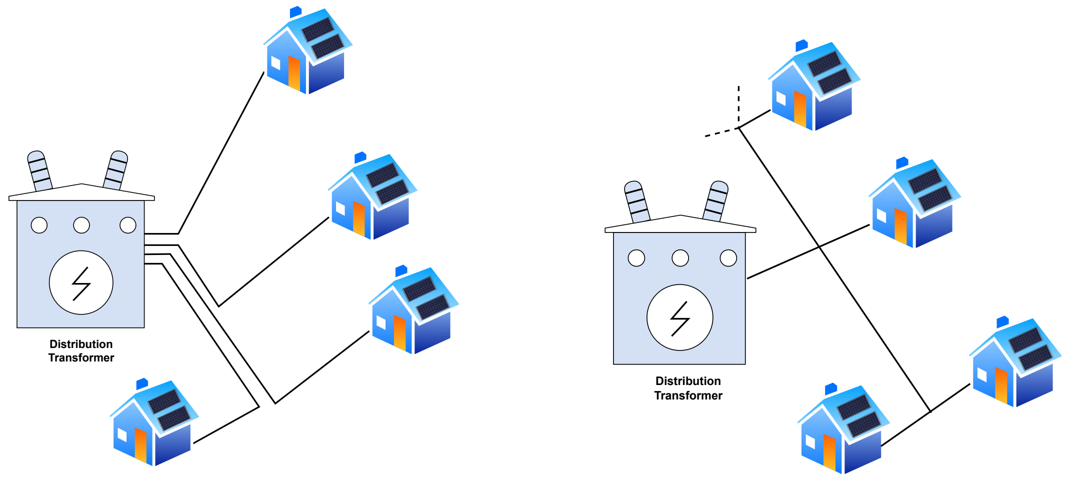

(a) Home Run (b) Shared Service

Figure 3.8: Typical secondary distribution configurations for residential services.

In the modeling of the feeder to be studied, the secondary side is considered. For this reason, the secondary configuration is modeled with the "Home Run" topology (figure 3.8a). The length of the secondary conductor will be 32.8 ft for all loads. The type of conductor to be used on the secondary side is 1/0 ACSR; its characteristics are described in Table 3.7.

Chapter 4

Research Methodology

4.1 Introduction

This section presents the methodology used to perform the study of ”Increasing hosting capacity of distribution feeders thru energy storage and smart inverter functions”. To achieve the proposed objective of this research, different methodologies were investigated to determine the accommodation capacity of a feeder and identify how to increase this accommodation capacity. Secondly, a typical urban feeder in Puerto Rico was searched (section 3). Next, the feeder was simulated using the OpenDSS simulation program, see reference [34]. To finalize the research using the simulated feeder, four case studies were proposed, which are described in Section 4.3 and the results of these case studies are shown in Section 5. Figure 4.1 shows the methodology used in this work.

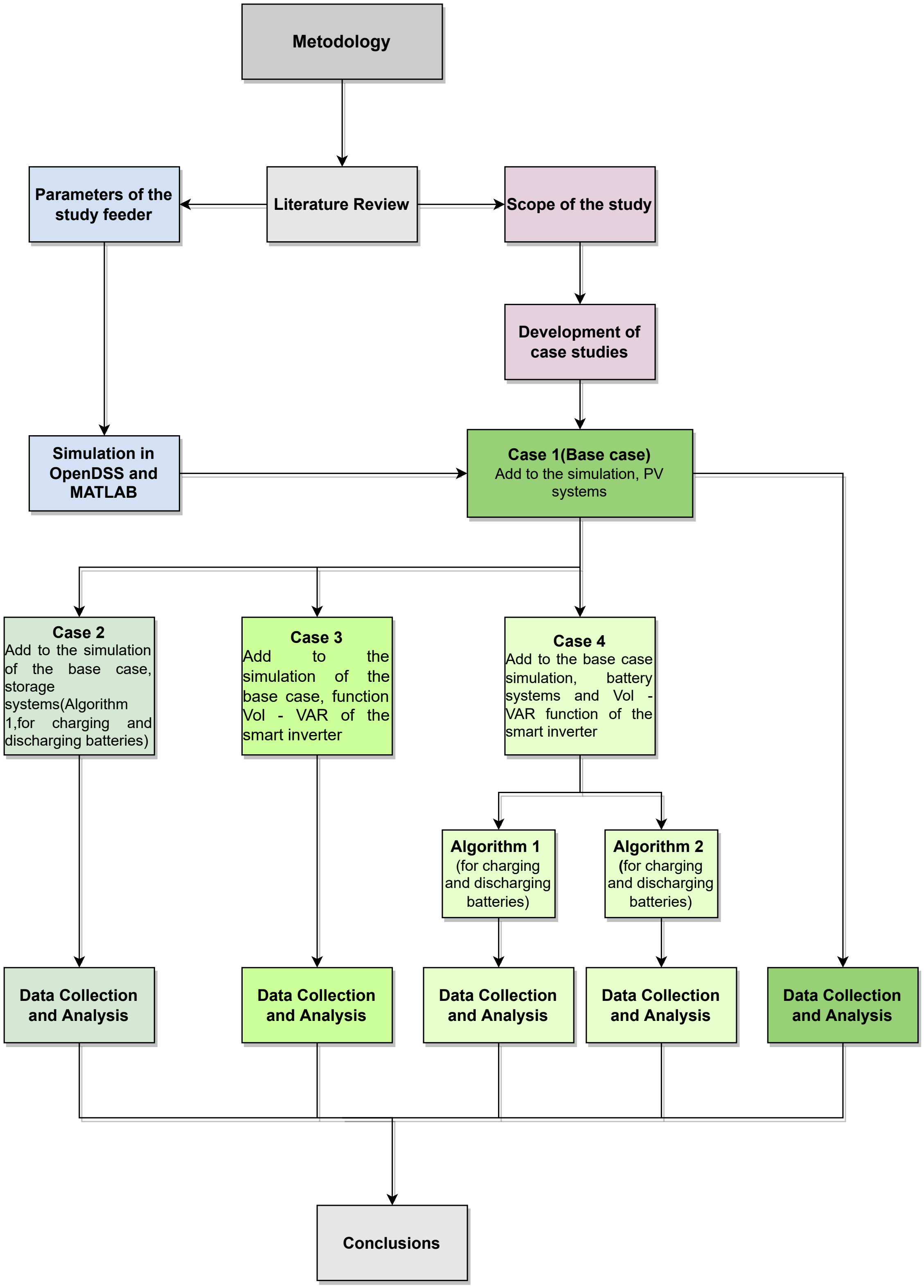

Figure 4.1: Diagram of the research methodology workflow.

4.2 Scope of the Research

The HC analysis is used to evaluate the amount of DER that can be added to a specific feeder without causing violations to the corresponding standards or requiring major modifications to the network infrastructure [35, 36]. In Table 4.1 we see different limits that must be considered to maintain the stability of an electrical distribution system, for this reason, it is important to define the limiting factors when performing the simulations.

When studying the maximum PV penetration capacity of the feeder, the variable behavior of loads, temperature, irradiance must be considered. The variable factors of temperature and irradiance make the generation of PV systems stochastic, in order to solve this problem and increase the level of PV penetration, it is possible to use batteries and intelligent inverters. For this reason, it is essential to perform the proper sizing and modeling of the PV penetration levels, battery banks, and smart inverters that will be part of the feeder under study.

Table 4.1: Monitoring Criteria and Flags for Distribution PV Analysis. (Source [37])

Category	Criteria	Basis	Flag
Voltage	Overvoltage	Feeder voltage	1.05 Vpu
	Voltage desviation	Deviation in voltaje from no PV to full PV	3% at primary 5% at secondary $\frac{1}{2}$ band at regulators
	Unbalance	Phase voltaje deviation from average	3% of phase voltage
Loading	Thermal	Element loading	100% normal rating
Protection	Element Fault Current	Deviation in fault current at each sectionalizing device	10% increase
	Sympathetic Breaker Tripping	Breaker zero sequence current due to an upstream fault	150A
	Breaker Reduction of Reach	Deviation in breaker fault current for feeder faults	10% decrease
	Breaker/Fuse Coordination	Fault current increase at fuse relative to change in breaker fault current	100A increase
Harmonics	Individual Harmonics	Harmonic magnitude	3%
	THDv	Total harmonic voltaje distortion	5%

4.2.1 Limiting Factors to Consider in HC Analysis

A high penetration of photovoltaic systems can cause distribution system power quality problems. Hence, limiting factors can limit the integration of DERs into distribution networks based on criteria defined by standards or norms to maintain power quality. The limiting factors that will be considered in this research are voltage and thermal violations, since they are the first limiting factors to appear when increasing the PV penetration level in a feeder. These types of violations are classified as steady-state problems, so these limiting factors will be analyzed at each hour of the day, running for 24 hours (1 day).

4.2.1.1 Voltage violations

To determine the hosting capacity of the feeder, over voltages and under voltages on the primary and secondary side of the system are considered. All feeder voltages are compared to the ANSI C84.1 range. For the steady state simulations (at each hour of the day), the acceptable voltage range is 0.975-1.05pu on the primary and secondary. Anything above or below this range is considered a voltage violation.

4.2.1.2 Thermal violations

Additionally, to determine the feeder's hosting capacity, thermal violations will be considered. Lines and feeder transformers have a rated current limit that they can withstand. Exceeding this limit due to reverse current flows due to excess generation from the PV systems causes these components to overheat, resulting in various faults, which is considered thermal violations in the study.

4.2.2 PV Penetration Scenarios

The implementation of PV systems can be on a residential scale on LV grids (120/240V) or can be directly on an MV grid (4.16kV, 13kV). The low voltage PV penetration level (PVLV) is defined as the percentage of LV customers of each secondary substation within the studied feeder, with a rooftop PV unit installation. In this work, PV systems were deployed on the load side; that is, LV. No PV systems were considered on the MV side.

The PV penetration levels considered in the simulations range between 0% to 150%, with 10% steps.

4.2.2.1 PV system design

To dimension the photovoltaic array on the roof of a house, the dimensions of the roof or available spaces must be obtained. In [27], researchers used ArcGeo's ArcMap program determined that most roofs have approximately 56 m2 or 64 m2 of available space.

A 56 m2 roof has dimensions of 6.4558 m × 7.7258 m, and 4.5508 m × 1.3229m for a total area of 55.89 m2 (figure 4.2).

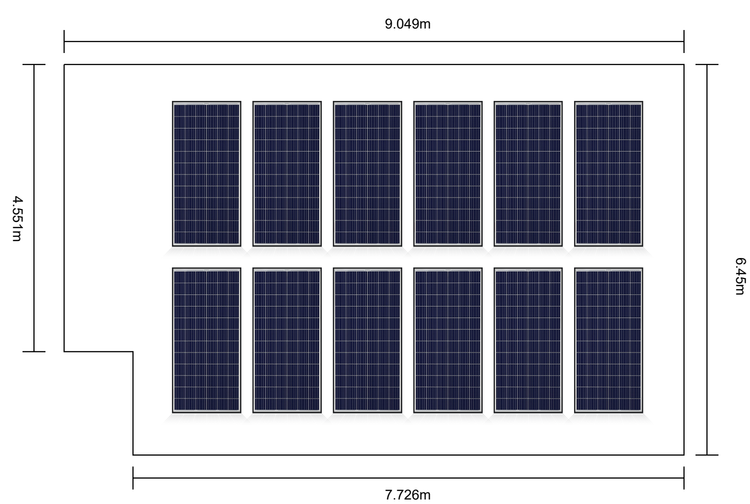

Figure 4.2: PV design for 56m2 house.

Similarly, a 64 m2 roof, has dimensions of 8.9697 m × 6.6675 m, and 3.5322 m × 1.0716 m, for a total area of 63.5906 m2 (figure 4.3).

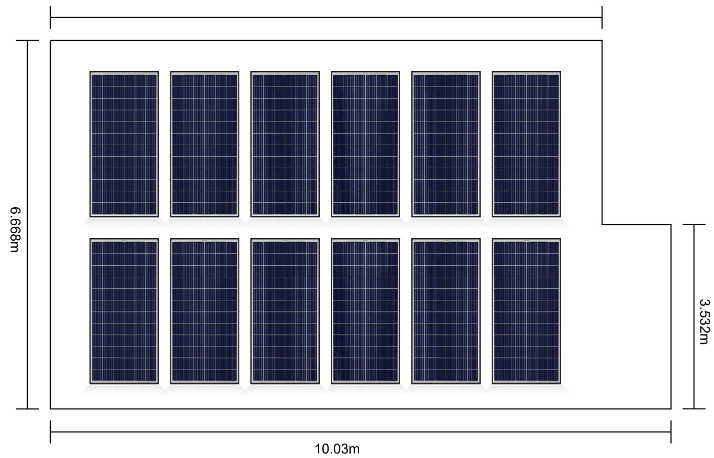

Figure 4.3: PV design for 64m2 house.

The number of PV panels that can be installed on the roofs with the above dimensions is 12 panels, since the dimensions of the PV panels considered in this study have dimensions of 0.992m x 1.956m, as shown in Figure 4.4.

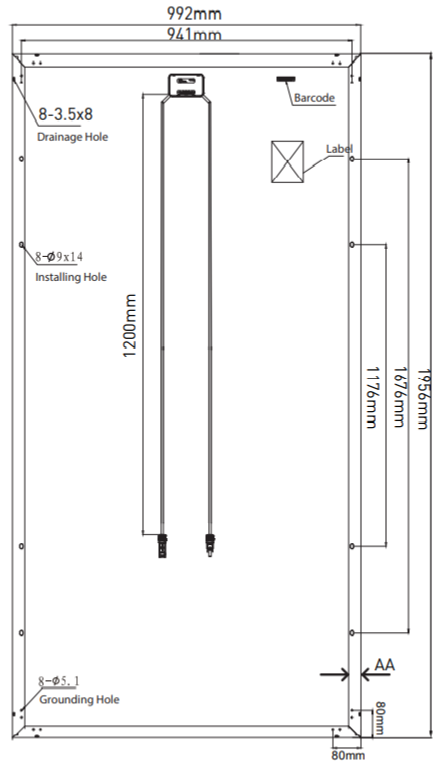

Figure 4.4: PV module dimensions.

Twelve photovoltaic panels installed per house will only be enough to supply a photovoltaic penetration up to 90% as detailed in table 6.2. From this percentage, some houses will require an increase in the number of panels, up to 22, to reach a penetration of 150% of PV. This is possible because most of the houses have a non-roofed space in the front or back of the house where extra PVs can be installed to achieve a higher PV generation.

4.2.2.2 Calculation of photovoltaic arrays and PV penetration levels

TThis subsection presents a basic numerical analysis that considers the demand profiles already described in Section 3.3, specifically in Table 3.4. The formulas used to determine the number of households (HH) required per transformer with photovoltaic installations to supply each penetration level to be studied are detailed. In addition, the formulas for sizing the PV arrays in households that require them are also shown. Table 6.2 shows the number of households with PV systems per transformer and the size of the PV arrays for each PV penetration level.

$$\begin{aligned} Total\ energy\ consumed\ in\ a\ day(kWh) = 33kW \times HH\_P1 + 22kWh \times HH\_P2 \\ +15kWh \times HH\_P3 + 10kWh \times HH\_P4 \\ +5.75kWh \times HH\_P5 \end{aligned} \tag{4.1}$$

$$Estimated\ load\ demand(kW) = \frac{Total\ energy\ consumed\ in\ a\ day(kWh)}{24\ hours} \tag{4.2}$$

$$Demand\ to\ be\ supplied\,(kWh) = \frac{Total\ energy\,(kWh) \times \%\ of\ load\ supplied\ by\ PV}{DC\ to\ AC\ Derated\ factor} \tag{4.3}$$

Photovoltaic panels have a power rating expressed in watts; this value indicates how much energy a photovoltaic module can produce. Derating factors can affect the amount of power generated by a solar panel. These factors can be environmental losses, such as a shadow on the panel or system losses, such as inverter losses, conductor losses and connection losses. The DC to AC derating factor takes these environmental and system losses and adds them into a percentage factor. This percentage indicates the overall efficiency of the PV module. In this work, the DC to AC derating factor is 0.9, considering the above-mentioned derating factors.

$$Required\ power\ of\ the\ PV\ system(kW) = \frac{Demand\ to\ be\ supplied(kWh)}{Sun\ peak\ hours(h)} \tag{4.4}$$

As described in section 3.2, the amount of peak sunshine hours in the area where the feeder is located is 5h.

$$Number\ of\ solar\ panels = \frac{Required\ power\ of\ the\ PV\ system(kW)}{Maximo\ power\ of\ panel(W)} \tag{4.5}$$

$$PV\ Power\,(kW) = Amount\ of\ solar\ panels \times Maximo\ power\ of\ panel\,(kW) \tag{4.6}$$

$$PV\ Energy\,(Wh) = PV\ Power\,(kW) \times\ Sun\ Peak\ Hour\,(h) \tag{4.7}$$

$$Number\ of\ PV\ systems\ HH = \frac{Amount\ of\ solar\ panels}{12\ panels\ per\ house} \tag{4.8}$$

$$Number\ of\ PV\ systems\ HH\ \leq\ Total\ HH \begin{cases} \text{Yes}, 12\ panels\ per\ house \\ \text{No}, 12\ panels\ per\ house\ + n \end{cases} \tag{4.9}$$

Where n is the number of additional solar panels needed to satisfy the condition.

$$PV\ Array\ Power\,(kW) = \#\ of\ Panel\ per\ House \times Maximo\ power\ of\ panel\,(kW) \tag{4.10}$$

An example of how to calculate the number of houses with PV systems needed in distribution transformer number seven (Table 4.2) to supply 50% and 150% of PV penetration is shown:

Table 4.2: Parameter of transformer T_7.

Transformer	Rating (kVA)	P1 33kWh	P2 22kWh	P3 15kWh	P4 10kWh	P5 5.75kWh	Total Houses
T_7	50	1	3	2	1	1	8

$Using\ equation$ 4.1 :

$$Total\ energy\ consumed\ in\ a\ day\,(kWh) = 33kW \times 1 + 22kWh \times 3 + 15kWh \times 2$$
$$+10kWh \times 1 + 5.75kWh \times 1$$
$$= 144.75kWh$$

$Using\ equation$ 4.2 :

$$Estimated\ load\ demand(kVA) = \frac{144.75kWh}{24\ hours} = 6.03kVA$$

The technical characteristics of the panels to be used are shown in Table 4.3.

Table 4.3: Parameters of panel.

Parameter	Value
Maximum Power (W)	330
Maximum Power Voltage (V)	37.8
Maximum Power Current (A)	8.73
Open Circuit Voltage (V)	46.2
Short Circuit Current (A)	9.33
Module Efficiency (%)	17
Temperature Coefficient of Voc (%/°C)	-0.32
Temperature Coefficient of Isc (%/°C)	0.055
Length (m)	1.956
Width (m)	0.992
Thickness (m)	0.035

- Example for 50%

  $Using\ equation$ 4.3 :

  $$Demand\ to\ be\ supplied = \frac{144.75kWh \times 0.5}{0.9} = 80.42kWh$$

$Using\ equation\ 4.4:$

$$Required\ power\ of\ the\ PV\ system = \frac{80.42kWh}{5h} = 16.08kW$$

$Using\ equation\ 4.5:$

$$Number\ of\ solar\ panels = \frac{16.08kW}{330W} = 48.7 \cong 49$$

$Using\ equation\ 4.6:$

$$PV\ Power\,(kW) = 49 \times 0.33kW = 16.17$$

$Using\ equation\ 4.7:$

$$PV\ Energy\,(Wh) = 16.17kW \times 5h = 80.85 \cong 81kWh$$

$Using\ equation\ 4.8:$

$$Number\ of\ PV\ systems\ HH = \frac{49}{12} = 4.08 \cong 5$$

$Using\ equation\ 4.9:$

$$Number\ of\ PV\ systems\ HH\ \leq\ Total\ HH \quad Yes,\ 12\ panels\ per\ house$$

$Using\ equation\ 4.10:$

$$PV\ Array\ Power\,(kW) = 12 \times 0.33kW = 3.96kW$$

- Example for 150%

$Using\ equation\ 4.3:$

$$Demand\ to\ be\ supplied = \frac{144.75kWh \times 1.5}{0.9} = 241.25kWh$$

$Using\ equation\ 4.4:$

$$Required\ power\ of\ the\ PV\ system = \frac{241.25kWh}{5h} = 48.25kW$$

$$Using\ equation\ 4.5:$$

$$Number\ of\ solar\ panels = \frac{48.25kW}{330W} = 146.21 \cong 147$$

$$Using\ equation\ 4.6:$$

$$PV\ Power\,(kW) = 147 \times 0.33kW = 48.51$$

$$Using\ equation\ 4.7:$$

$$PV\ Energy\,(Wh) = 48.51kW \times 5h = 242.55 \cong 243kWh$$

$$Using\ equation\ 4.8:$$

$$Number\ of\ PV\ systems\ HH = \frac{147}{12} = 12.25 \cong 13$$

$$Using\ equation\ 4.9:$$

$$Number\ of\ PV\ systems\ HH\ \leq\ Total\ HH \quad No,\ 12\ panels\ per\ house\ +\ n$$

$$Restating\ equation\ 4.8:\ para\ n = 8$$

$$Number\ of\ PV\ systems\ HH = \frac{49}{(12+8)} = 7.35 \cong 8$$

$$Checking\ equation\ 4.9:$$

$$Number\ of\ PV\ systems\ HH\ \leq\ Total\ HH \quad Yes,\ 20\ panels\ per\ house$$

$$Using\ equation\ 4.10:$$

$$PV\ Array\ Power\,(kW) = 20 \times 0.33kW = 6.6kW$$

Table 4.4 shows a summary of the calculations performed.

Table 4.4: Number of panels and HH to supply 50% and 150% of PV penetration.

Trans.	Rating (kVA)	Total Houses	Demand		50% PV		150% PV	
			Total(kWh)	Total(KVA)	HH with pv	# panels per house	HH with pv	# panels per house
T7	50	8	144.75	6.0	5	12	8	20

4.2.3 Residential Energy Storage Systems (RESS)

As mentioned previously, this study considers residential PV systems connected to a low voltage distribution system. Assuming that the maximum PV generation occurs at midday when there is low residential load consumption, high PV penetration can cause reverse flows and overvoltage in the feeder. To lessen the impact of high PV penetration, one solution is implementing ESS. Residential PV systems generally operate in conjunction with RESS systems in Puerto Rico. RESSs are used in small-scale energy systems and are mostly customer-owned. For this reason, the electric power authority has no control over RESS systems. The technologies implemented for RESSs are mostly solid-state batteries (lead-acid, lead-carbon and lithium-ion).

In this work, we implemented ESSs at each household with a PV system installed to increase the HC of the study feeder. The critical load analysis of a typical household was used for sizing the ESS systems, so all households have the same ESS capacity.

4.2.3.1 Critical load of a household

HHouseholds are composed of various types of loads, but there are essential or critical loads that must remain energized when a fault occurs in the electrical system. The essential electrical appliances of a household have been identified to be energized with the ESS. Table 4.5 describes these essential loads, their energy consumption, and hours of use. With this data, the energy consumed in the day by each load can be calculated (equation 4.11). The daily essential energy consumption value is used to size the capacity of the ESS.

$$Daily\ Energy\ Consumption\,(kWh) = Units \times\ Power\,(W) \times\ Hours\ of\ Use\,(h) \tag{4.11}$$

Table 4.5: Critical load.

Loads	Unit	Power (W)	Hours of Use(hrs)	Daily Energy Consumption (kWh/D)
Refrigerator	1	140	24	3.36
Pedestal Fan	2	100	6	0.6
Ceiling Fan	1	75	4	0.3
LCD TV	1	105	4	0.42
Radio	1	7	12	0.084
Smart Phone	2	6	4	0.024
Light Buld	4	20	8	0.16
			Total	5

4.2.3.2 Battery selection by performance

There are several types of batteries on the market, so it is important to select a battery that offers the best cost-performance ratio. The battery to be used was chosen by means of a price per kilowatt-hour analysis (equation 4.12). Table 4.6 shows different types of batteries and their characteristics.

$$\frac{\$}{kWh} = \frac{Price\ of\ the\ Battery \times\ 1000}{Nominal\ Voltage \times\ Capacity \times \%DoD \times\ Life\ Cycle} \tag{4.12}$$

Table 4.6: Comparison of battery performance.

Battery	Type	Capacity (Ah)	Nominal Voltage	Life Cycles 50% DoD	Price	$/kWh
Trojan T-105	Lead acid	225	6	1600	250	0.231
Crow CR-235	Lead acid	235	6	1200	200	0.236
Outback 106 WC	Lead acid	106	12	2750	286	0.164
Vitron Energy	Lithium Ion	100	12	1000	295	0.492
US Battery US	Lead acid	232	6	1150	153	0.191

The battery that offers the best cost-performance ratio is the Outback 106 WC, which uses sealed lead AGM technology, and is therefore, maintenance-free.

4.2.3.3 Battery Bank Sizing

Next, we describe the equations used to determine the number of batteries needed to supply the critical load of a household, identified in Table 4.5. Additionally, for the calculation of the battery bank, we considered two days of autonomy and a 50% depth of discharge (DoD).

$$Battery\ Bank\ Power\ Capacity\,(kWh) = \frac{DEC \times\ Days\ of\ Autonomy}{DoD} \tag{4.13}$$

$$Individual\ Battery\ Power\,(kWh) = NBV \times\ Battery\ Capacity \tag{4.14}$$

$$System\ Battery\ Capacity = \frac{Battery\ Bank\ Power\ Capacity}{Nominal\ System\ Voltage} \times 1000 \tag{4.15}$$

$$Number\ of\ Batteries = \frac{Battery\ Bank\ Power\ Capacity}{Individual\ Battery\ Power} \tag{4.16}$$

$$Batteries\ in\ Series = \frac{Nominal\ System\ Voltage}{Nominal\ Battery\ Voltage} \tag{4.17}$$

$$Batteries\ in\ Parallel = \frac{Number\ of\ Batteries}{Batteries\ in\ Series} \tag{4.18}$$

$$New\ number\ of\ batteries = Batteries\ in\ Series \times\ Batteries\ in\ Parallel \tag{4.19}$$

$$New\ battery\ bank\ power\ capacity\,(kWh) = \frac{BS \times\ NBV \times\ BP \times\ BC}{1000} \tag{4.20}$$

where:

- DEC: Daily energy consumption

- NBV: Nominal Battery Voltage
- BS: Batteries in series
- BP: Batteries in Parallel
- BC: Battery Capacity

Replacing the above equations with the corresponding values will give the following results:

$$Using\ equation\ 4.13:$$

$$Battery\ Bank\ Power\ Capacity\,(kWh) = \frac{5kWh \times\ 2}{0.5} = 20kWh$$

$$Using\ equation\ 4.14:$$

$$Individual\ Battery\ Power\,(kWh) = 12V \times\ 106Ah = 1.2kWh$$

$$Using\ equation\ 4.15:$$

$$System\ Battery\ Capacity\,(Ah) = \frac{20kWh}{48V} \times 1000 = 416.7Ah$$

$$Using\ equation\ 4.16:$$

$$Number\ of\ Batteries = \frac{20kWh}{1.2kWh} = 16.6$$

$Using\ equation\ 4.17:$

$$Batteries\ in\ Series = \frac{48V}{12V} = 4$$

$Using\ equation\ 4.18:$

$$Batteries\ in\ Parallel = \frac{16}{4} = 4$$

$Using\ equation\ 4.19:$

$$New\ number\ of\ batteries = 4 \times\ 4 = 16$$

$Using\ equation\ 4.20:$

$$New\ battery\ bank\ power\ capacity\,(kWh) = \frac{4 \times\ 12V \times\ 4 \times\ 106Ah}{1000} = 20.35kWh$$

Summarizing, the battery bank will consist of 16 batteries, at a 48 V nominal system voltageand 20.35kWh capacity. Figure 4.5 shows how the battery bank will be configured.

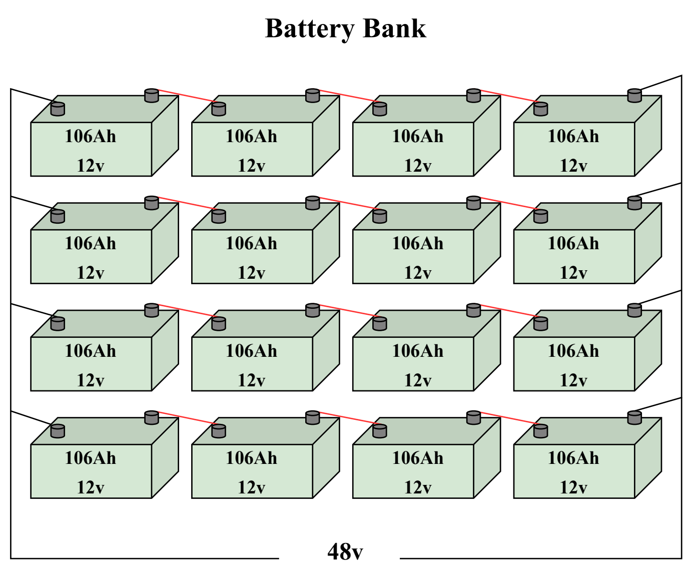

Figure 4.5: Battery bank.

4.2.4 Function Volt-VAR of Smart Inverter

The high penetration of PV systems increases voltage problems in distribution systems. For this reason, different methodologies have been proposed in the literature to control the active and reactive power, by means of intelligent inverter functions to maintain stable system voltage levels.

The most widely used method to regulate the voltage is to apply a Volt-VAR control curve to the PV system. The Volt-VAR control delivers a fraction of the available VARs based on the voltage measured at the common connection point of the PV system. A deadband near the desired voltage ensures that the control does not oscillate and only acts to reduce significant voltage deviations [24].

This document studies the use of the Volt-VAR function of the smart inverter as voltage support, and the impact that this type of control can have on the feeder HC increase.

4.2.4.1 Volt-VAR Curve

The Volt-VAR(VVC) control characteristics are shown in Figure 4.6. The VVC center defines the desired voltage of the smart inverters; this means that if the smart inverter voltage is at the VVC center, it does not require VAR support. The VVC width determines the VVC slope and how much reactive power the inverter delivers to bring the voltage back to the VVC center. So the smaller the VVC width, the steeper the slope. The deadband defines the voltage range around the VVC center in which the inverter would not deliver any reactive power [38].

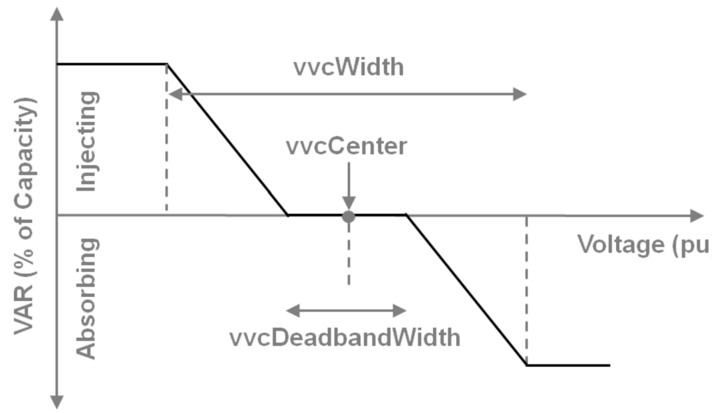

Figure 4.6: VVC Characteristics. (Source [38])

The maximum reactive power delivery from either injection or absorption is limited to 44% of rated capacity per Hawaii Rule 14H and IEEE 1547 default settings category B (high PV penetration, table 4.7) and 30% in California Rule 21 [25].

Table 4.7: Minimum reactive power injection and absorption capability. (Source [39])

Category	**Injection capability as % of nameplate apparent power (kVA) rating**	**Absorption capability as % of nameplate apparent power (kVa) rating**
A (at DER rated voltage)	44	25
B (over the full extent of ANSI C84.1 range A)	44	44

The IEEE Voltage Regulation Subgroup, in coordination with the IEEE 1547 update, proposed a default VVC curve type that aims to improve DER integration without causing adverse impact. This curve is shown in Figure 4.7. The Volt-VAR configuration shown is intended to be a default, out-of-the-box configuration that works in any given scenario [40].

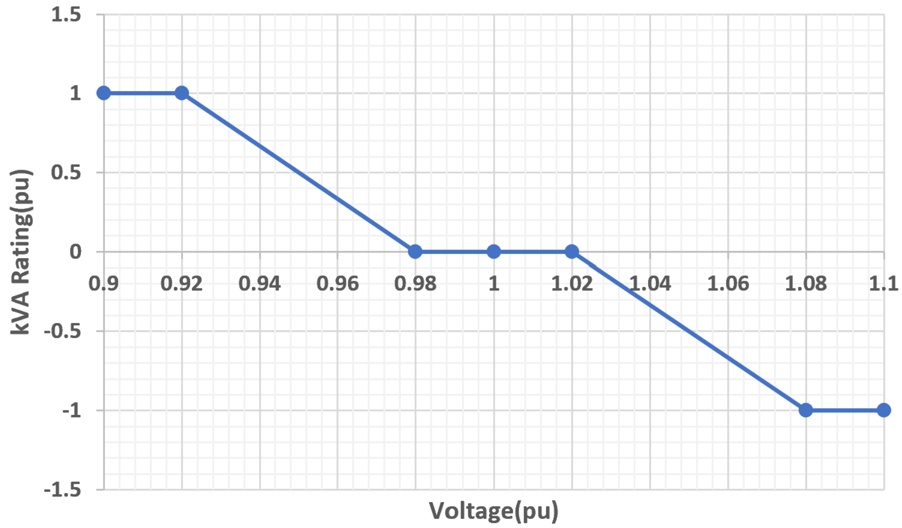

Figure 4.7: IEEE Voltage Regulation Subgroup Proposed Volt-VAR Settings. (Source [40])

Hence, this VVC configuration is used in this work to model the inverter.

4.2.4.2 Inverter Sizing

This section discusses the numerical analysis performed to determine the parameters needed to model the inverter.

A photovoltaic array can never deliver the maximum power for which it is designed, because there are efficiency losses due to temperature losses, and irradiance levels, among others. For this reason, inverters are often sized smaller than the maximum power that the PV array can deliver.

The DC-to-AC ratio is the ratio between the installed DC capacity (PV array power) and the rated AC power of the inverter. Figure 4.8 shows what happens when the DC-to-AC ratio of the inverter is high or low.

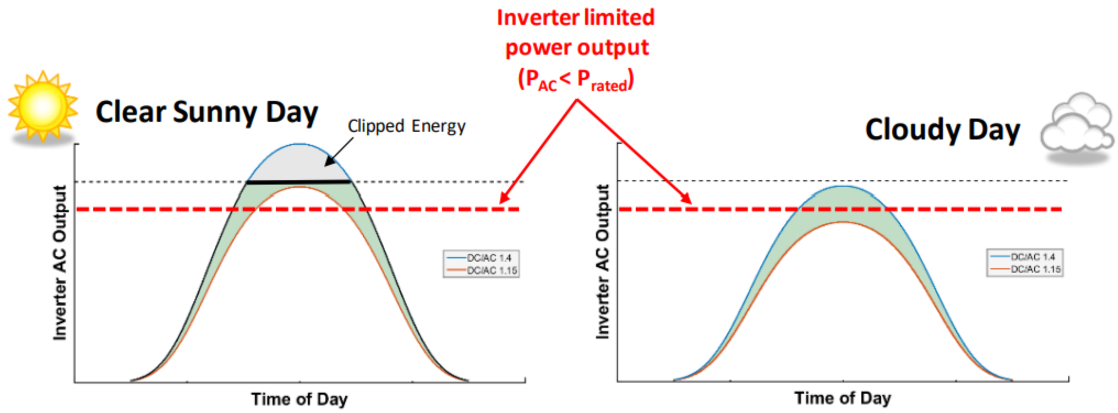

Figure 4.8: Inverter AC Output Over the Course of a Day. (Source [41])

If the inverter needs to limit its active power output to generate the reactive power required by the voltage control function, the energy loss will be higher in systems with a higher DC-to-AC ratio.

To better explain the equations used to determine the DC-to-AC ratio and rated power for inverter modeling, an example is used. In the example, the parameters of an inverter are calculated for a photovoltaic array composed of 12 panels, with 3.96 kW capacity. This was calculated in section 4.2.2.2 in the example for a penetration of 50% using equation 4.10.

Table 4.8: Schneider SW 4048 parameters.

Electrical specifications - inverter	**SW 4048 120/240**
Output power (continuous) at 25°C	3800 W
Peak current	41 A
Output frequency	50 / 60 Hz selectable
Output voltage	120 / 240 Vac
Nominal output voltage	48 Vdc

As explained above, it is advisable to use an inverter of lower power than the PV array. Hence, a Schneider SW 4048 120/240 inverter is used which has an output power of

3.8Kw (see Table 4.8).

$$DC\ to\ AC = \frac{PV\ \ Array\ Power\,(kW)}{Inverter\ Output\ Power\,(kW)} \tag{4.21}$$

$Using\ equation$ 4.21 :

$$DC\ to\ AC = \frac{3.96kW}{3.8kW} = 1.04$$

The maximum reactive demand when using the default VVC curve (Figure 4.7) is approximately 44% of the inverter's kVA rating. This amount of reactive power is equivalent to operating at a power factor of 90% during maximum output.

As seen in Figure 4.8, the inverter output power given in the datasheet is different from the rated power when the active output power needs to be limited to control the voltage. In equation 4.22, we can see how the rated power is calculated for the inverter modeling in the simulation:

$$P_{rated}(kVA) = \frac{Inverter\ Output\ Power(kW)}{Power\ Factor} \tag{4.22}$$

$Using\ equation$ 4.22 :

$$P_{rated}(kVA) = \frac{3.8kW}{0.9} = 4.22$$

As mentioned in section 4.2.2, when having different PV penetration levels, we will have different PV array sizes, as shown in Table 4.9. For this reason, the inverter seen in the example cannot be used in all PV penetration levels, as a consequence, it was decided that the DC-to-AC ratio seen in the example is the same for all PV penetration levels. Table 4.9, also describes which will be the inverter output power values for the different PV array sizes.

Table 4.9: Inverter output power, for different PV array sizes.

PV Array Paneles	PV Array Power(kW)	Inverter Output Power(kW)	DC-to-AC Ratio
12	3.96	3.8	1.04
14	4.62	4.4	1.04
16	5.28	5.1	1.04
18	5.94	5.7	1.04
20	6.6	6.3	1.04
22	7.26	7.0	1.04

4.3 Hosting Capacity Case Studies

This section describes the methodology followed in the simulation in each case study to determine the HC. The HC analysis is performed for a period of 24 hours with steps of one hour. The type of simulation performed is quasi-static, since for each hour of the day, a static power flow analysis is performed.

The HC analysis methodology used in the simulation, in all case studies, is divided into two groups. The first block refers to the simulation actions that are performed in the OpenDSS program environment. OpenDSS is a useful tool for distributed system simulation and HC analysis. Although OpenDSS is highly efficient software, it is difficult to perform the analysis and comparison of the results it delivers since they are in extensive ".txt" format. However, this drawback can be solved through its COM interface, which allows the user to connect OpenDSS with MATLAB and other programs (Visual Basic, Excel, Python). This interaction between programs provides a great capacity for information analysis, and to implement algorithms that use the results of OpenDSS simulations. The latter is what is done in the second block in MATLAB.

MATLAB is a programming software with great capabilities and many built-in functions such as the GRIDPV toolbox that allows graphing the results obtained from OpenDSS.

Taking control of OpenDSS from MATLAB enhances its functionality and makes it easy to process the results. Additionally, MATLAB can be used to control and modify the simulations performed by OpenDSS.

The codes used in OpenDSS and MATLAB for the simulation of these case studies can be found in Annex B and C. Additionally, the guidelines for the modeling of each component of the power supply, PV systems, ESS and Volt-VAR inverter function can be found in [34, 42–48].

4.3.1 Case 1: PV Only

For this case, the distribution system is modeled, using the information collected in Section 3, regarding the technical characteristics of the feeder under study. Then, the OpenDSS files of the different PV penetration scenarios are created, considering the PV penetration range from 0 to 150% (10% step). After the above steps, the power flow for the different PV penetration scenarios and each hour of the day can be solved. MATLAB collects all the information obtained from the power flow solution in OpenDSS. Additionally, MATLAB initializes the data collection for a PV penetration of 0% and the first hour of the morning at 1:00hrs (t=1). Then, it compares the voltage and current levels at each system node with the limits and constraints set(constraints described in section 4.2.1). Finally, MATLAB displays a summary of the constraint violations found for each PV penetration level. The entire methodology used for the simulation of this case is described in Figure 4.10. The way the PV systems are implemented on a distribution transformer is shown in Figure 4.9.

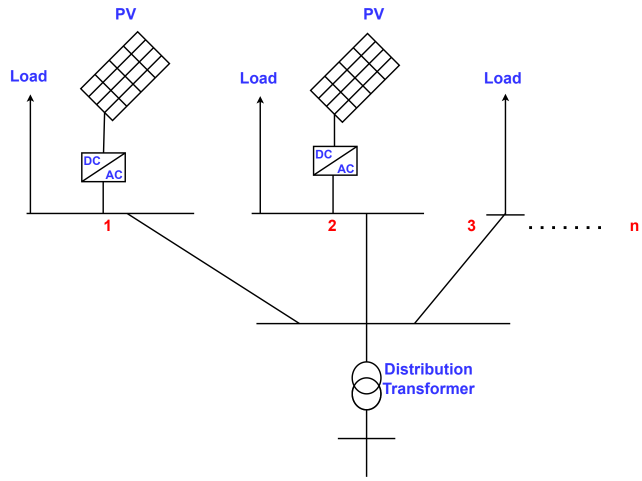

Figure 4.9: Single-line diagram Case 1.

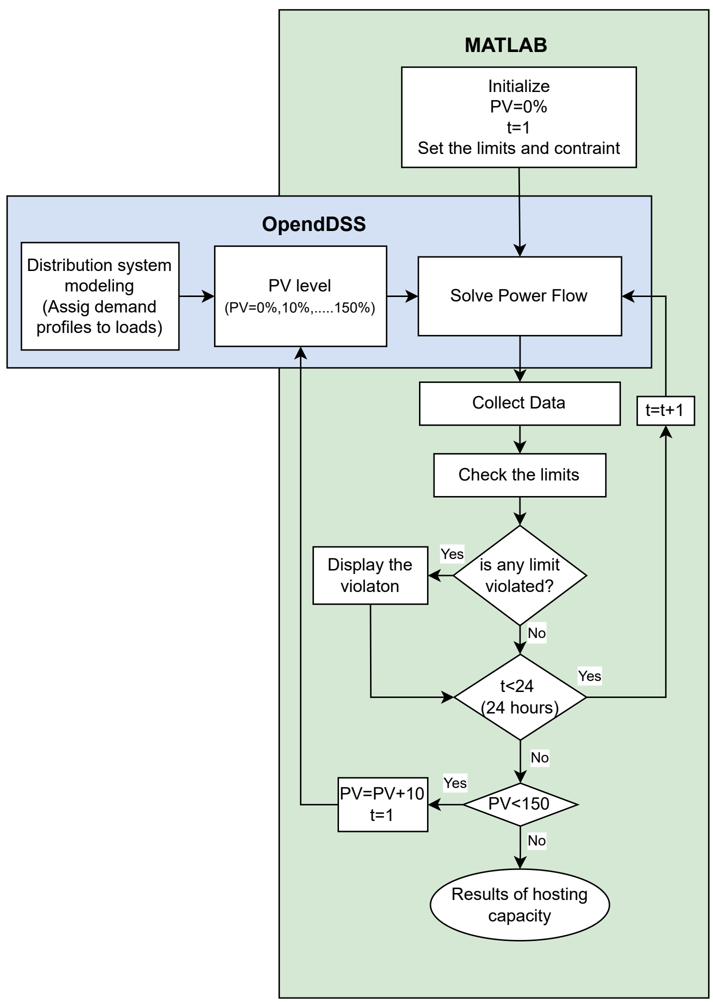

Figure 4.10: Methodology to evaluate the HC of PV systems, Caso 1.

4.3.2 Case 2: PV and Batteries

For the second case study, once the housing capacity has been evaluated in case 1 or also called a base case, RESS systems are added to the model to improve the HC. The implementation of the RESS systems to the simulation is done as illustrated in Figure 4.11 (i.e., if a household has a PV system, it also has a RESS system),applied to all PV penetration scenarios.

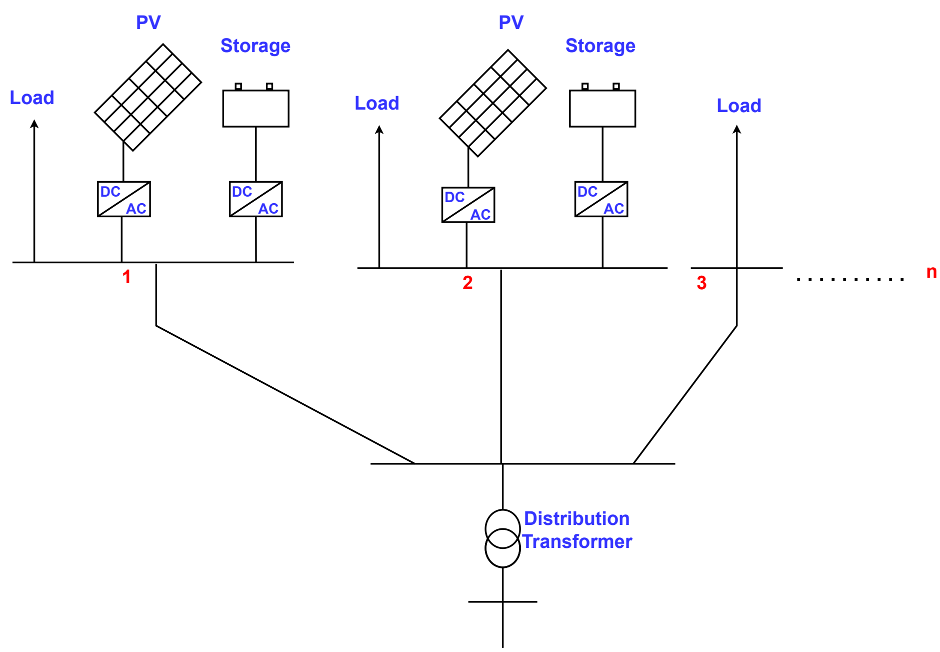

Figure 4.11: Single-line diagram Case 2.

For the analysis of the HC including the ESS, the same methodology described in case 1 is used, with the difference that a charging and discharging algorithm for the batteries (Figure 4.17) iis added in the MATLAB block, as seen in Figure 4.12, implemented after the power flow data collection. The battery discharge algorithm is designed to reduce the power consumption from the grid.

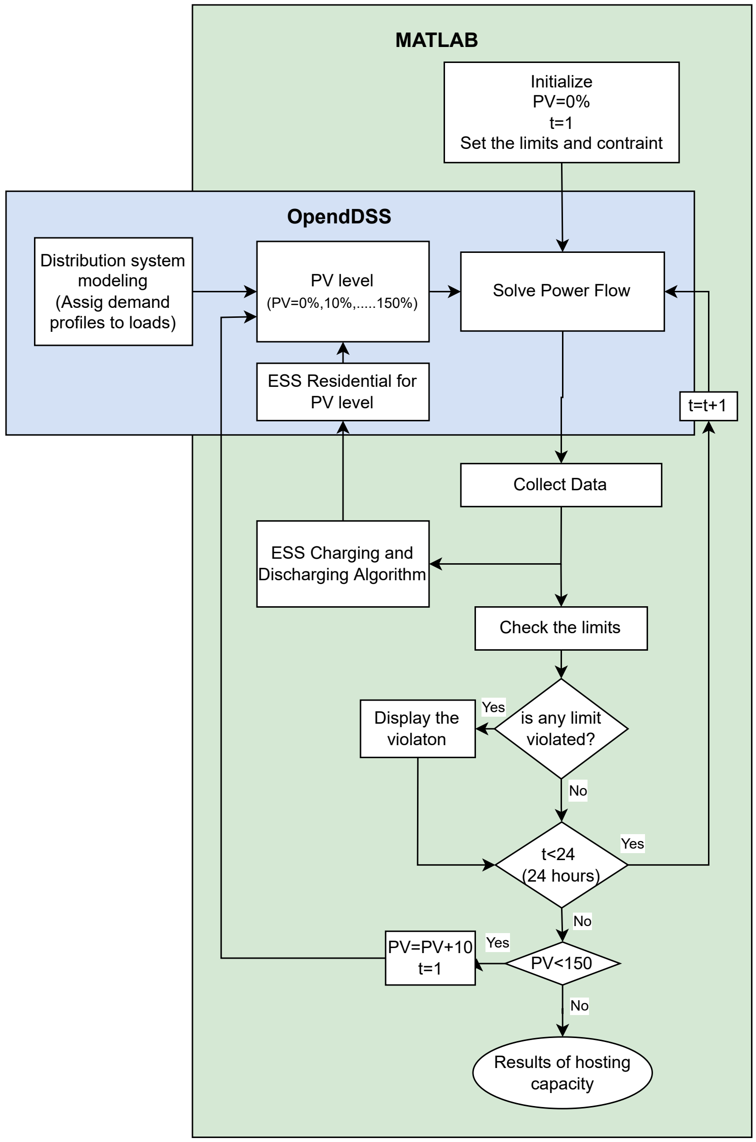

Figure 4.12: Methodology to evaluate the HC of PV systems, Case 2.

4.3.3 Case 3: PV and Smart Inverter

In the third case study, the Volt-VAR function of smart inverters is added to improve the HC. In the base case, the modeling of an ideal inverter is already included, see [34]]. But for this case, the Volt-VAR function is included in the inverter. For this reason, a new file is created in OpenDSS where the control method of all existing inverters in the different scenarios of PV penetration will be indicated. Additionally, in this file, the different parameters of the Volt-VAR function of the inverter described in section 4.2.4.2 are included. The methodology used for the simulation of this case is described in Figure 4.14.

The implementation of the Volt-VAR function is done as depicted in Figure 4.13, The figure we can observe that, if a household has a PV system, this system contains a smart inverter. This applies to all PV penetration scenarios.

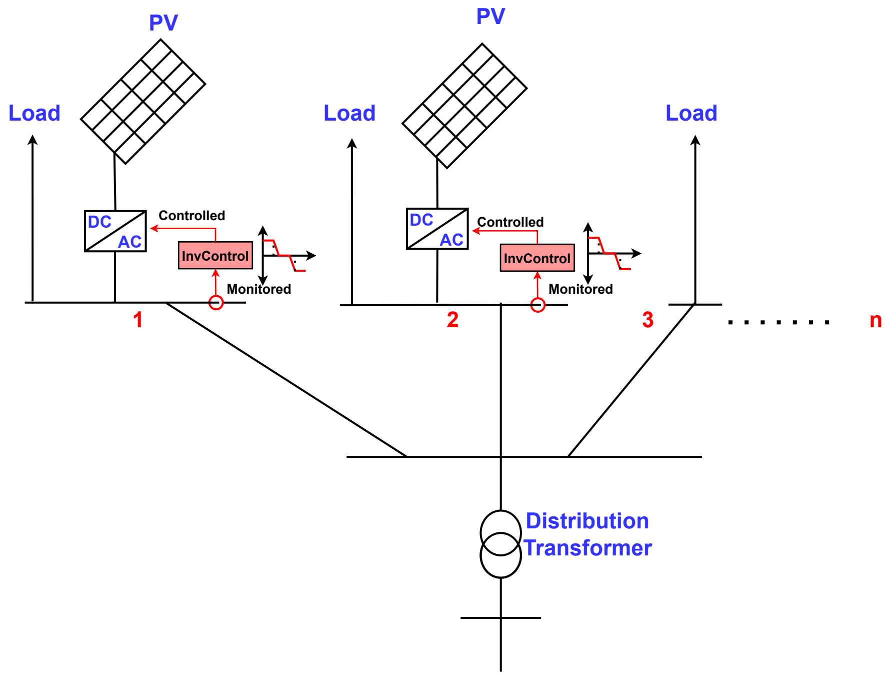

Figure 4.13: Single-line diagram Case 3.

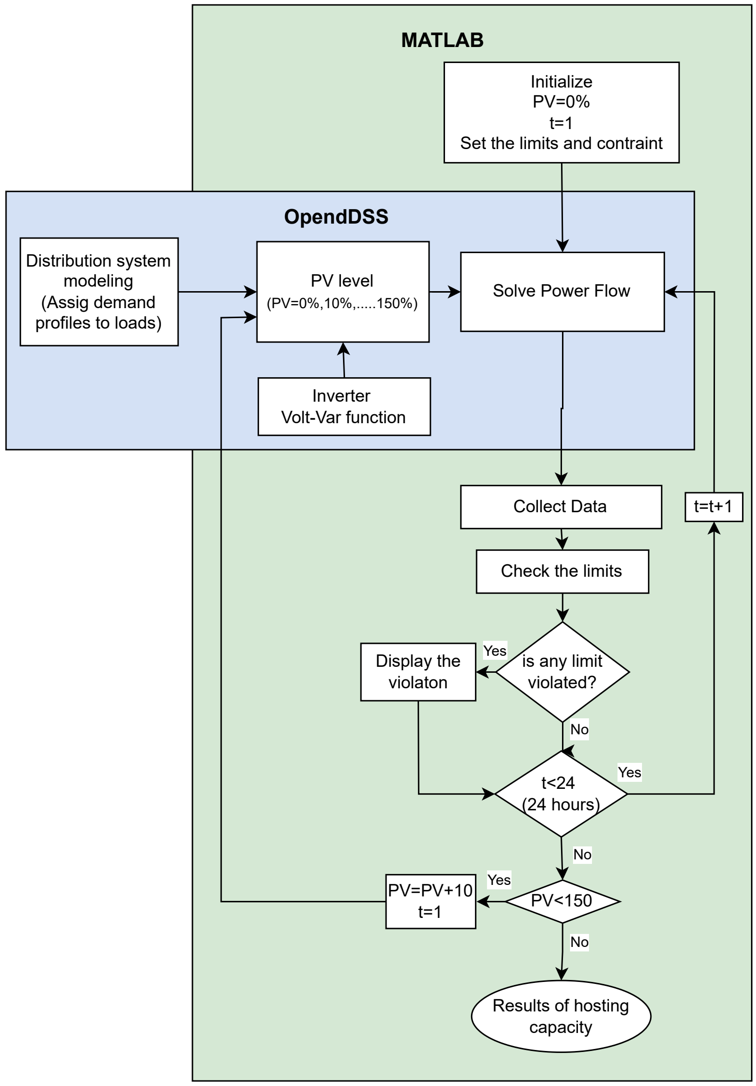

Figure 4.14: Methodology to evaluate the HC of PV systems, Case 3.

4.3.4 Case 4: PV, Batteries and Smart Inverter

Case 4 combines cases 1, 2 and 3. In the simulation of this case, as a method to improve the HC, the base case, RESS systems and the Volt-VAR function of the intelligent inverter were included. The implementation of these systems in the simulation is done as shown in Figure 4.15. The charge and discharge control of RESS can be governed by different parameters, generation cost, reduce grid consumption, voltage support, reverse current reduction, among others. For this reason, two algorithms for charging and discharging of RESS were implemented.

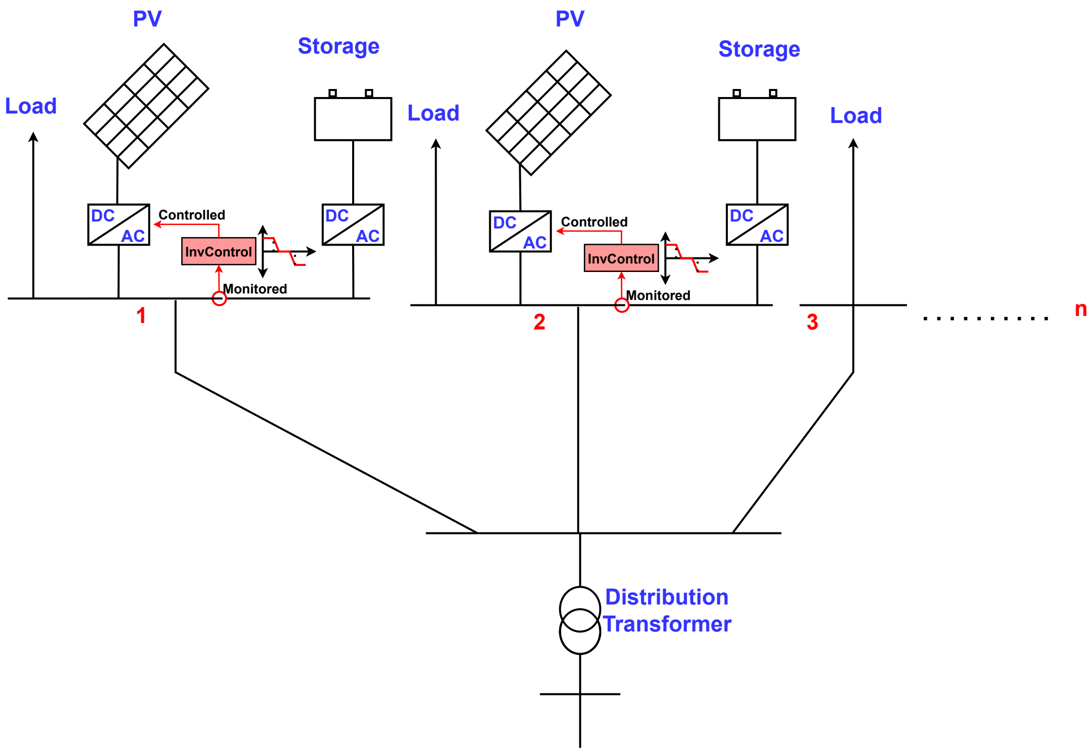

Figure 4.15: Single-line diagram Case 4.

4.3.4.1 Case 4.1: Battery algorithm 1

The methodology used for the simulation of this case is described in Figure 4.16, where the battery discharge algorithm is oriented to reduce the power consumption of the grid for a house. This algorithm is described in Figure 4.17. Therefore, the battery is discharged when the power demanded by the household load is higher than the power generated by the PV systems.

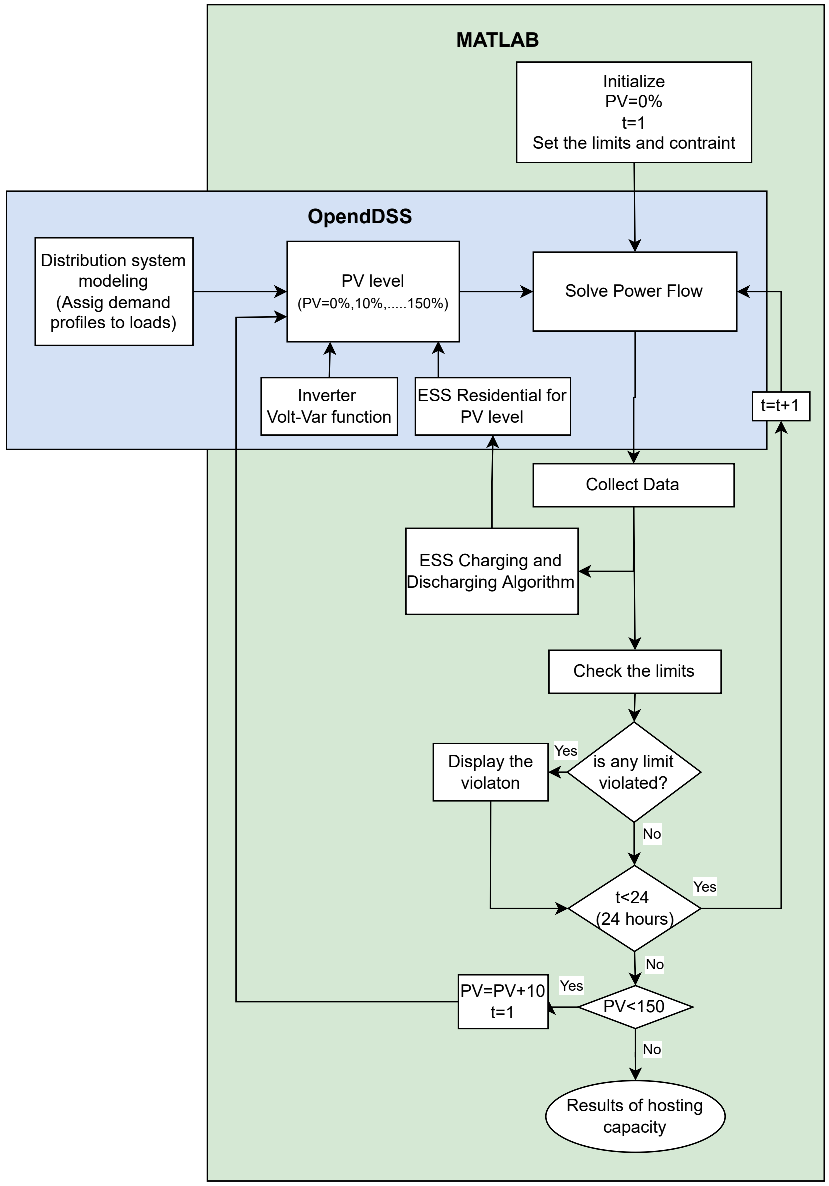

Figure 4.16: Methodology to evaluate the HC of PV systems, Case 4.

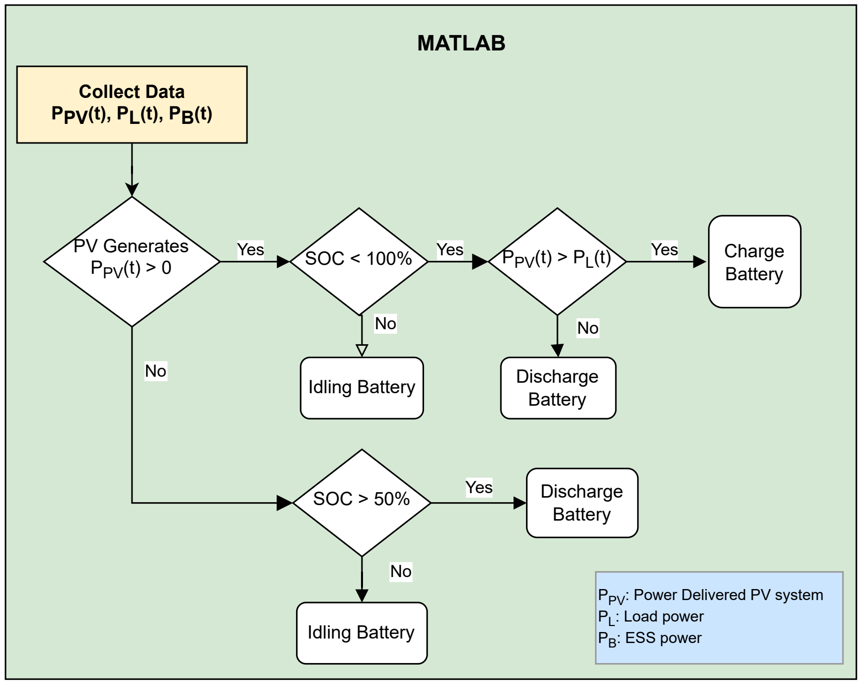

Figure 4.17: Flowchart of the battery charging and discharging algorithm 1.

4.3.4.2 Case 4.2: Battery algorithm 2

The methodology used for the simulation of this case is described in Figure 4.16, where the battery discharge algorithm is oriented to reduce the reverse current that causes voltage and thermal violations. This algorithm is described in Figure 4.17. Therefore, the battery is discharged when the reverse flow power reaching the distribution transformer is higher than the transformer rating.

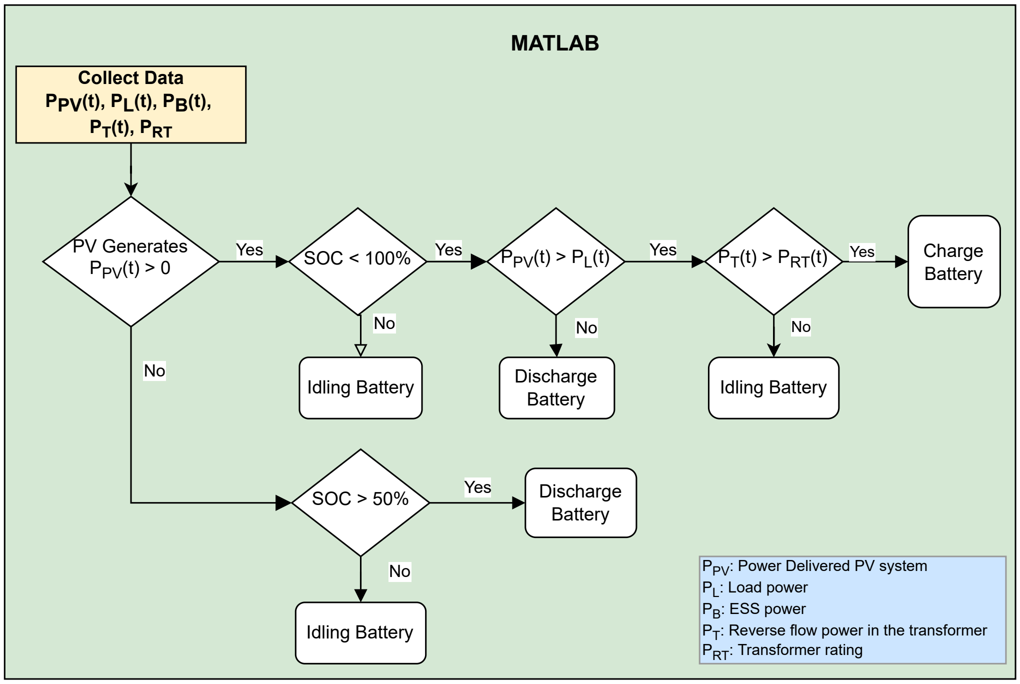

Figure 4.18: Flowchart of the battery charging and discharging algorithm 2.

Chapter 5

Results

5.1 Introduction

This chapter shows the results obtained in the case studies. The power flow analysis made it possible to determine the HC of PV systems for each case study.

To obtain the results described in this chapter, the first step was to collect information from the feeder and generate the temperature and irradiance curves of the area where it is located, as described in Chapter 3.

Subsequently, the development of the study was divided into four case. In the first phase, case one was established, in which first the feeder was simulated, and power flow was calculated for each hour of the day. For phase 2, different levels of PV penetration were implemented to determine the HC. In the second case study, a battery bank was implemented in the PV systems to improve the HC. Similarly, in case three, the Volt-VAR function of smart inverters is implemented in the PV systems to calculate the HC. Finally, case four combined the three previous cases. The case was divided into two parts because it analyzes different algorithms for charging and discharging battery banks to evaluate how this affects the HC of PV systems.

The results for each case study are presented through figures and tables that summarize the findings of the simulation data collection for each case. Power flow data is collected for each hour of the day, with each PV penetration level, i.e., for each case the power flow will be analyzed 3600 times so that the HC can be calculated.

5.2 Case 1: Only PV

5.2.1 Feeder Power Flow

The behavior of power and current in the feeder for a period of one day is shown in Figure 5.1. As shown in Figure 5.1a, the phase with the highest active and reactive power demand is phase one, also known as phase A. Figure 5.1b shows that the current in phase A is higher than the other phases with similar demands. On the other hand, we observe that the lowest power consumption in the feeder occurs in the early morning hours and the peak demand occurs at 20:00 hrs.

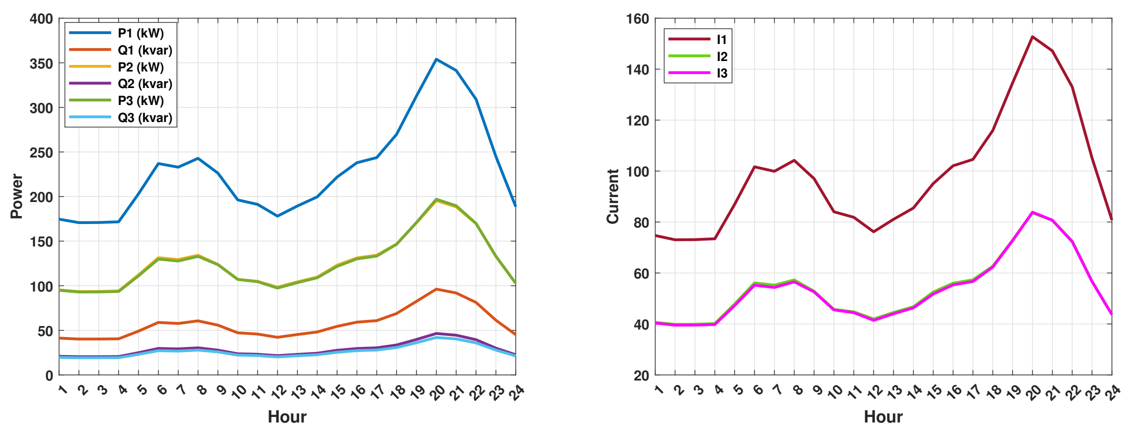

(a) Power demanded in the substation (b) Current demanded in the substation

Figure 5.1: Power flow of the feeder, in one day.

Figure 5.2 shows the current profile of the primary side of the feeder. This profile shows the current flowing through the last primary line where the load is lower up to the line leaving the substation where all the feeder demand comes together. Therefore the graph has a staggering shape. Figure 5.2a represents the demanded current for 13:00 hours, where it can be observed that the average current demand at the substation is 56.52A. On the other hand, the average current demand at the same point for 20:00 hours is 106.74A, almost double the demand at 13:00 hours. In addition, it is observed in Figure 5.2 that the current passing through the feeder lines is much lower than the rating of the lines.

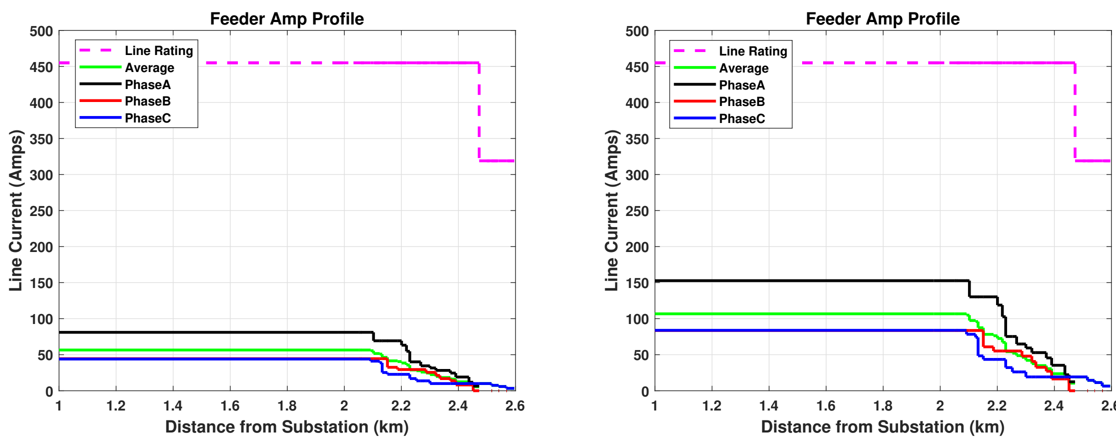

(a) Current profile for 13:00

(b) Current profile for 20:00

Figure 5.2: Feeder current profile.

Figure 5.3 shows the feeder power profile. Figure 5.3a shows that the average active power demanded at 13:00 hours is 132.4kW. While the average peak power demanded is 248.82kW (Figure 5.3b).

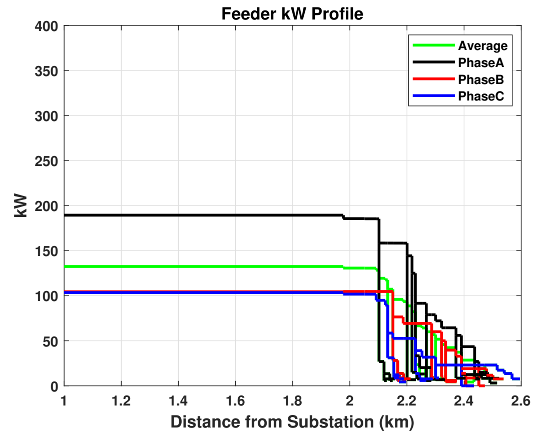

(a) active power profile for 13:00 (b) active power profile for 20:00

Figure 5.3: Active power profile on the feeder.

Figure 5.4a represents the feeder voltage profile for 13:00 hours, as can be seen in the figure, phase A has the highest voltage drop. In addition, for 13:00 hours it is observed that all phases are within the allowed voltage range. But this does not occur for 20:00 hours. In Figure 5.4b we observe that with the higher load at this time phase A is overloaded and violates the voltage limit.

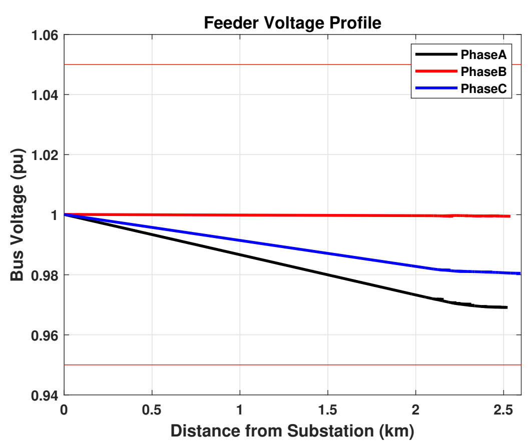

(a) Voltage profile for 13:00 (b) Voltage profile for 20:00

Figure 5.4: Feeder voltage profile.

5.2.2 PV Systems Hosting Capacity

This section presents the HC results of the PV system feeder. Different PV penetration scenarios were added to the feeder simulation to obtain these results, as described in Section 4.3.1.

Table 5.1 summarizes the maximum PU voltage values found on the feeder at each hour of the day for each PV penetration level described in the table. As can be seen in this table, for 60% PV penetration, from 11:00 to 13:00 hours, voltage levels very close to the allowed limit of 1.05pu are found. Therefore, for 70% PV penetration in the hours mentioned above, the voltage level exceeds the permitted limit. From this level of PV penetration, the percentage of violation of the voltage limits will increase.

Table 5.1: Maximum PU voltage per hour of the day, Case 1.

PV Level	**Hora**											
	<6:00	**7:00**	**8:00**	**9:00**	**10:00**	**11:00**	**12:00**	**13:00**	**14:00**	**15:00**	**16:00**	**>17:00**
10% PV	1.000	1.000	1.000	1.000	1.000	1.000	1.000	1.000	1.000	1.000	1.000	1.000
20% PV	1.000	1.000	1.000	1.000	1.002	1.004	1.006	1.005	1.001	1.000	1.000	1.000
30% PV	1.000	1.000	1.000	1.000	1.010	1.014	1.015	1.014	1.009	1.000	1.000	1.000
40% PV	1.000	1.000	1.000	1.006	1.020	1.024	1.026	1.025	1.019	1.007	1.000	1.000
50% PV	1.000	1.000	1.000	1.013	1.028	1.034	1.035	1.034	1.028	1.013	1.000	1.000
60% PV	1.000	1.000	1.003	1.020	1.038	1.045	1.046	1.045	1.038	1.020	1.003	1.000
70% PV	1.000	1.000	1.007	1.026	1.046	1.054	1.055	1.054	1.046	1.027	1.007	1.000
80% PV	1.000	1.000	1.012	1.034	1.056	1.064	1.065	1.063	1.055	1.034	1.012	1.000
90% PV	1.000	1.000	1.016	1.040	1.063	1.072	1.073	1.071	1.062	1.040	1.016	1.000
100% PV	1.000	1.000	1.020	1.046	1.071	1.081	1.082	1.081	1.071	1.046	1.020	1.000
110% PV	1.000	1.000	1.023	1.051	1.077	1.087	1.089	1.087	1.077	1.052	1.023	1.000
120% PV	1.000	1.001	1.029	1.060	1.088	1.100	1.101	1.099	1.088	1.060	1.029	1.000
130% PV	1.000	1.003	1.033	1.066	1.096	1.109	1.110	1.108	1.095	1.066	1.033	1.000
140% PV	1.000	1.006	1.039	1.074	1.107	1.122	1.124	1.122	1.106	1.074	1.039	1.000
150% PV	1.000	1.008	1.043	1.079	1.115	1.132	1.133	1.131	1.114	1.079	1.043	1.000

Figure 5.5 shows voltage profiles for 12:00. In these figures, the voltage profile varies as the PV penetration level increases. For a level of 20% PV penetration, we can see that in all phases the voltage level is close to unity. At 60% PV penetration, the voltage levels in phases A and B are close to the maximum allowable limit. At 70% PV penetration, phases A and B violating the voltage limit in the farthest areas of the substation. The

same will occur for PV penetration levels higher than 70% with the difference that the higher the penetration level, the closer the violations will occur to the substation, as shown in Figure 5.5d.

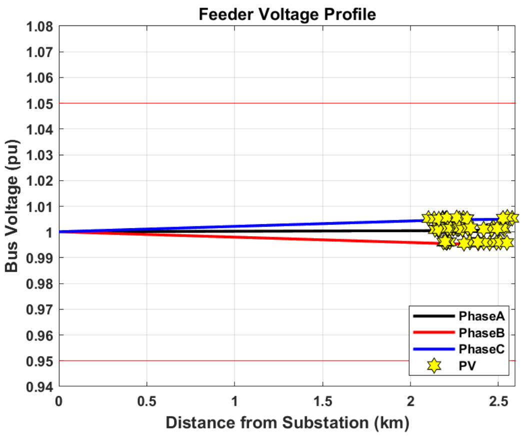

(a) 20% PV

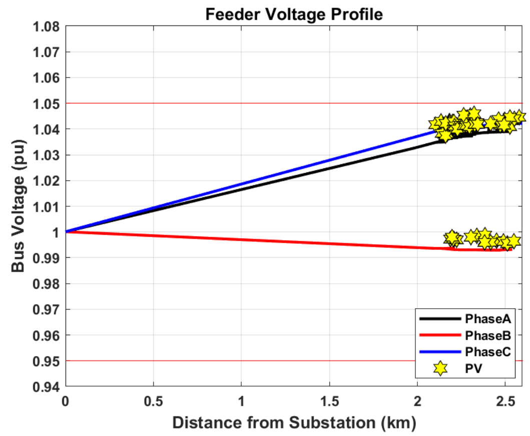

(b) 60% PV

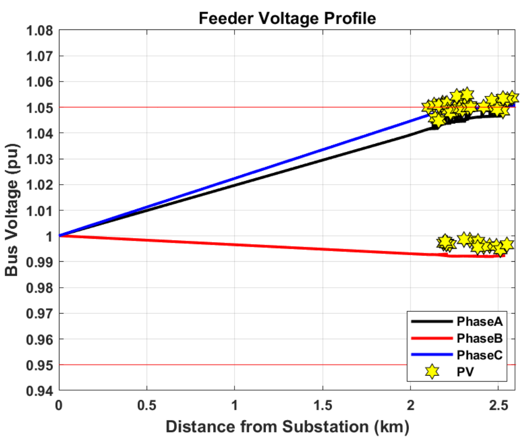

(c) 70% PV

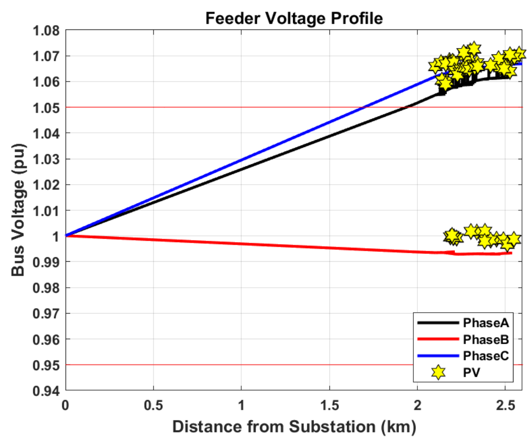

(d) 90% PV

Figure 5.5: Voltage Profile at 12:00 hrs, Case 1.

Figure 5.6 shows the mid-day feeder current profile for different PV penetration levels. In Figure 5.6a, the current flowing through the lines does not violate the conductor's capacity, as it occurs in Figures 5.6b and 5.6c. In addition, we can observe a greater increase in the current in phase A concerning the other phases. In Figure 5.6d, for a penetration level of 140%, the amount of current flowing through the phase A conductor manages to violate the conductor capacity very close to the substation.

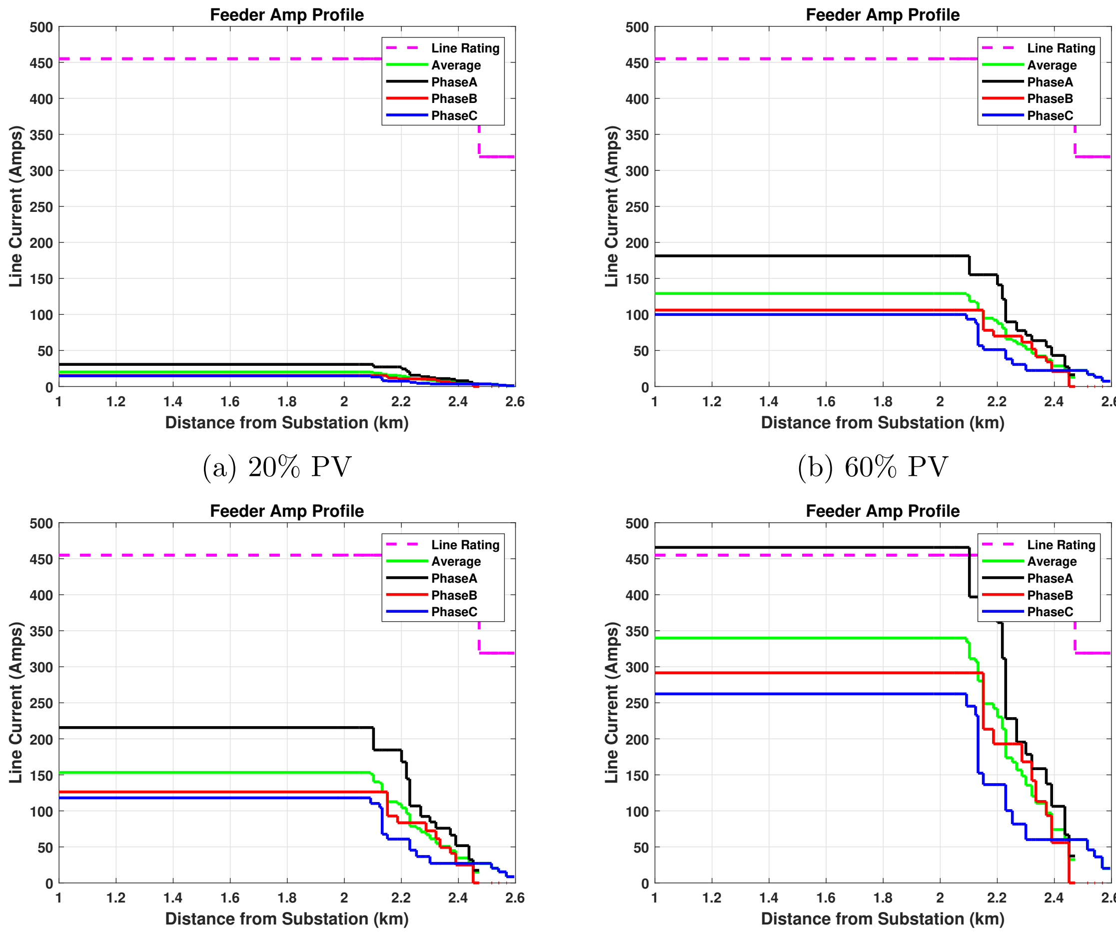

(a) 20% PV

(b) 60% PV

(c) 70% PV

(d) 140% PV

Figure 5.6: Current profile, Case 1.

Figure 5.7shows the power at the nodes where the distribution transformers are located for a PV penetration percentage of 60%; additionally, it is observed that the power in the transformers does not violate their capacity. But this does not occur for a penetration percentage of 90%, as shown in Figure 5.7b. In transformer number 51, the power exceeds its capacity. From this percentage of PV penetration, the thermal violations in the transformers will continue, as shown in Figure 5.7c for a penetration level of 140%, where the number of transformers that suffer thermal violations increases.

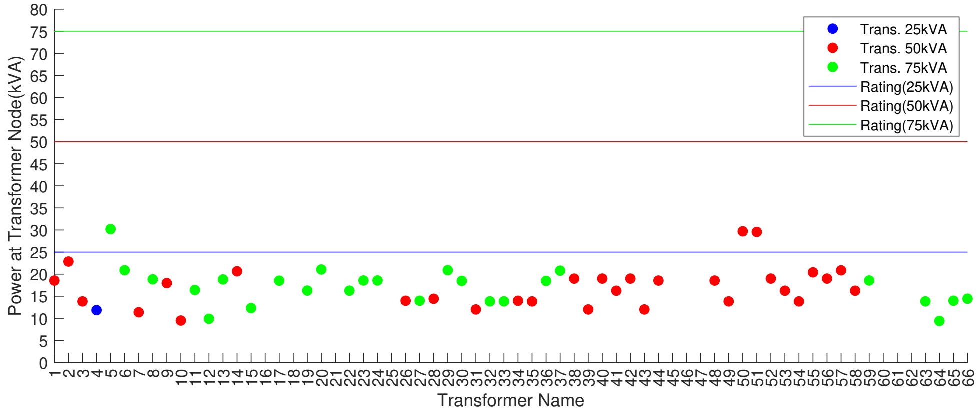

(a) 60% PV

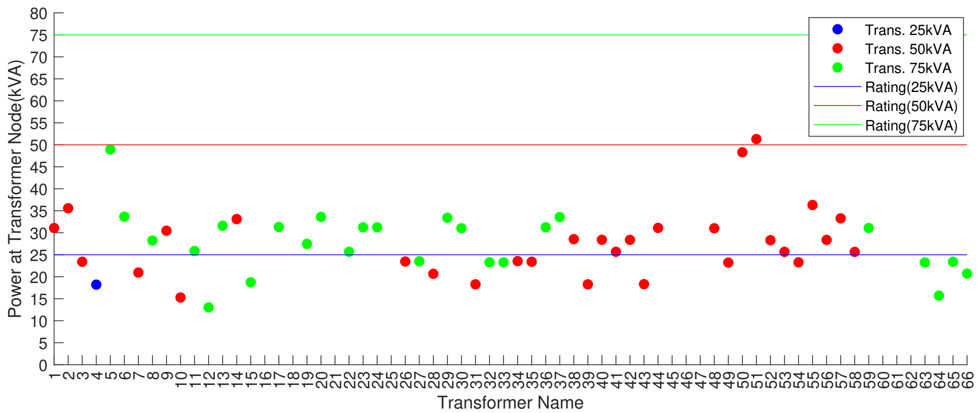

(b) 90% PV

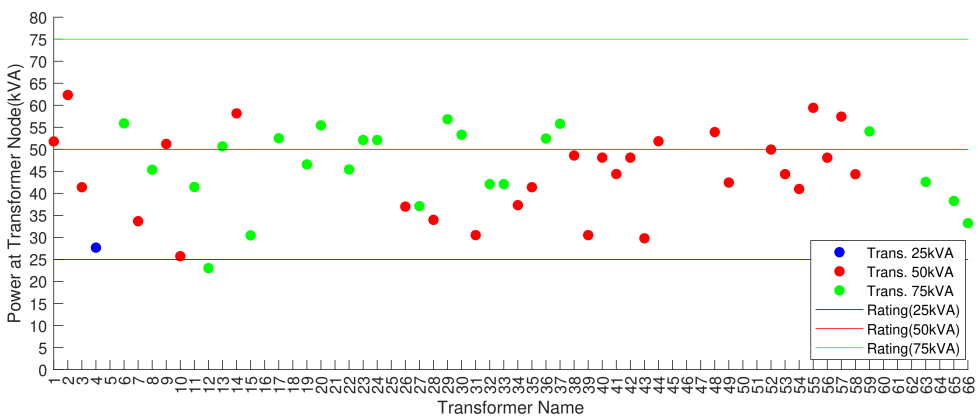

(c) 140% PV

Figure 5.7: Power at the distribution transformer nodes, Case 1.

Table 5.2 shows the transformers where thermal violations occur, the time of occurrence and the percentage of violation.

Table 5.2: Percentage of transformer capacity violations, Case 1.

Transformer	Hour						
	9:00	**10:00**	**11:00**	**12:00**	**13:00**	**14:00**	**15:00**
T_1	0.00%	0.00%	8.38%	9.23%	8.11%	0.00%	0.00%
T_2	0.00%	19.71%	33.92%	34.08%	32.81%	17.60%	0.00%
T_4	0.00%	15.43%	30.36%	31.60%	30.69%	16.26%	0.00%
T_5	0.00%	3.74%	17.36%	18.20%	16.91%	2.70%	0.00%
T_9	0.00%	0.00%	10.39%	11.67%	10.49%	0.00%	0.00%
T_14	0.00%	7.29%	22.51%	24.52%	23.14%	8.03%	0.00%
T_38	0.00%	0.00%	0.84%	1.38%	0.55%	0.00%	0.00%
T_40	0.00%	0.00%	0.00%	0.37%	0.00%	0.00%	0.00%
T_42	0.00%	0.00%	0.00%	0.35%	0.00%	0.00%	0.00%
T_44	0.00%	0.00%	8.18%	8.83%	7.94%	0.00%	0.00%
T_48	0.00%	0.00%	14.13%	15.12%	13.82%	0.00%	0.00%
T_50	6.07%	53.56%	74.45%	75.78%	73.85%	52.30%	5.84%
T_51	7.54%	55.80%	77.06%	78.61%	76.67%	54.84%	7.69%
T_52	0.00%	0.00%	5.03%	5.94%	4.68%	0.00%	0.00%
T_55	0.00%	12.60%	26.47%	27.20%	26.15%	11.87%	0.00%
T_56	0.00%	0.00%	0.00%	0.33%	0.00%	0.00%	0.00%
T_57	0.00%	7.54%	24.54%	25.69%	24.11%	6.32%	0.00%

Figures 5.8classifies HC and voltage or thermal violations into regions. The green region represents the allowed PV penetration levels that do not cause violations. As shown in the graph, the maximum HC of PV systems allowed for the first case study is 60%. Above this level of PV penetration, the red region indicates voltage violations. If the PV penetration continues to increase above 60%, the percentage of violation of the allowed limit will also increase (this is represented on the y-axis). This can also be seen in Table 5.3. For a PV penetration of 70%, we have a violation of 0.5% of the allowable limit. But for 90% penetration, we have voltage violations up to 2.2% of the allowed limit. Additionally, the blue region indicates thermal violations in the Figure. As can be seen, these violations occur for PV penetration levels greater than 80%. Table 5.3 shows that for 90% PV penetration, a 2.6% violation of the allowed limit is reached. This percentage increases for penetration levels higher than 90%.

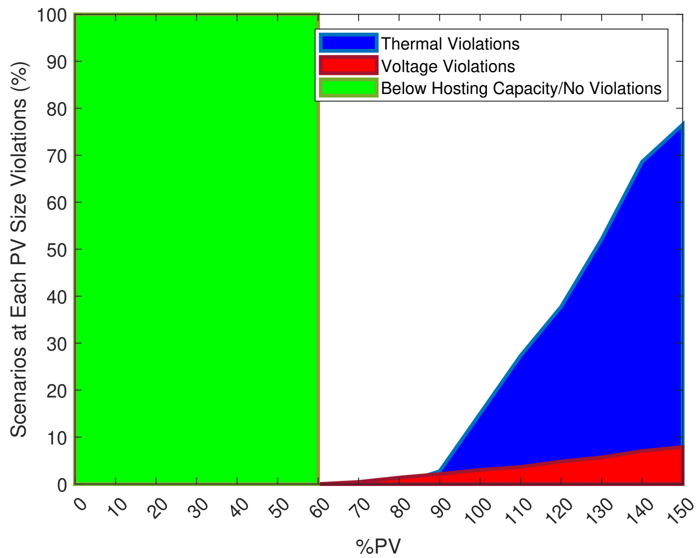

Figure 5.8: Results of HC analysis, Case 1.

Table 5.3: HC Analysis Results, Case 1.

PV% Level	**Violations**	
	Voltage(%)	**Thermal(%)**
<60	0.0	0.0
70	0.5	0.0
80	1.4	0.0
90	2.2	2.6
100	3.0	14.9
110	3.7	27.2
120	4.8	37.6
130	5.7	51.9
140	7.0	69.5
150	7.9	78.6

Figure 5.9a shows the nodes on the feeder where voltage violations first occur for 70% PV penetration. Similarly, Figure 5.9b shows the node where the first thermal violation occurs for 90% PV penetration. The detailed feeder with the names of the distribution nodes and transformers can be found in Appendix A.

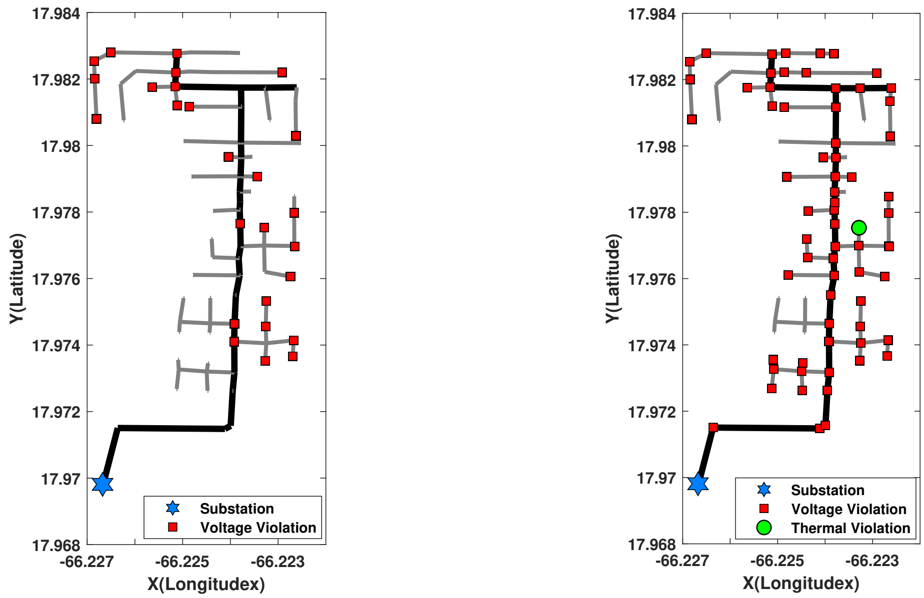

(a) 70% PV

(b) 90% PV

Figure 5.9: Network topology showing nodes where violations occur, Case 1.

5.3 Case 2: PV and Batteries

This section presents the results of the feeder HC analysis of case 2. Different PV penetration scenarios were added to the feeder simulation to obtain these results. The PV systems will be implemented with recurring ESS, as described in Section 4.3.2. Table 5.4 summarizes the maximum PU voltage values found on the feeder at each hour of the day for each PV penetration level described in the table.

As can be observed in this table, for 120% PV penetration, the maximum voltage found at 14:00 hrs is 1.051pu, which violates the allowed limit of 1.05pu. Therefore, we can observe that for penetration levels higher than 120%, voltage violations will occur from 13:00 to 14:00 hrs.

Table 5.4: Maximum PU voltage per hour of the day, Case 2.

PV Level	Hora											
	<6:00	**7:00**	**8:00**	**9:00**	**10:00**	**11:00**	**12:00**	**13:00**	**14:00**	**15:00**	**16:00**	**>17:00**
10% PV	1.000	1.000	1.000	1.000	1.000	1.000	1.000	1.000	1.000	1.000	1.000	1.000
20% PV	1.000	1.000	1.000	1.000	1.000	1.000	1.000	1.000	1.000	1.000	1.000	1.000
30% PV	1.000	1.000	1.000	1.000	1.000	1.000	1.000	1.000	1.000	1.000	1.000	1.000
40% PV	1.000	1.000	1.000	1.001	1.000	1.000	1.000	1.000	1.000	1.000	1.000	1.000
50% PV	1.000	1.000	1.004	1.005	1.000	1.000	1.000	1.000	1.000	1.000	1.000	1.000
60% PV	1.000	1.002	1.008	1.010	1.000	1.000	1.000	1.000	1.000	1.000	1.000	1.000
70% PV	1.000	1.006	1.012	1.014	1.002	1.000	1.000	1.000	1.002	1.004	1.000	1.000
80% PV	1.000	1.009	1.017	1.018	1.005	1.000	1.000	1.000	1.008	1.009	1.000	1.000
90% PV	1.000	1.012	1.019	1.021	1.006	1.000	1.000	1.000	1.014	1.012	1.000	1.000
100% PV	1.000	1.015	1.022	1.024	1.008	1.000	1.000	1.004	1.020	1.017	1.000	1.000
110% PV	1.000	1.017	1.025	1.027	1.009	1.000	1.000	1.004	1.032	1.020	1.000	1.000
120% PV	1.002	1.021	1.028	1.029	1.010	1.000	1.003	1.023	1.051	1.028	1.000	1.000
130% PV	1.004	1.024	1.031	1.032	1.011	1.000	1.011	1.061	1.060	1.032	1.000	1.000
140% PV	1.007	1.028	1.035	1.035	1.012	1.002	1.031	1.092	1.072	1.037	1.000	1.000
150% PV	1.008	1.030	1.037	1.036	1.015	1.011	1.043	1.108	1.078	1.041	1.000	1.000

Figure 5.10 shows voltage profiles for 14:00 hrs of the day where most of the voltage violations occur, as seen in Table 5.4. These figures show how the voltage profile varies as the PV penetration level increases. For a level of 20% PV penetration (Figure 5.10a) all phases are within the allowed limits. For 110% PV penetration (Figure 5.10b)), it is observed that the voltage levels in phases A and B increase because there is a greater

load on these phases; therefore, there is greater penetration of PV systems. For 120% PV penetration (Figure 5.10c)), phases A and B in the farthest areas of the substation begin to violate the voltage limits. The same will occur for PV penetration levels higher than 120% with the difference that the higher the penetration level, the more violations will occur closer to the substation, as shown in Figure 5.10d.

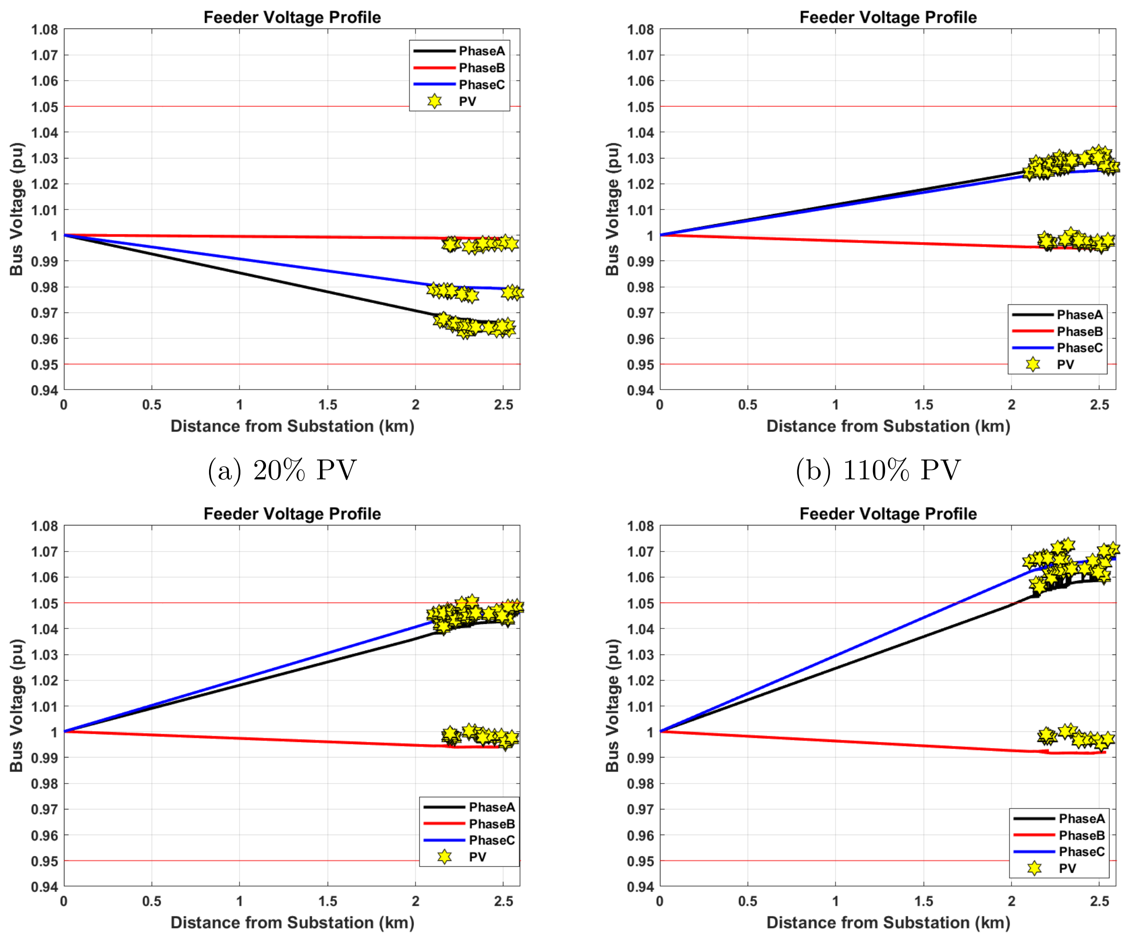

(a) 20% PV

(b) 110% PV

(c) 120% PV

(d) 140% PV

Figure 5.10: Voltage Profile at 14:00 hrs, Case 2.

Figure 5.11shows the feeder current profile at 13:00 hrs for different PV penetration levels. Figure 5.11a shows that the current flowing through the lines does not violate the conductor's capacity, as it occurs in Figures 5.11b, 5.11c, and 5.11d. However, we see that at higher PV penetration levels, the reverse current flow in the phases increases. A greater increase in the current in phase A with respect to the other phases is observed because there is a greater number of distributed PV systems in this phase.

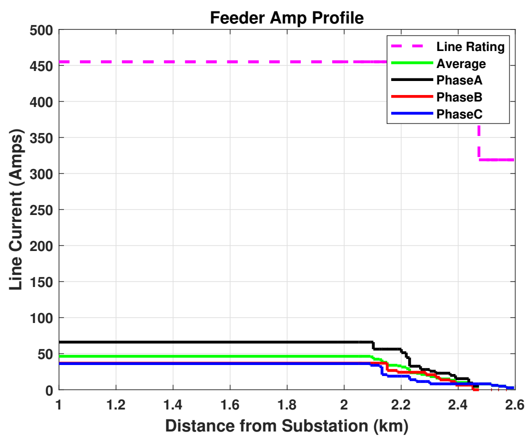

(a) 20% PV

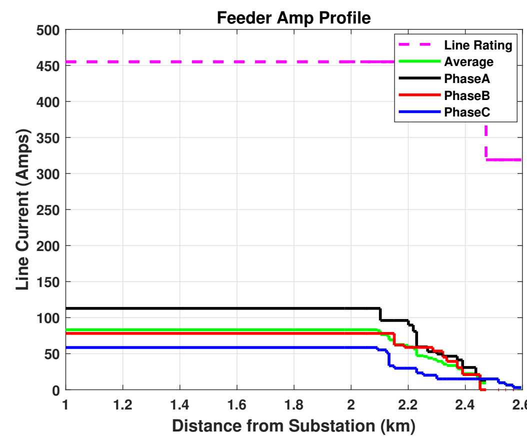

(b) 110% PV

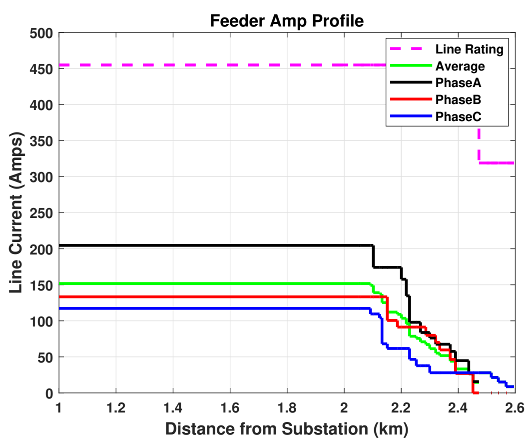

(c) 120% PV

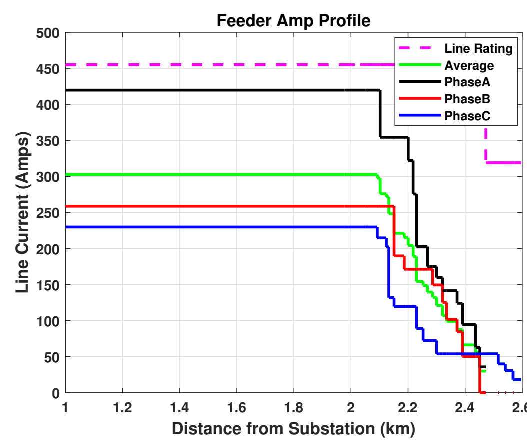

(d) 150% PV

Figure 5.11: Current profile, Case 2.

Figure 5.12 shows the power at the nodes where the distribution transformers are located. Figure 5.12a refers to a PV penetration percentage of 60%, where the power in the transformers does not violate their capacity. However, this does not occur for a penetration percentage of 130%, as shown in Figure 5.12b. In transformer number 51, the power exceeds its capacity. From this percentage of PV penetration, the thermal violations in the transformers will continue. As we can see in Figure 5.12c for a penetration level of 140%, the number of transformers that suffer thermal violations increases.

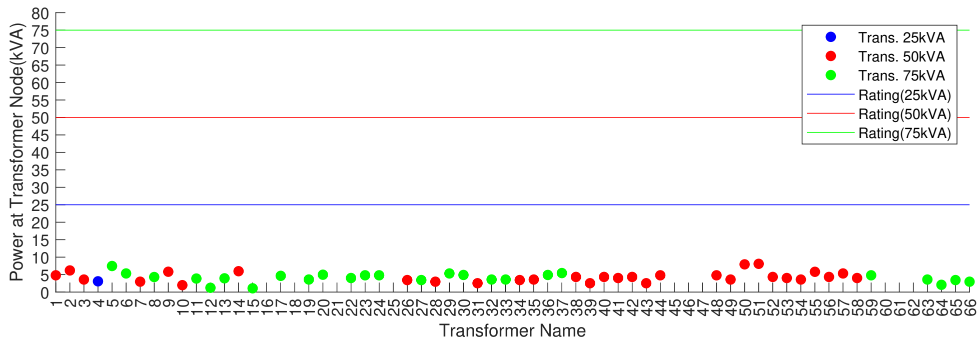

(a) 60% PV

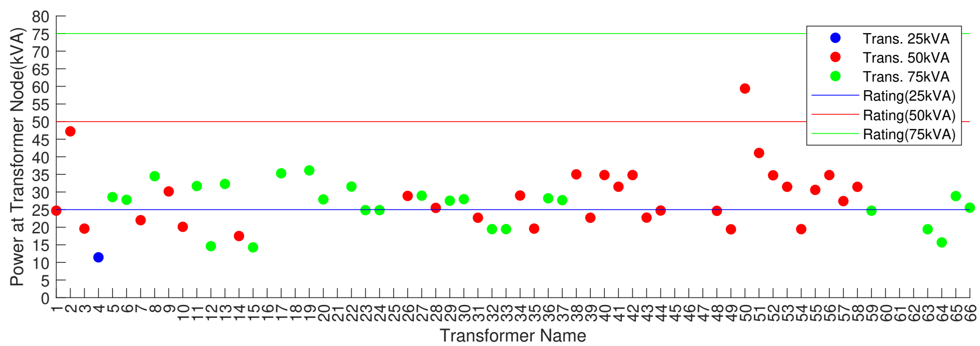

(b) 130% PV

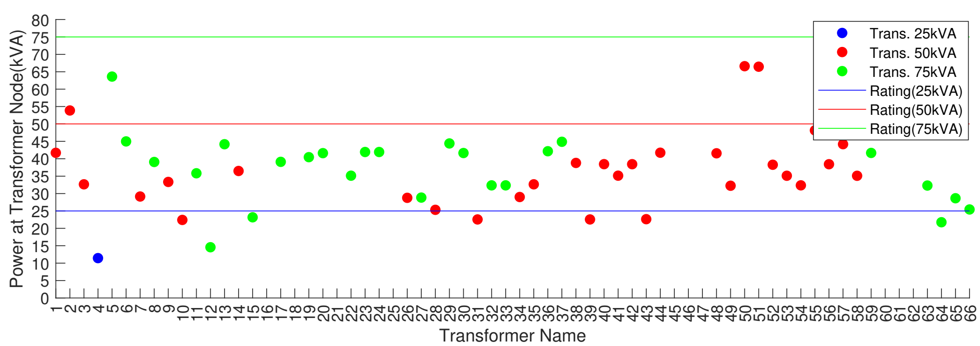

(c) 140% PV

Figure 5.12: Power at the Distribution Transformer Nodes, Case 2.

Table 5.5 shows the transformers where thermal violations occur, the time of occurrence, and the percentage of violations.

Table 5.5: Percentage of transformer capacity violations, Case 2.

Transformer	Hour	
	13:00	**14:00**
T_2	16.19%	0.00%
T_5	1.59%	0.00%
T_50	50.64%	4.02%
T_51	39.98%	5.61%
T_55	3.83%	0.00%

Figures 5.13 shows the result of the HC analysis for the case 2.The green region represents the allowed PV penetration levels that do not cause violations. As we can see in the graph, the maximum HC of PV systems allowed for the second case study is 110%. Above this level of PV penetration, the red-colored region appears, indicating voltage violations. If the PV penetration continues to increase above 110%, the percentage of violations of the allowable limit will also increase. This is also seen in Table 5.6. For a PV penetration of 120%, we have a violation of 0.05% of the allowable limit. But for a 140% penetration, voltage violations up to 3.98% of the allowable limit are observed. Additionally, the blue region indicates thermal violations. As can be seen, these violations can occur for PV penetration levels greater than 120%. Table 5.6 shows that for 130% PV penetration, a 19.30% violation of the allowed limit occurs. This percentage increases for higher penetration levels.

Table 5.6: HC Analysis Results, Case 2.

PV% level	Violations	
	Voltage	**Thermal**
<110	0.00	0.00
120	0.05	0.00
130	1.07	19.30
140	3.98	33.26
150	5.54	50.64

Figure 5.14a shows the nodes on the feeder where voltage violations first occur for 120% PV penetration. Similarly, Figure 5.14b shows the node where the first thermal violation occurs for 130% PV penetration.

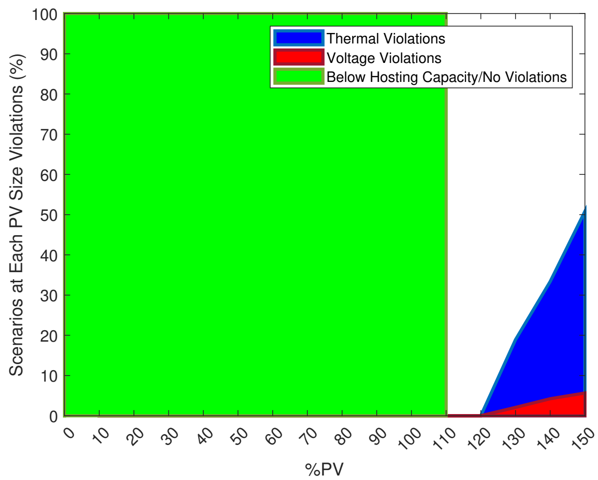

Figure 5.13: Results of HC analysis, Case 2.

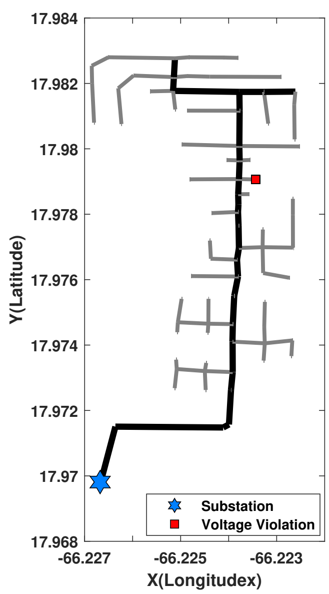

(a) 120% PV

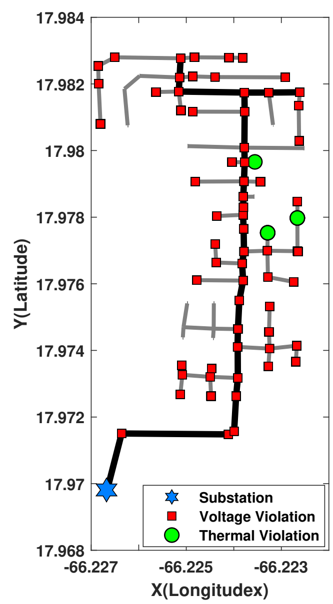

(b) 140% PV

Figure 5.14: Network topology showing nodes where violations occur, Case 2.

An important aspect to show in this case with RESS where the charging and discharging algorithm is designed to reduce the power consumption of the household grid is that during the hours of peak PV generation the batteries will be charged so that at night, they can supply the household load. Figure 5.15 compares voltage profiles for the 20 hours with different levels of PV penetration. Figure 5.15a with no PV penetration shows that at peak hour phase A, which contains the largest feeder load, violates the voltage limits. But this situation is remedied as seen in Figures 5.15b, 5.15c, and 5.15d where the feeder simulation includes PV systems with RESS.

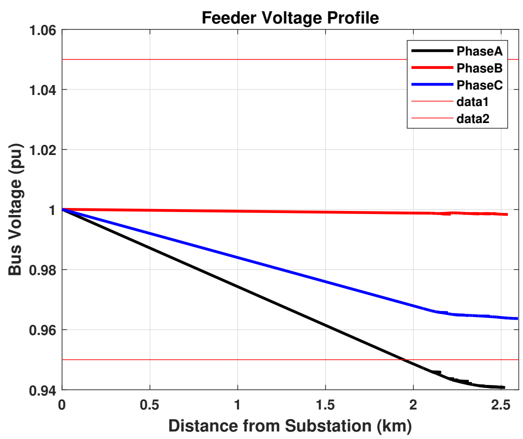

(a) No PV

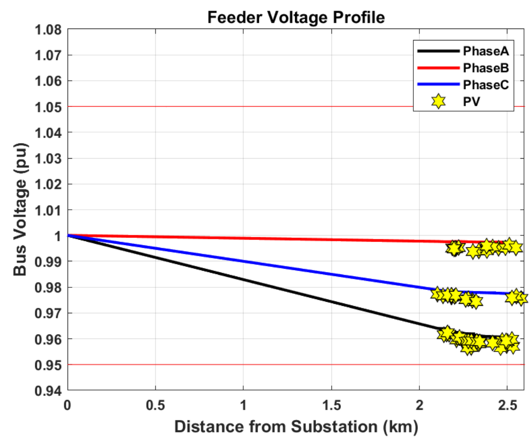

(b) 20% PV

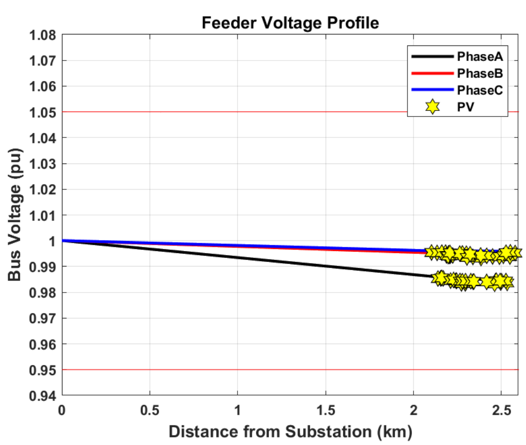

(c) 80% PV

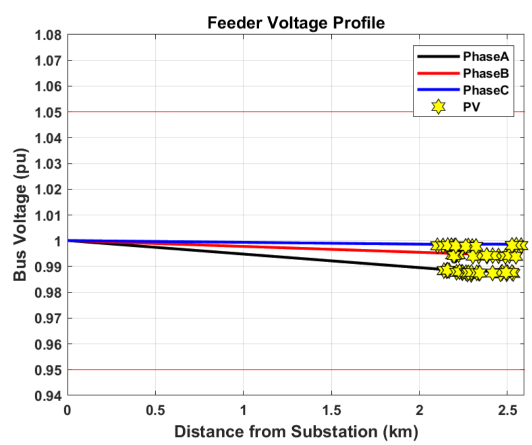

(d) 150% PV

Figure 5.15: Voltage Profile at 20:00 hrs, Case 2.

5.4 Case 3: PV and Smart Inverter

This section presents the results of the feeder HC analysis of case 3. Different PV penetration scenarios were added to the feeder simulation to obtain these results. The PV systems will have smart inverters where the Volt-VAR function is used, as described in Section 4.3.3.

Table 5.7 summarizes the maximum PU voltage values found on the feeder at each hour of the day, for each PV penetration level described in the table. As can be seen in this table, the highest voltage values occur between 10:00 and 14:00 hrs. These voltage values are below the maximum allowable limit of 1.05pu. These voltage values are below the maximum allowable limit of 1.05pu. Therefore, in this case, there are no voltage violations.

Table 5.7: Maximum PU voltage per hour of the day, Case 3.

PV Level	**Hora**											
	<6:00	**7:00**	**8:00**	**9:00**	**10:00**	**11:00**	**12:00**	**13:00**	**14:00**	**15:00**	**16:00**	**>17:00**
10% PV	1.000	1.000	1.000	1.000	1.000	1.000	1.000	1.000	1.000	1.000	1.000	1.000
20% PV	1.000	1.000	1.000	1.000	1.001	1.004	1.006	1.005	1.001	1.000	1.000	1.000
30% PV	1.000	1.000	1.000	1.000	1.010	1.014	1.015	1.014	1.009	1.000	1.000	1.000
40% PV	1.000	1.000	1.000	1.006	1.020	1.023	1.024	1.023	1.019	1.006	1.000	1.000
50% PV	1.000	1.000	1.001	1.013	1.024	1.027	1.028	1.027	1.024	1.013	1.000	1.000
60% PV	1.000	1.000	1.002	1.020	1.028	1.031	1.031	1.030	1.027	1.020	1.002	1.000
70% PV	1.000	1.000	1.006	1.023	1.030	1.033	1.034	1.033	1.030	1.022	1.006	1.000
80% PV	1.000	1.000	1.011	1.025	1.033	1.036	1.036	1.035	1.032	1.025	1.011	1.000
90% PV	1.000	1.000	1.015	1.027	1.034	1.037	1.038	1.037	1.034	1.026	1.015	1.000
100% PV	1.000	1.000	1.019	1.028	1.036	1.039	1.040	1.039	1.036	1.028	1.019	1.000
110% PV	1.000	1.000	1.021	1.029	1.037	1.040	1.040	1.040	1.036	1.029	1.021	1.000
120% PV	1.000	1.000	1.022	1.031	1.039	1.042	1.042	1.041	1.038	1.031	1.022	1.000
130% PV	1.000	1.000	1.023	1.031	1.039	1.042	1.043	1.042	1.039	1.031	1.023	1.000
140% PV	1.000	1.000	1.024	1.033	1.041	1.044	1.044	1.043	1.040	1.032	1.024	1.000
150% PV	1.000	1.000	1.024	1.033	1.041	1.045	1.045	1.044	1.041	1.033	1.025	1.000

Figure 5.16 shows voltage profiles at 12:00 hrs where the voltage level is higher as we saw in Table 5.7. These figures show how the voltage profile varies as the PV penetration level increases. For 20% PV penetration (Figure 5.16a), all phases are within the allowed limits with values very close to unity. For 80% PV penetration (Figure 5.16b),

the voltage levels increase in all three phases. This occurs similarly for the different penetration levels.

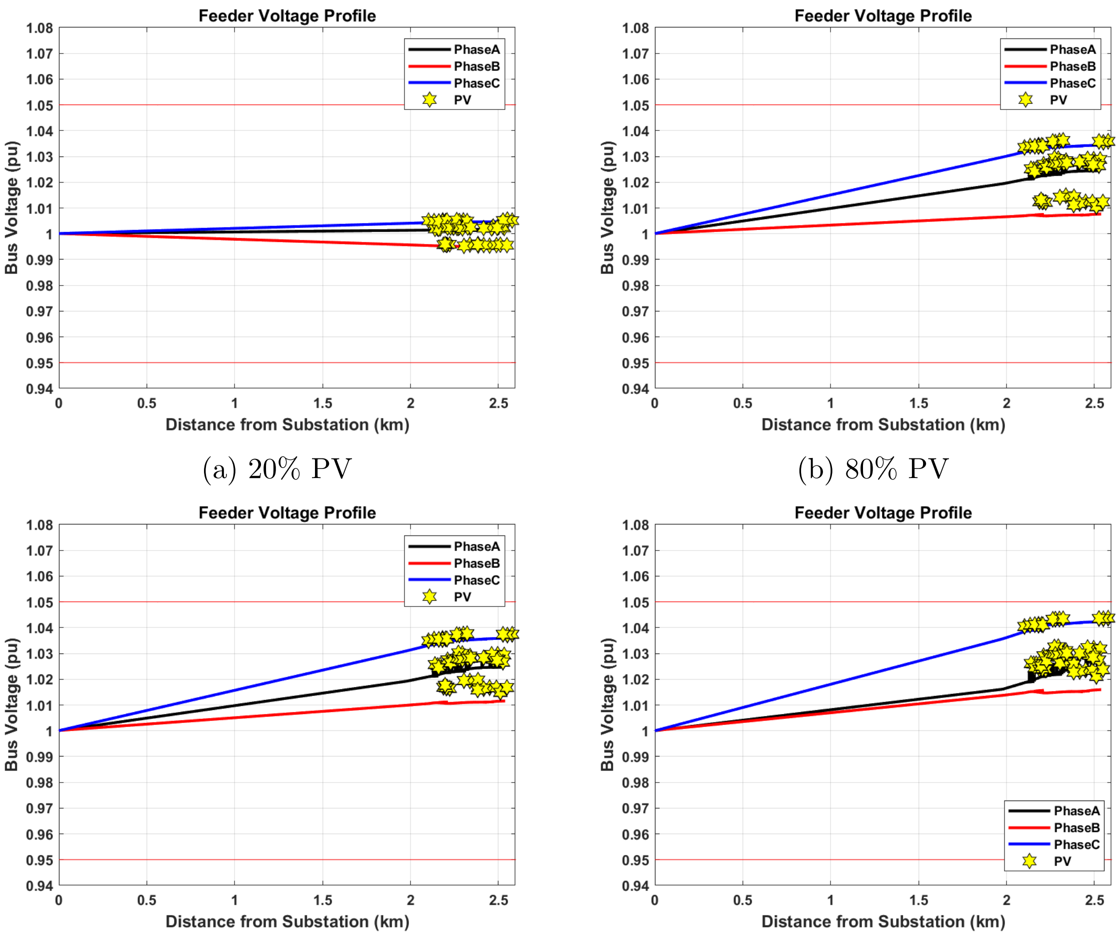

(a) 20% PV

(b) 80% PV

(c) 90% PV

(d) 140% PV

Figure 5.16: Voltage Profile at 12:00 hrs, Case 3.

Figure 5.17 shows the feeder current profile at 12:00 hrs, for different PV penetration levels. In Figure 5.17a, the current flowing through the lines does not violate the conductor's capacity. This can also be seen for 80% and 90% PV penetration (Figure 5.17b and 5.17c, respectively). For a PV penetration of 130% (Figure 5.17d), the reverse current flowing through the phase A conductor violates the conductor rating near the substation.

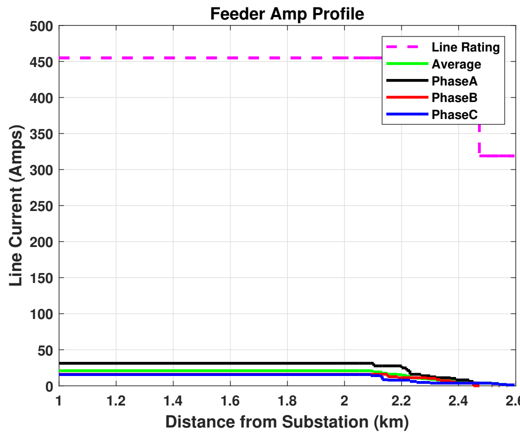

(a) 20% PV

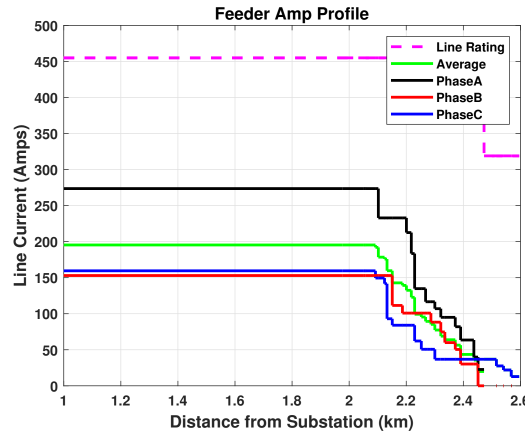

(b) 80% PV

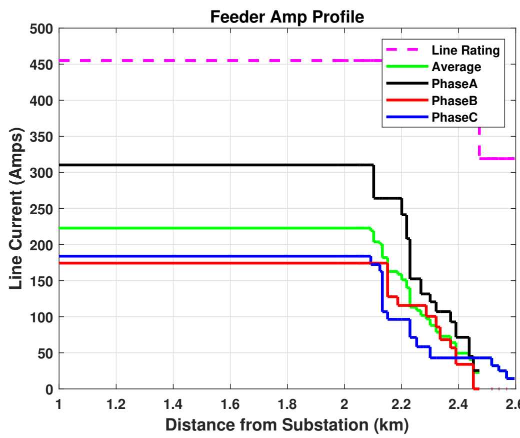

(c) 90% PV

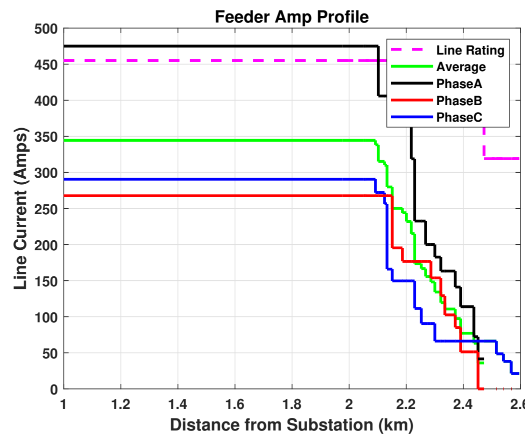

(d) 130% PV

Figure 5.17: Current Profile, Case 3.

Figure 5.18a shows the power at the nodes where the distribution transformers are located for a PV penetration percentage of 60%; additionally, it is observed that the power at the transformers does not violate their capacity. But this does not occur for a penetration percentage of 90%, as shown in Figure 5.18b. The power at the nodes of distribution transformers number 50 and 51 exceeds their capacity. From this percentage of PV penetration, the thermal violations in the transformers will continue. As we can see in Figure 5.18c for a penetration level of 140%, the number of transformers suffering thermal violations increases.

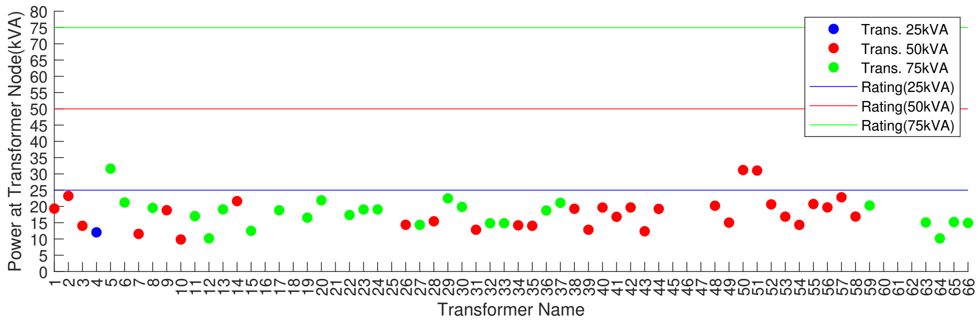

(a) 60% PV

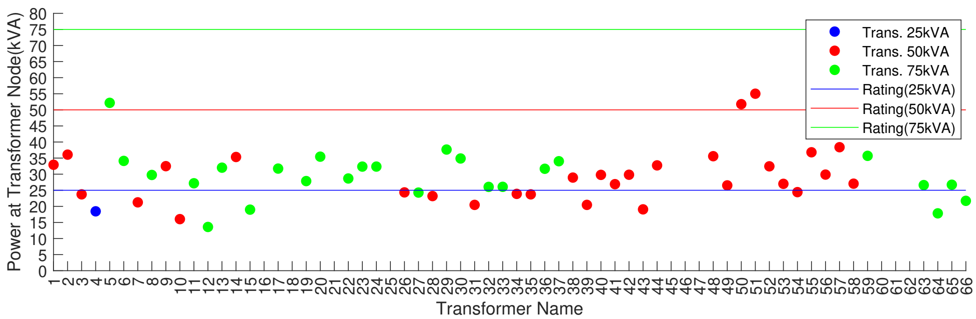

(b) 90% PV

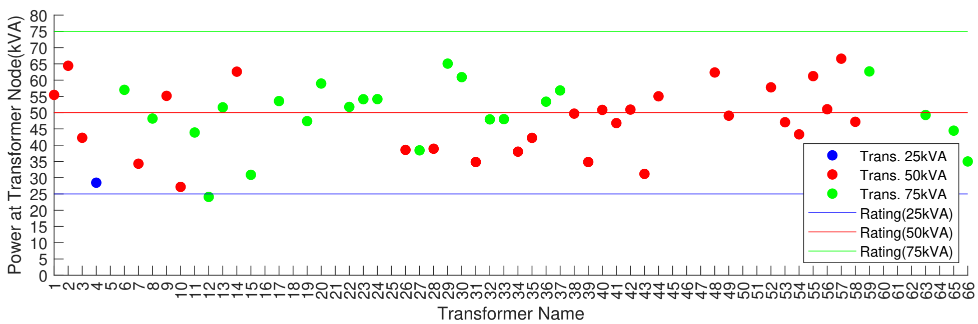

(c) 140% PV

Figure 5.18: Power at the distribution transformer nodes, Case 3.

Table 5.8 shows the transformers where thermal violations occur, the time of occurrence, and the percentage of violations.

Table 5.8: Percentage of transformer capacity violations, Case 3.

Transformer	Hour						
	9:00	**10:00**	**11:00**	**12:00**	**13:00**	**14:00**	**15:00**
T_1	0.00%	2.11%	15.70%	16.30%	15.49%	2.48%	0.00%
T_2	0.00%	22.99%	38.66%	38.83%	37.64%	20.94%	0.00%
T_4	0.00%	18.46%	34.82%	36.04%	35.19%	19.35%	0.00%
T_5	0.00%	10.98%	25.58%	26.22%	25.29%	11.06%	0.00%
T_9	0.00%	3.63%	18.26%	19.25%	18.41%	5.08%	0.00%
T_14	0.00%	15.24%	31.39%	33.00%	32.01%	17.12%	0.00%
T_38	0.00%	0.00%	3.36%	3.90%	3.11%	0.00%	0.00%
T_40	0.00%	0.00%	5.97%	6.36%	5.41%	0.00%	0.00%
T_42	0.00%	0.00%	5.28%	6.18%	5.51%	0.00%	0.00%
T_44	0.00%	1.33%	14.67%	15.39%	14.57%	1.55%	0.00%
T_48	0.00%	15.46%	30.83%	31.50%	30.55%	15.07%	0.00%
T_50	13.52%	67.80%	87.49%	88.53%	87.15%	65.46%	13.64%
T_51	15.08%	70.21%	90.33%	91.54%	90.17%	68.14%	15.57%
T_52	0.00%	6.39%	20.45%	21.07%	20.16%	5.83%	0.00%
T_55	0.00%	15.37%	30.58%	31.30%	30.32%	14.69%	0.00%
T_56	0.00%	0.00%	5.43%	6.26%	5.48%	0.00%	0.00%
T_57	0.00%	26.43%	43.00%	43.76%	42.60%	25.49%	0.00%

Figures 5.19 shows the result of the HC analysis for the Case 3. The green region represents the permitted PV penetration levels that do not cause violations. As we can see in the graph the maximum HC of PV systems allowed for the third case study is 80%. From this level of PV penetration, a blue region appears, indicating thermal violations. As can be seen, these violations can occur for PV penetration levels higher than 80%. Table 5.9 shows that for 90% PV penetration, a 10% violation of the allowed limit is observed. This percentage increases for higher penetration levels.

Table 5.9: HC Analysis Results, Case 3.

PV% level	Violations	
	Voltage	**Thermal**
<80	0.00	0.00
90	0.00	10.00
100	0.00	23.68
110	0.00	37.60
120	0.00	49.29
130	0.00	65.39
140	0.00	83.30
150	0.00	91.54

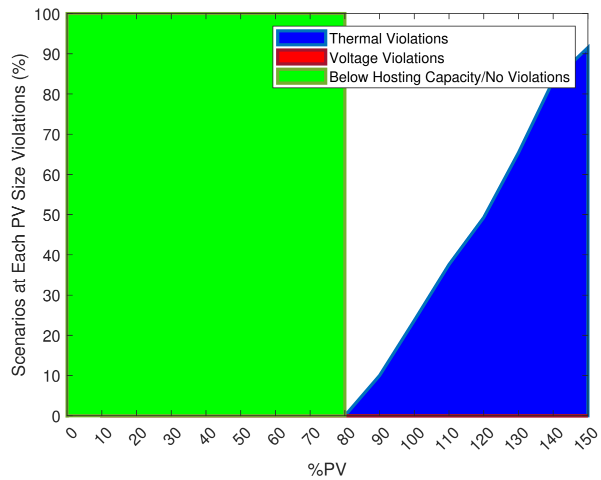

Figure 5.19: Results of HC analysis, Case 3.

Figure 5.20a shows the feeder node where thermal violations first occur for 120% PV penetration. Similarly, Figure 5.20b shows the nodes where these violations occur for 140% PV penetration.

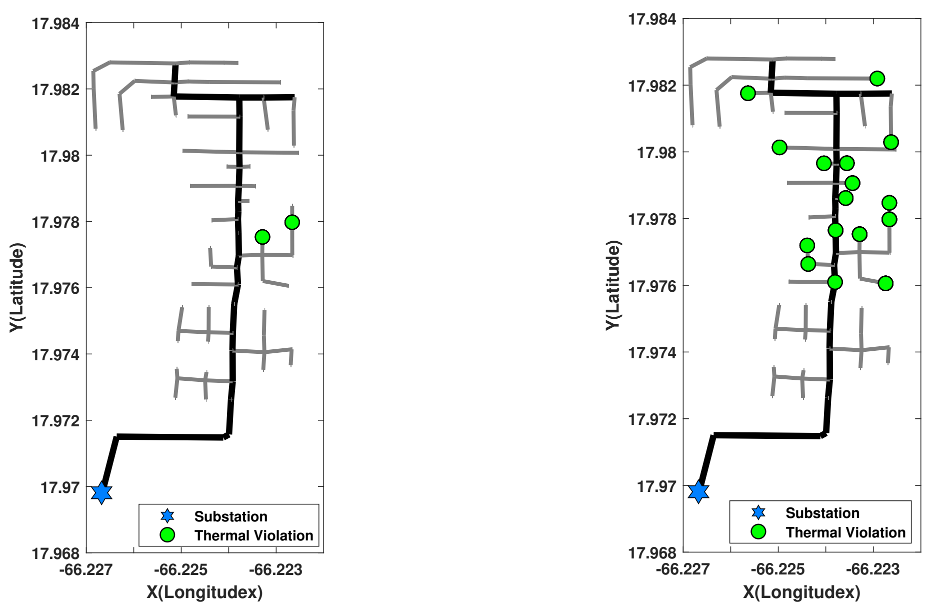

(a) 120% PV

(b) 140% PV

Figure 5.20: Network topology showing nodes where violations occur, Case 3.

5.5 Case 4: PV, Batteries and Smart Inverter

This case study links the photovoltaic battery systems and the Volt-VAR function of smart inverters. Additionally, this case is divided into two sub-cases. In the first sub-case, the battery charging and discharging algorithm are oriented to minimize the grid consumption of a household, while the second battery control algorithm is oriented to minimize reverse flows that cause voltage violations.

5.5.1 Case 4.1: Battery algorithm 1

This section presents the results of the HC analysis of the feeder in case 4.1. Different PV penetration scenarios were added to the feeder simulation to obtain these results. The PV systems will have smart inverters and RESS systems as described in Section 4.3.4.1. Table 5.10 summarizes the maximum PU voltage values found on the feeder at each hour of the day for each PV penetration level described in the table. As can be seen in this table, the highest voltage values occur between 13:00 and 14:00 hrs. These voltage values are below the maximum allowable limit of 1.05pu. Therefore, in this case, there are no voltage violations.

Table 5.10: Maximum PU voltage per hour of the day, Case 4.1.

PV Level	**Hora**											
	<6:00	**7:00**	**8:00**	**9:00**	**10:00**	**11:00**	**12:00**	**13:00**	**14:00**	**15:00**	**16:00**	**>17:00**
10% PV	1.000	1.000	1.000	1.000	1.000	1.000	1.000	1.000	1.000	1.000	1.000	1.000
20% PV	1.000	1.000	1.000	1.000	1.000	1.000	1.000	1.000	1.000	1.000	1.000	1.000
30% PV	1.000	1.000	1.000	1.000	1.000	1.000	1.000	1.000	1.000	1.000	1.000	1.000
40% PV	1.000	1.000	1.000	1.001	1.000	1.000	1.000	1.000	1.000	1.000	1.000	1.000
50% PV	1.000	1.001	1.003	1.005	1.000	1.000	1.000	1.000	1.000	1.000	1.000	1.000
60% PV	1.000	1.001	1.008	1.010	1.000	1.000	1.000	1.000	1.000	1.000	1.000	1.000
70% PV	1.000	1.005	1.012	1.014	1.002	1.000	1.000	1.000	1.000	1.003	1.000	1.000
80% PV	1.000	1.010	1.016	1.018	1.005	1.000	1.000	1.000	1.007	1.008	1.000	1.000
90% PV	1.000	1.014	1.019	1.021	1.006	1.000	1.000	1.000	1.012	1.011	1.000	1.000
100% PV	1.000	1.020	1.021	1.022	1.008	1.000	1.000	1.005	1.019	1.016	1.000	1.000
110% PV	1.000	1.022	1.022	1.023	1.009	1.000	1.000	1.004	1.023	1.019	1.000	1.000
120% PV	1.000	1.023	1.022	1.022	1.010	1.000	1.000	1.024	1.029	1.022	1.000	1.000
130% PV	1.000	1.023	1.023	1.024	1.011	1.000	1.000	1.031	1.030	1.023	1.000	1.000
140% PV	1.000	1.024	1.023	1.024	1.012	1.001	1.007	1.037	1.032	1.024	1.000	1.000
150% PV	1.000	1.025	1.024	1.024	1.014	1.012	1.014	1.040	1.033	1.025	1.000	1.000

Figure 5.21 shows voltage profiles at 13:00 hrs where the voltage level is higher, as seen in Table 5.10. These figures show how the voltage profile varies as the PV penetration level increases. For 20% and 100% PV penetration (Figure 5.21a and 5.21b, respectively), all phases operate within the allowed limits with values below unity. For 130% and 150% PV penetration (Figure 5.21c and 5.21d, respectively), the voltage levels increase above unity in all three phases.

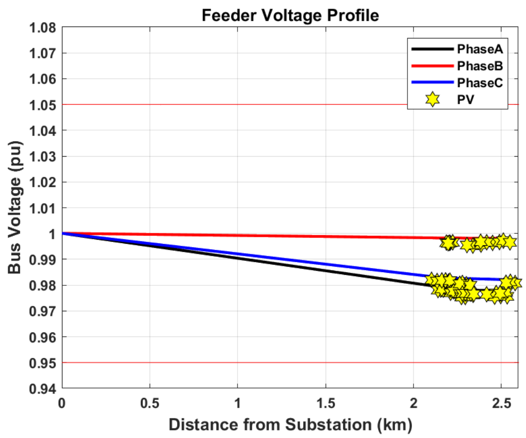

(a) 20% PV

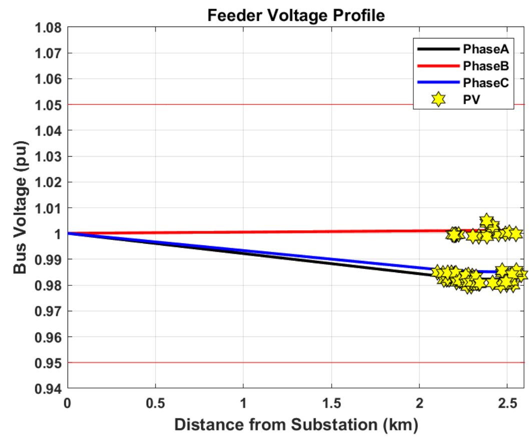

(b) 100% PV

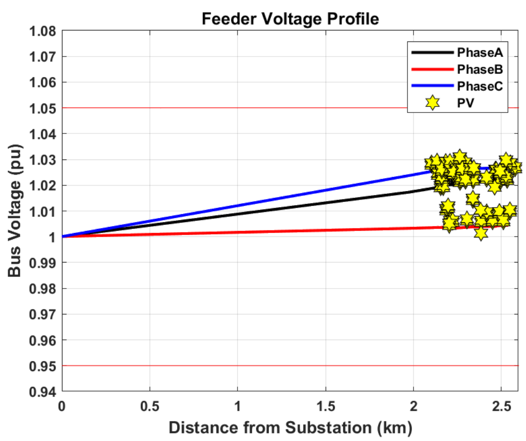

(c) 130% PV

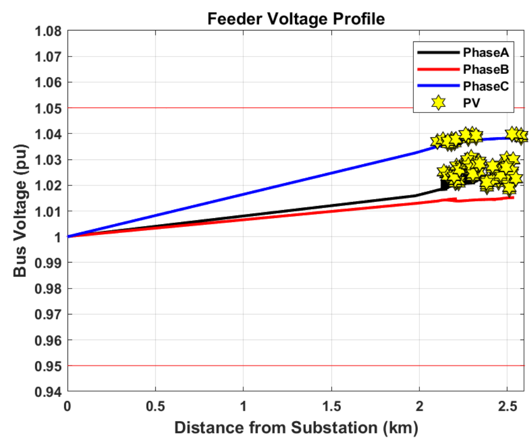

(d) 150% PV

Figure 5.21: Voltage Profile at 13:00 hrs, Case 4.1.

Figure 5.22 shows the current profile at 13:00 hrs for different PV penetration levels. In Figure 5.22a, the current flowing through the lines does not violate the conductor's capacity; the same occurs for 120% and 130% PV penetration (Figures 5.22b and 5.22d, respectively). For a PV penetration of 150%, the reverse current flowing through the phase A conductor violates the conductor rating near the substation.

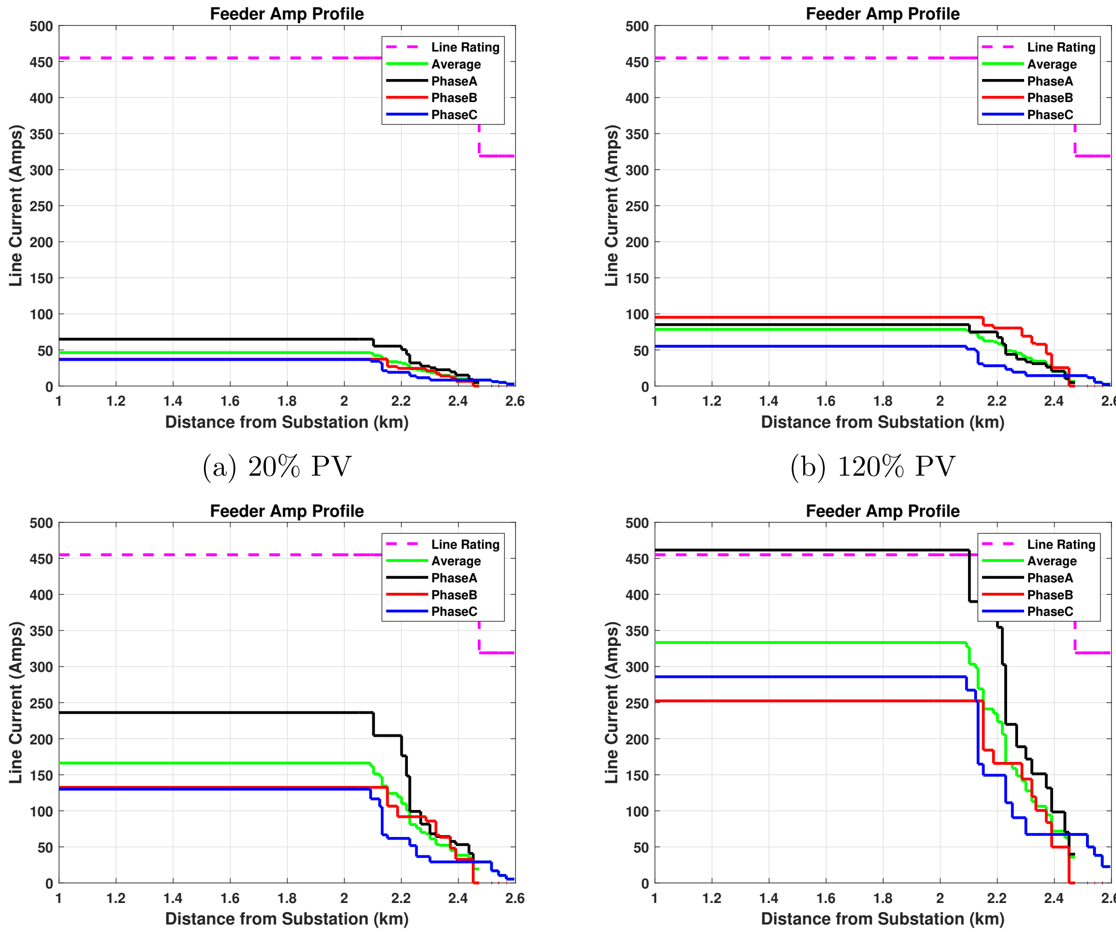

(a) 20% PV

(b) 120% PV

(c) 130% PV

(d) 150% PV

Figure 5.22: Current Profile,, Case 4.1.

Figure 5.23a shows the power at the nodes where the distribution transformers are located for a PV penetration percentage of 60%; additionally, it is observed that the power at the transformers does not violate their capacity. But this does not occur for a penetration percentage of 130%, as shown in Figure 5.23b. The power at the nodes of distribution transformer number 50 exceeds its capacity. From this percentage of PV penetration, the thermal violations in the transformers will continue, as seen in Figure 5.23c. For a penetration level of 150%, the number of transformers suffering thermal violations increases.

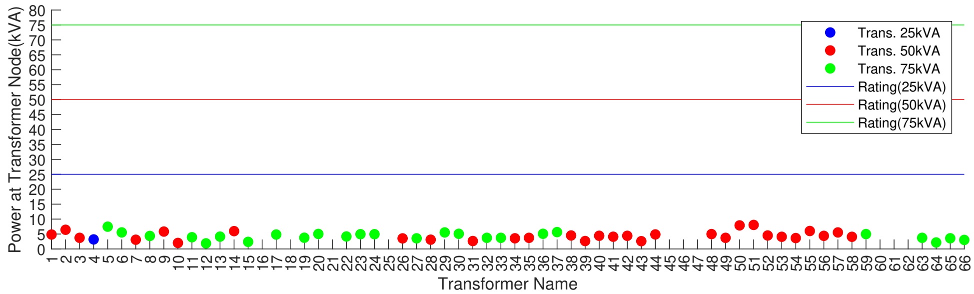

(a) 60% PV

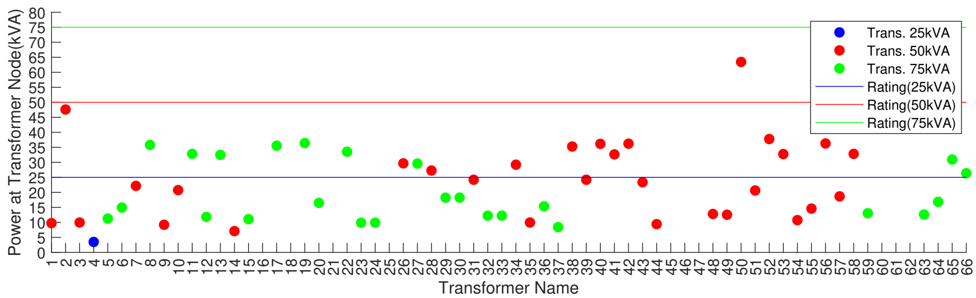

(b) 130% PV

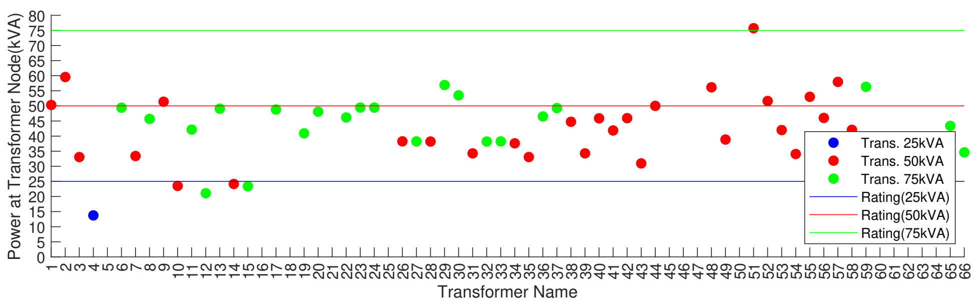

(c) 150% PV

Figure 5.23: Power at the distribution transformer nodes, Case 4.1.

Table 5.11 shows the transformers where thermal violations occur, the time of occurrence, and the percentage of violations.

Table 5.11: Percentage of transformer capacity violations, Case 4.1.

Transformer	Hour	
	13:00	**14:00**
T_1	0.60%	0.00%
T_2	19.12%	0.00%
T_5	8.89%	0.00%
T_9	2.77%	0.00%
T_44	0.01%	0.00%
T_48	12.32%	0.00%
T_50	62.80%	11.65%
T_51	51.45%	12.89%
T_52	3.24%	0.00%
T_55	6.02%	0.00%
T_57	15.90%	0.00%

Figures 5.24 shows the result of the HC analysis for case 4.1. The green region represents the allowed PV penetration levels that do not cause violations. As we can observe in the graph, the maximum HC of PV systems allowed for the Case 4.1 study is 120%. From this level of PV penetration, the blue region appears, indicating thermal violations. As can be seen, these violations can occur for PV penetration levels higher than 130%. Table 5.12 shows that for 130% PV penetration, a 26.91% violation of the allowed limit is observed. This percentage increases for higher penetration levels.

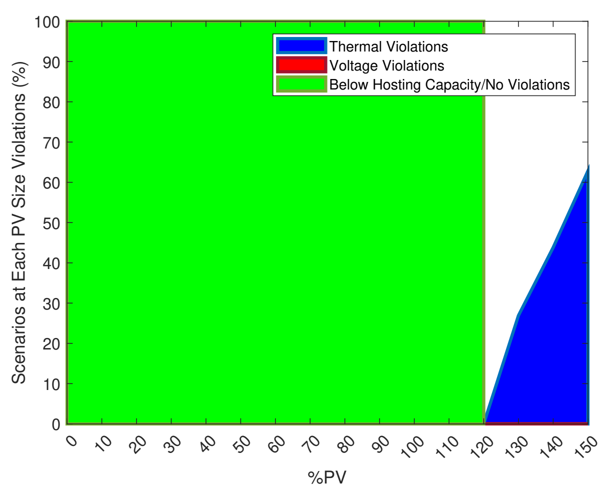

Figure 5.24: Results of HC analysis, Case 4.1.

Table 5.12: HC Analysis Results, Case 4.1.

PV% level	Violations	
	Voltage	Thermal
<120	0.00	0.00
130	0.00	26.91
140	0.00	43.82
150	0.00	62.80

Figure 5.25a shows the feeder node where thermal violations first occur for 130% PV penetration. Similarly, Figure 5.25b shows the nodes where these violations occur for 140% PV penetration.

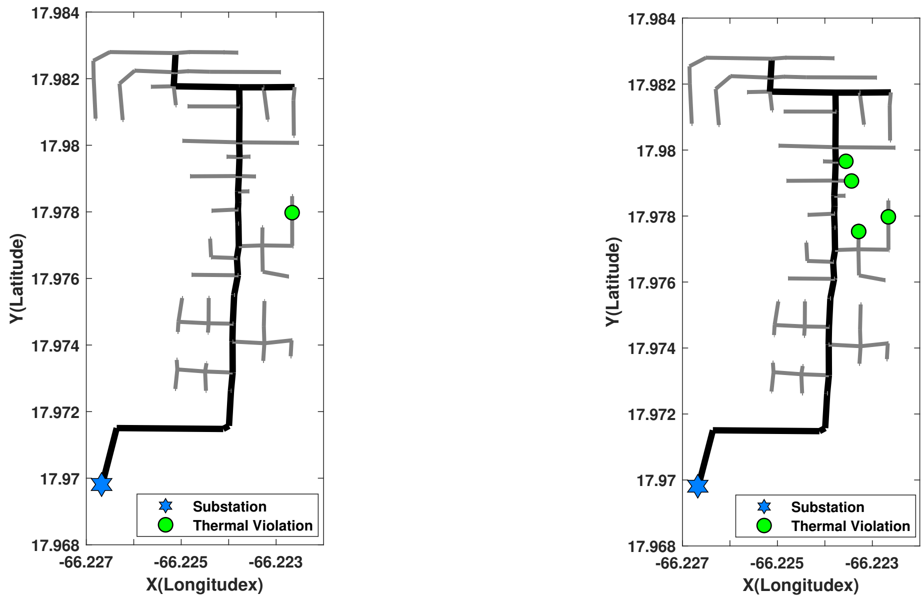

(a) 130% PV

(b) 140% PV

Figure 5.25: Network topology showing nodes where violations occur, Case 4.1.

5.5.2 Case 4.2: Battery algorithm 2

This section presents the results of the HC analysis of the feeder in case 4.2. Different PV penetration scenarios were added to the feeder simulation to obtain these results. The PV systems have smart inverters and ESS systems as described in Section 4.3.4.2. Table 5.13 summarizes the maximum PU voltage values found on the feeder at each hour of the day for each PV penetration level described in the table. As can be seen in this table, the highest voltage values occur between 09:00 to 14:00 hrs. These voltage values are below the maximum allowable limit of 1.05pu. Therefore, in this case, there are no voltage violations.

Table 5.13: Maximum PU voltage per hour of the day, Case 4.2.

PV Level	**Hora**											
	<6:00	**7:00**	**8:00**	**9:00**	**10:00**	**11:00**	**12:00**	**13:00**	**14:00**	**15:00**	**16:00**	**>17:00**
10% PV	1.000	1.000	1.000	1.000	1.000	1.000	1.000	1.000	1.000	1.000	1.000	1.000
20% PV	1.000	1.000	1.000	1.000	1.001	1.002	1.000	1.000	1.000	1.000	1.000	1.000
30% PV	1.000	1.000	1.000	1.009	1.011	1.007	1.000	1.000	1.000	1.000	1.000	1.000
40% PV	1.000	1.000	1.005	1.019	1.010	1.023	1.000	1.000	1.000	1.000	1.001	1.000
50% PV	1.000	1.001	1.011	1.022	1.022	1.024	1.000	1.000	1.000	1.000	1.000	1.000
60% PV	1.000	1.001	1.019	1.022	1.026	1.025	1.000	1.000	1.000	1.000	1.000	1.000
70% PV	1.000	1.005	1.022	1.024	1.024	1.033	1.000	1.000	1.000	1.000	1.000	1.000
80% PV	1.000	1.010	1.023	1.026	1.025	1.031	1.000	1.000	1.000	1.000	1.000	1.000
90% PV	1.000	1.014	1.024	1.028	1.026	1.034	1.000	1.000	1.000	1.000	1.000	1.000
100% PV	1.000	1.020	1.025	1.028	1.027	1.035	1.000	1.000	1.005	1.001	1.000	1.000
110% PV	1.000	1.022	1.025	1.029	1.028	1.031	1.000	1.000	1.000	1.009	1.000	1.000
120% PV	1.000	1.023	1.026	1.030	1.028	1.029	1.000	1.001	1.021	1.019	1.000	1.000
130% PV	1.000	1.023	1.027	1.030	1.028	1.031	1.000	1.023	1.024	1.022	1.000	1.000
140% PV	1.000	1.024	1.028	1.030	1.032	1.028	1.005	1.030	1.028	1.024	1.000	1.000
150% PV	1.000	1.025	1.028	1.032	1.030	1.031	1.013	1.035	1.030	1.024	1.000	1.000

Figure 5.26 shows voltage profiles at 13:00 hrs where the voltage level is higher, as seen in Table 5.13. In these figures, we can observe how the voltage profile varies as the PV penetration level increases. For 20% and 100% PV penetration (Figures 5.26a and 5.26b, respectively) all phases are within the allowed limits with values below unity. For 130% and 150% PV penetration (Figures 5.26c and 5.26d, respectively) the voltage levels in phases A and B increase above unity in both phases.

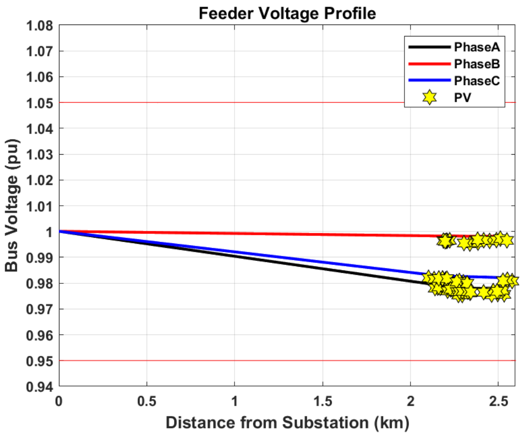

(a) 20% PV

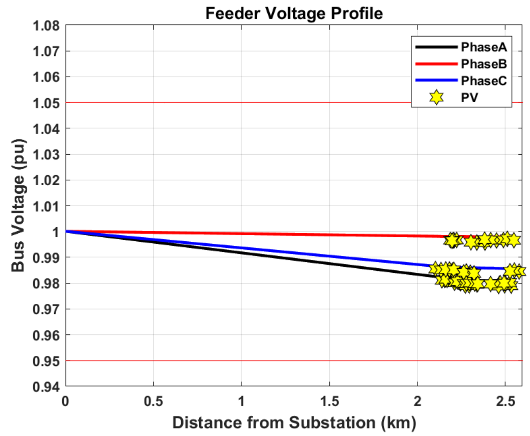

(b) 100% PV

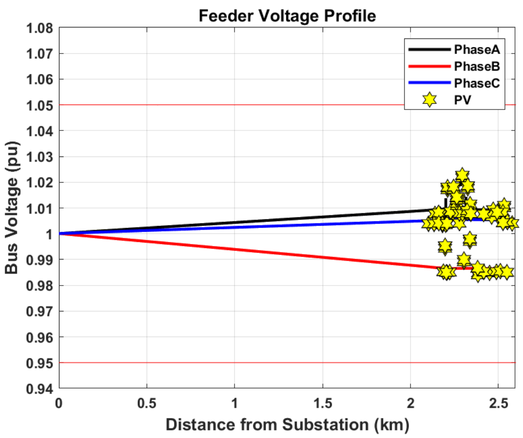

(c) 130% PV

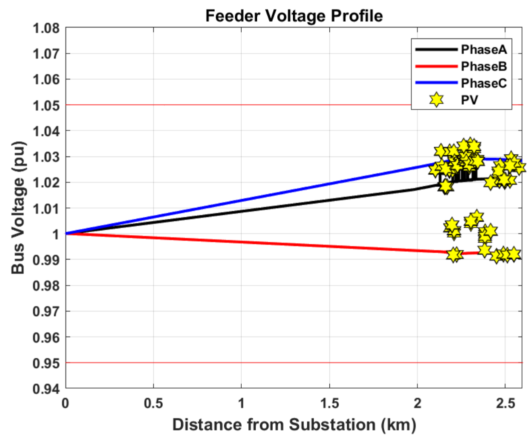

(d) 150% PV

Figure 5.26: Voltage Profile at 13:00 hrs, Case 4.2.

Figure 5.27 shows the feeder current profile at 13:00 hrs, for different PV penetration levels. Figure 5.27a shows that the current flowing through the lines does not violate the conductor's capacity, as it occurs for 120% and 130% PV penetration (Figures 5.27b and 5.27c, respectively). For a PV penetration of 150%(Figure 5.27d), the reverse current flowing through the phase A conductor increases abruptly but does not exceed the conductor rating.

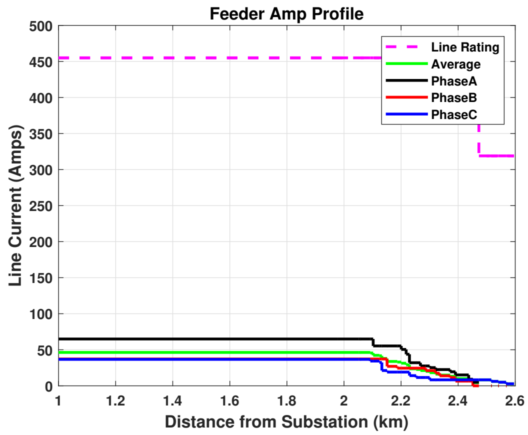

(a) 20% PV

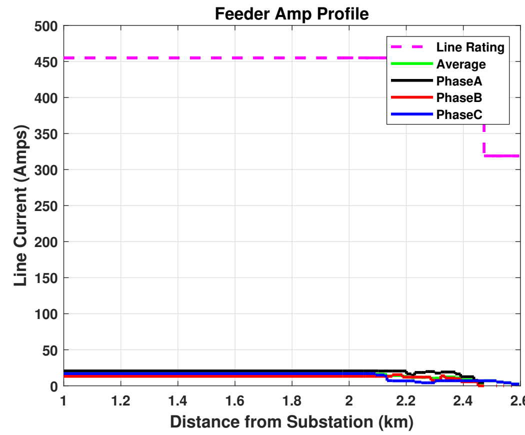

(b) 120% PV

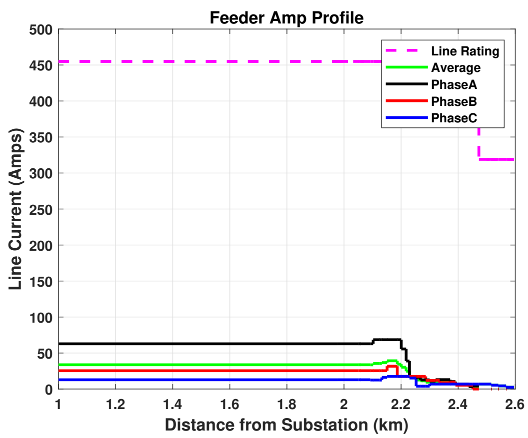

(c) 130% PV

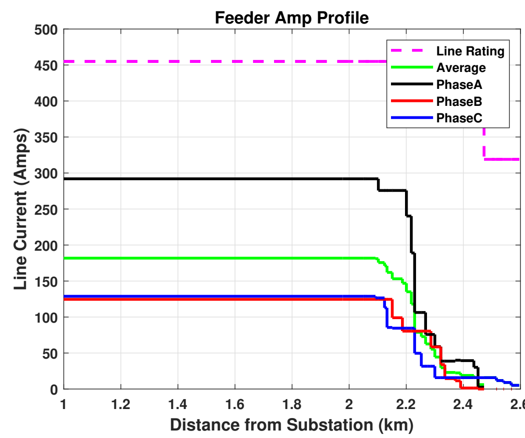

(d) 150% PV

Figure 5.27: Current Profile, Case 4.2.

Figure 5.28a shows the power at the nodes where the distribution transformers are located for a PV penetration percentage of 60%; additionally, it is observed that the power at the transformers does not violate their capacity. But this does not occur for a penetration percentage of 130%, as shown in Figure 5.28b. The power at the nodes of distribution transformer number 50 exceeds its capacity. From this percentage of PV penetration, the thermal violations in the transformers will continue, as seen in Figure 5.28c. For a penetration level of 150%, the number of transformers suffering thermal violations increases.

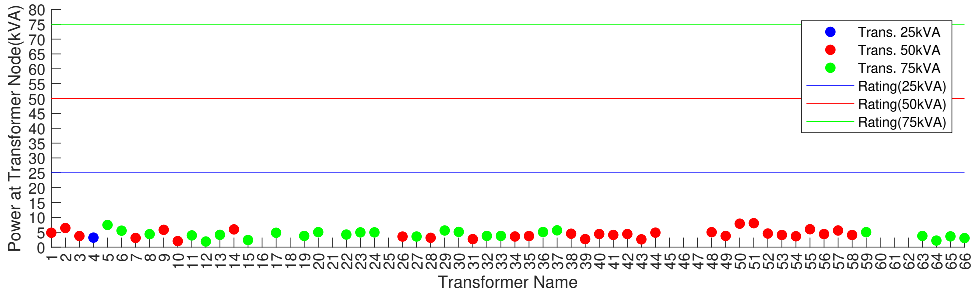

(a) 60% PV

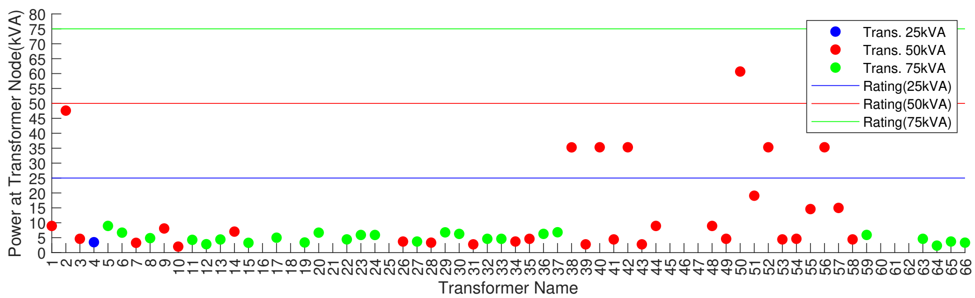

(b) 130% PV

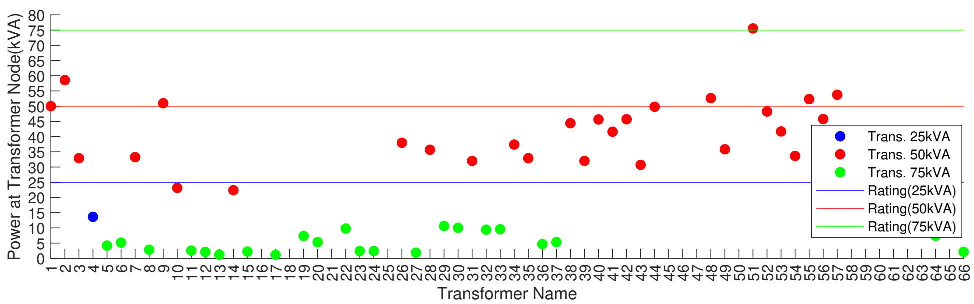

(c) 150% PV

Figure 5.28: Power at the distribution transformer nodes, Case 4.2.

Table 5.14 shows the transformers where thermal violations occur, the time of occurrence, and the percentage of violations.

Table 5.14: Percentage of transformer capacity violations, Case 4.2.

Transformer	**Hour**	
	13:00	**14:00**
T_1	0.01%	0.00%
T_2	17.14%	0.00%
T_9	1.95%	0.00%
T_48	5.27%	0.00%
T_50	62.67%	12.37%
T_51	51.09%	14.35%
T_55	4.64%	0.00%
T_57	7.52%	0.00%

Figure 5.29 shows the result of the HC analysis for case 4.2. The green region represents the allowed PV penetration levels that do not cause violations. As seen in the graph, the maximum HC of PV systems allowed for this case study is 120%. From this level of PV penetration, a blue region appears, indicating thermal violations. As can be seen, these violations can occur for PV penetration levels higher than 130%. Table 5.15 shows that for 130% PV penetration, a 20.68% violation of the allowed limit is obtained. This percentage increases for higher penetration levels.

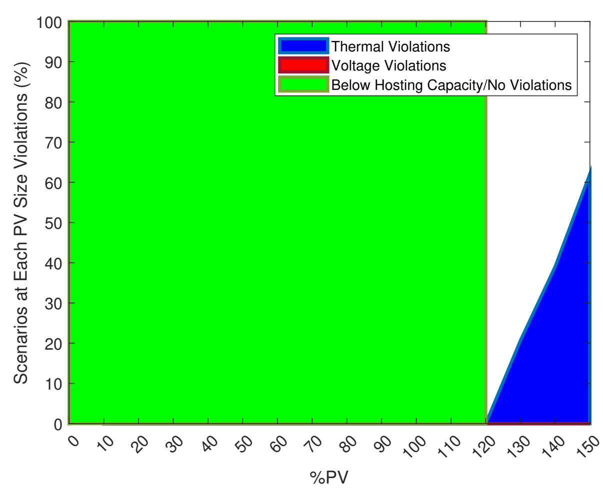

Figure 5.29: Results of HC analysis, Case 4.2.

Table 5.15: HC Analysis Results, Case 4.2.

PV% level	**Violations**	
	Voltage	**Thermal**
<120	0.00	0.00
130	0.00	20.68
140	0.00	39.05
150	0.00	62.11

Figure 5.30a shows the feeder node where thermal violations first occur for 130% PV penetration. Similarly, Figure 5.30b shows the nodes where these violations occur for 140% PV penetration.

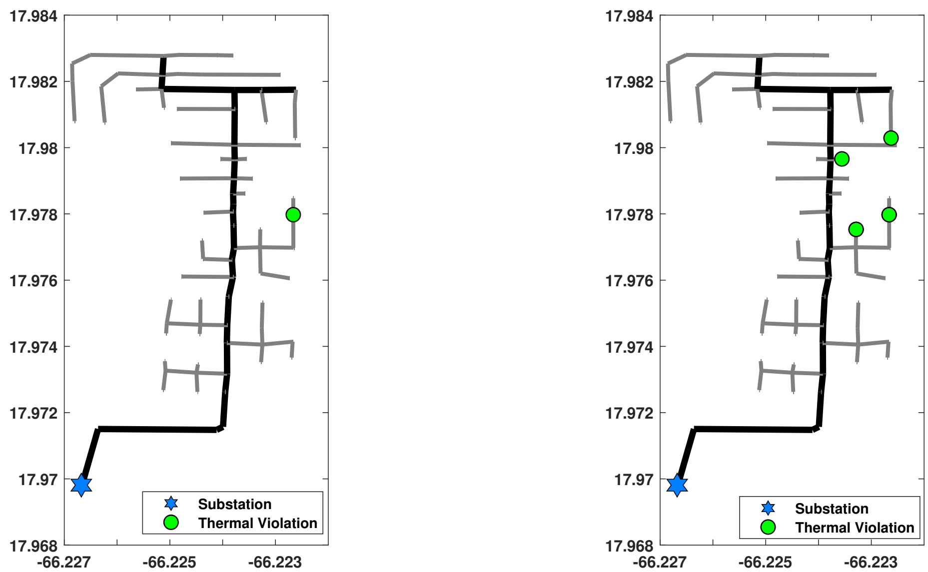

(a) 130% PV

(b) 140% PV

Figure 5.30: Network topology showing nodes where violations occur, Case 4.2.

Chapter 6

Conclusions

6.1 Conclusions

Energy demand is increasing worldwide, leading to the search for more efficient electricity generation. Distributed generation with photovoltaic systems makes efficient use of the solar resource and offer greater security in the event of electrical system failure. But a high penetration of distributed photovoltaic systems can cause several problems in power quality. This thesis aims to examine the factors that limit the HC of distributed photovoltaic systems in a typical urban feeder model distribution systems under different levels of PV penetration and propose methods to increase the HC of the feeder.

In this research, the behavior of a feeder was analyzed temporally against different PV penetration scenarios and methodologies to increase the HC. The analysis period was performed for 24 hours a day with one-hour steps. Hence, the simulation is of a quasi-static type. The penetration levels of photovoltaic systems q selected to supply a percentage of the feeder load. These penetration levels range from 10% to 150% (at 10% steps).

In the first part of the research, phase A accounted for much of the feeder load, followed by phase B, and phase C. It was also found that some areas of the feeder that are part of phase A experienced low voltage problems during peak demand hours. From this simulation, four case studies were established.

Case one analyzed the maximum HC of the PV system feeder. It was found that the feeder supported up to 60% PV penetration. When reaching a PV penetration level of 70%, there were no overvoltages in the substation, but there were overvoltages in some feeder nodes. Also, as the penetration percentage continued to increase, the number of nodes where voltage violations occurred also increased. In this case, thermal violations appeared for the first time for 90% PV penetration.

In case two, residential energy storage systems were proposed as a method to increase the HC of distributed PV systems. In this case, it was possible to increase the maximum HC up to 110% PV penetration. From this penetration level, voltage violations occurred. For 130% PV penetration, thermal violations occured in different distribution transformers. The charging and discharging algorithm of the RESS in this case was designed to minimize the energy consumption of the household grid. The RESSs reduced the feeder load at peak hours and voltage drops due to the overloading of the phases, as was the case with phase A.

In case three, the use of the Volt-VAR function of smart inverters was proposed as a method to increase the HC of feeder PV systems. Using this method, it was possible to increase the HC up to 80% of PV penetration. Smart inverters prevented voltage violations from occurring on the feeder by ensuring reactive compensation. But this did not happen with thermal violations that started occurring at a penetration level of 90%, as thermal violations are related to reversed power flow.

In case four, the use of RESS and the Volt-VAR function of smart inverters was proposed to increase the HC of PV systems on the feeder. This case was divided into two subcases, differentiated by the battery charging and discharging algorithm.

For the first sub-case, the battery charging and discharging algorithm was equal to case three. Using this method, it was possible to increase the HC up to 120% of PV penetration. In this case, no voltage violations occurred since the Volt-VAR function of the inverter was used. But there were still thermal violations from 130% PV penetration. In the second sub-case, the battery charging and discharging algorithm was designed to reduce the reversed power flow. The same maximum HC as the first sub-case was obtained, except that the violation percentages occurring, in this case, were lower than in sub-case one.

Additionally, it was observed during the simulations of the four cases, that the transformers where the thermal violations occurred were the same in each case. Transformers number 50 and 51, where thermal violations always occurred, had the highest feeder loads, predisposing them to suffer thermal violations. The identification of the transformers where thermal violations occur frequently is important because as a solution to increase the HC, the capacity of these transformers could be increased.

From the above, case four proved to be the best method to increase the HC of distributed PV systems of the feeder under study. Smart inverters prevented voltage violations from occurring during maximum PV generation through reactive compensation. Battery charging during maximum PV generation reduced reverse flows, and therefore, reduced thermal violations. Additionally, RESSs during peak hours reduced the load on the feeder, improving grid stability by reducing voltage sags.

6.2 Future Work

This work paves the way for further analysis and comparison of methods to help increase the HC of feeders. The following topics could be considered extensions of this research:

- Include limiting factors, such as harmonics and protection in the HC analysis, and evaluate how these affect the increased penetration of distributed PV systems.
- Replicate the OpenDSS and MATLAB analysis and programming to determine the HC of other feeders and compare the results.
- Utilize more features of smart inverters and evaluate the impact on increasing the HC of PV systems.
- Include the study of centralized battery banks to increase the HC.
- Evaluate the reliability of the system by integrating batteries and smart inverters to maximize the HC.
- Conduct a study of the optimal location of PV systems to maximize PV system penetration.

References

[1] V. Silva and C. Daniel, *"Determinación de la capacidad máxima permitida de generación solar fotovoltaica en redes de distribución"*. PhD thesis, Escuela Colombiana de Ingeniería Julio Garavito, 2020.

[2] C. Edvard, "The structure of electric power systems (generation, distribution and transmission of energy)." https://electrical-engineering-portal.com/electricpower-systems. (accessed: 09.16.2022).

[3] A. Sallam and O. Malik, *Electric distribution systems*. John Wiley & Sons, 2018.

[4] M. NAVFAC, "Electric power distribution systems operations," 1990.

[5] L. Rogers, J. Smith, and M. Rylander, "Distribution feeder hosting capacity: What matters when planning for der?," *Electri Power Research Institute*, vol. 3002004777, 2015.

[6] ANSI, "Standard c84.1-2011 american national standard for electric power systems and equipment - voltage ratings (60 hz)," tech. rep., ANSI, 2011.

[7] M. J. Reno, K. Coogan, J. Seuss, and R. J. Broderick, "Novel methods to determine feeder locational pv hosting capacity and pv impact signatures," tech. rep., Sandia National Lab.(SNL-NM), Albuquerque, NM (United States), 2017.

[8] M. Zain ul Abideen, O. Ellabban, and L. Al-Fagih, "A review of the tools and methods for distribution networks' hosting capacity calculation," *Energies*, vol. 13, no. 11, p. 2758, 2020.

[9] S. Stanfield, S. Safdi, and S. Mihaly, "Hosting capacity analyses for distributed energy resources," *IREC publications*, p. 63, 2017.

[10] M. Bartecka, G. Barchi, and J. Paska, "Time-series pv hosting capacity assessment with storage deployment," *Energies*, vol. 13, no. 10, p. 2524, 2020.

[11] A. Maitra, M. Rylander, and R. Dungan, "Analysis of distribution system effects of energy storage through simulation and modeling," *Electri Power Research Institute*, vol. 1024285, 2012.

[12] G. Effect, E. Storage, and T. Simulation, "Understanding energy storage solutions and capabilities on utility distribution systems," *Electri Power Research Institute*, vol. 1021938, 2011.

[13] H. E. O. Farias and L. N. Canha, "Battery energy storage systems (bess) overview of key market technologies," in *2018 IEEE PES Transmission & Distribution Conference and Exhibition-Latin America (T&D-LA)*, pp. 1–5, IEEE, 2018.

[14] A. Haque and M. A. Rahman, "Study of a solar pv-powered mini-grid pumped hydroelectric storage & its comparison with battery storage," in *2012 7th International Conference on Electrical and Computer Engineering*, pp. 626–629, IEEE, 2012.

[15] C. Yang, *Storing Energy.* International series of monographs on physics, Elsevier, 2016.

[16] K. T. Lulbadda and K. U. Hemapala, "Novel concepts for additional functions of smart pv inverters," in *2020 IEEE International Conference on Computing, Power and Communication Technologies (GUCON)*, pp. 740–744, IEEE, 2020.

[17] K. T. Lulbadda and K. Hemapala, "The additional functions of smart inverters," *Aims Energy*, vol. 7, no. 6, pp. 971–988, 2019.

[18] R. D. A. Maitra, M. Rylander, "Common functions for smart inverters," *Electri Power Research Institute*, vol. 1023059, 2011.

[19] J. Peppanen, M. Bello, and M. Rylander, "Service entrance hosting capacity," in *2018 IEEE 7th World Conference on Photovoltaic Energy Conversion (WCPEC)(A Joint Conference of 45th IEEE PVSC, 28th PVSEC & 34th EU PVSEC)*, pp. 1451–1456, IEEE, 2018.

[20] V. Quintero-Molina, M. Romero-L, and A. Pavas, "Assessment of the hosting capacity in distribution networks with different dg location," in *2017 IEEE Manchester PowerTech*, pp. 1–6, IEEE, 2017.

[21] B. B. Navarro and M. M. Navarro, "A comprehensive solar pv hosting capacity in mv and lv radial distribution networks," in *2017 IEEE PES Innovative Smart Grid Technologies Conference Europe (ISGT-Europe)*, pp. 1–6, IEEE, 2017.

[22] P. H. Divshali and L. Söder, "Improvement of res hosting capacity using a central energy storage system," in *2017 IEEE PES Innovative Smart Grid Technologies Conference Europe (ISGT-Europe)*, pp. 1–6, IEEE, 2017.

[23] S. Hashemi and J. Østergaard, "Efficient control of energy storage for increasing the pv hosting capacity of lv grids," *IEEE Transactions on Smart Grid*, vol. 9, no. 3, pp. 2295–2303, 2016.

[24] J. Seuss, M. J. Reno, R. J. Broderick, and S. Grijalva, "Improving distribution network pv hosting capacity via smart inverter reactive power support," in *2015 IEEE Power & Energy Society General Meeting*, pp. 1–5, IEEE, 2015.

[25] K. Rahimi, H. Chun, R. Moghe, D. Tholomier, F. Wong, A. Hirayama, and M. Asano, "Impact of advanced vol-v ar control devices on increasing pv hosting capacity of distribution systems," in *2020 IEEE/PES Transmission and Distribution Conference and Exposition (T&D)*, pp. 1–5, IEEE, 2020.

[26] E. O'Neill-Carrillo, I. Jordan, A. Irizarry-Rivera, and R. Cintron, "The long road to community microgrids: Adapting to the necessary changes for renewable energy implementation," *IEEE Electrification magazine*, vol. 6, no. 4, pp. 6–17, 2018.

[27] G. A. Carrión Hernández, R. A. Cintrón Cuevas, M. A. Rodríguez Pérez, and W. E. Sanabria Octaviani, *Final Progress Report INEL 5195-Capstone "Community Microgrid"*. PhD thesis, UPRM, 31 May 2018.

[28] A. J. Burgos Cintrón, M. A. Rosario Angleró, and P. E. A. Cruz Cabrera, *Final Progress Report INEL 5195-Capstone "El Coquí"*. PhD thesis, UPRM, 14 May 2018.

[29] G. Carrión, R. Cintrón, M. Rodríguez, W. Sanabria, R. Reyes, and E. O'Neill-Carrillo, "Community microgrids to increase local resiliency," in *2018 IEEE International Symposium on Technology and Society (ISTAS)*, pp. 1–7, IEEE, 2018.

[30] OpenDSSWiki, "Technote modeling single phase, center tapped distribution transformers," *EPRI, OpenDSS*, 30 Jan 2015.

[31] AEE, "Patrones de construcción de distribución aérea." https://aeepr.com/es-pr/Site-Servicios/Manuales. (accessed: 09.12.2022).

[32] AEE, "Comunicados y circulares tecnicas 2012." https://aeepr.com/es-pr/Site-Servicios/ComunicadosTecnicos/Comunicados %20Tecnicos%202012%20.pdf. (accessed: 09.12.2022).

[33] AEE, "Comunicados y circulares tecnicas 1980 - 1999." https://aeepr.com/es-pr/Site-Servicios/ComunicadosTecnicos/Comunicados%20Tecnicos%201980-1999.pdf. (accessed: 09.12.2022).

[34] E. P. R. Institute, "Opendss pvsystem element model," *EPRI, OpenDSS*, 2011.

[35] K. A. Horowitz, F. Ding, B. A. Mather, and B. S. Palmintier, "The cost of distribution system upgrades to accommodate increasing penetrations of distributed photovoltaic systems on real feeders in the united states," tech. rep., National Renewable Energy Lab.(NREL), Golden, CO (United States), 2018.

[36] S. B. Gahl D. and U. R., "Hosting capacity: using increased transparency of grid constraints to accelerate interconnectio processes.," tech. rep., Solar Energy Industries Association, Washington, NW (United States), 2017.

[37] J. Smith, "Distributed photovoltaic feeder analysis preliminary findings from hosting capacity analysis of 18 distribution feeders," *EPRI, OpenDSS*, 12 2013.

[38] F. Ding, A. Nagarajan, S. Chakraborty, M. Baggu, A. Nguyen, S. Walinga, M. McCarty, and F. Bell, "Photovoltaic impact assessment of smart inverter volt-var control on distribution system conservation voltage reduction and power quality," tech. rep., National Renewable Energy Lab.(NREL), Golden, CO (United States), 2016.

[39] D. G. Photovoltaics and E. Storage, "Ieee standard for interconnection and interoperability of distributed energy resources with associated electric power systems interfaces," *IEEE Std*, pp. 1547–2018, 2018.

[40] M. Rylander, H. Li, J. Smith, and W. Sunderman, "Default volt-var inverter settings to improve distribution system performance," in *2016 IEEE Power and Energy Society General Meeting (PESGM)*, pp. 1–5, IEEE, 2016.

[41] P. Radatz(EPRI), "Opendss training workshop - 2021." https://sourceforge.net/p/electricdss/code/HEAD/tree/trunk/Training/Virtual-2021/Session3/PVSystem_InvControl/OpenDSS_day3_PauloRadatz.pdf. (accessed: 10.01.2022).

[42] R. C. Dugan and D. Montenegro, "Reference guide: The open distribution system simulator," in *EPRI*, 2013.

[43] C. Rocha, J. Peppanen, P. Radatz, M. Rylander, and D. R, "Storage element," *EPRI, OpenDSS*, 2020.

[44] C. Rocha, J. Peppanen, P. Radatz, M. Rylander, and D. R, "Storage controller element," *EPRI, OpenDSS*, 2020.

[45] E. P. R. Institute, "Storage model dynamics dll," *EPRI, OpenDSS*, 2020.

[46] J. Smith, "Modeling high-penetration pv for distribution interconnection studies," *Electric Power Research Institute, Tech. Rep*, 2013.

[47] P. Radatz, C. Rocha, W. Sunderman, M. Rylander, and J. Peppanen, "Opendss pvsystem and invcontrol element models," *EPRI, OpenDSS*, 2020.

[48] C. Rocha, J. Peppanen, P. Radatz, M. Rylander, and D. R, "Inverter modelling," *EPRI, OpenDSS*, 2020.

Appendix A: Feeder Data

This section shows more detailed data of the feeder.

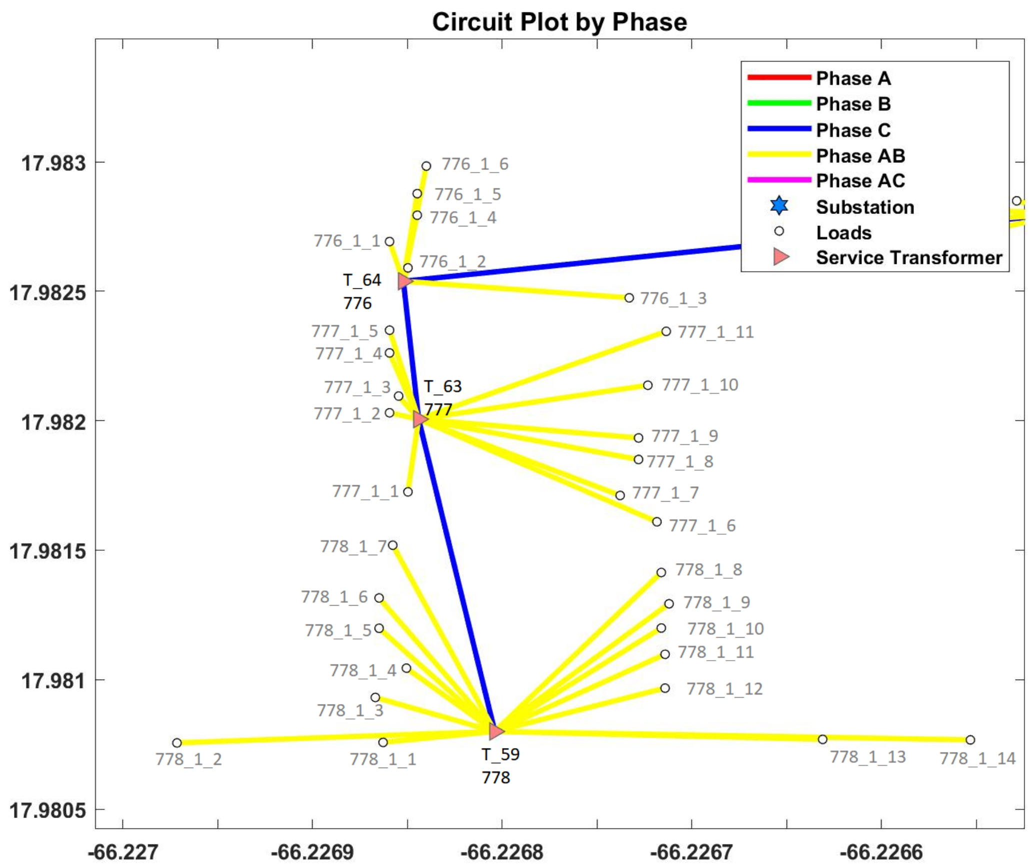

Figure 6.1: Arrangement of the loads in the feeder.

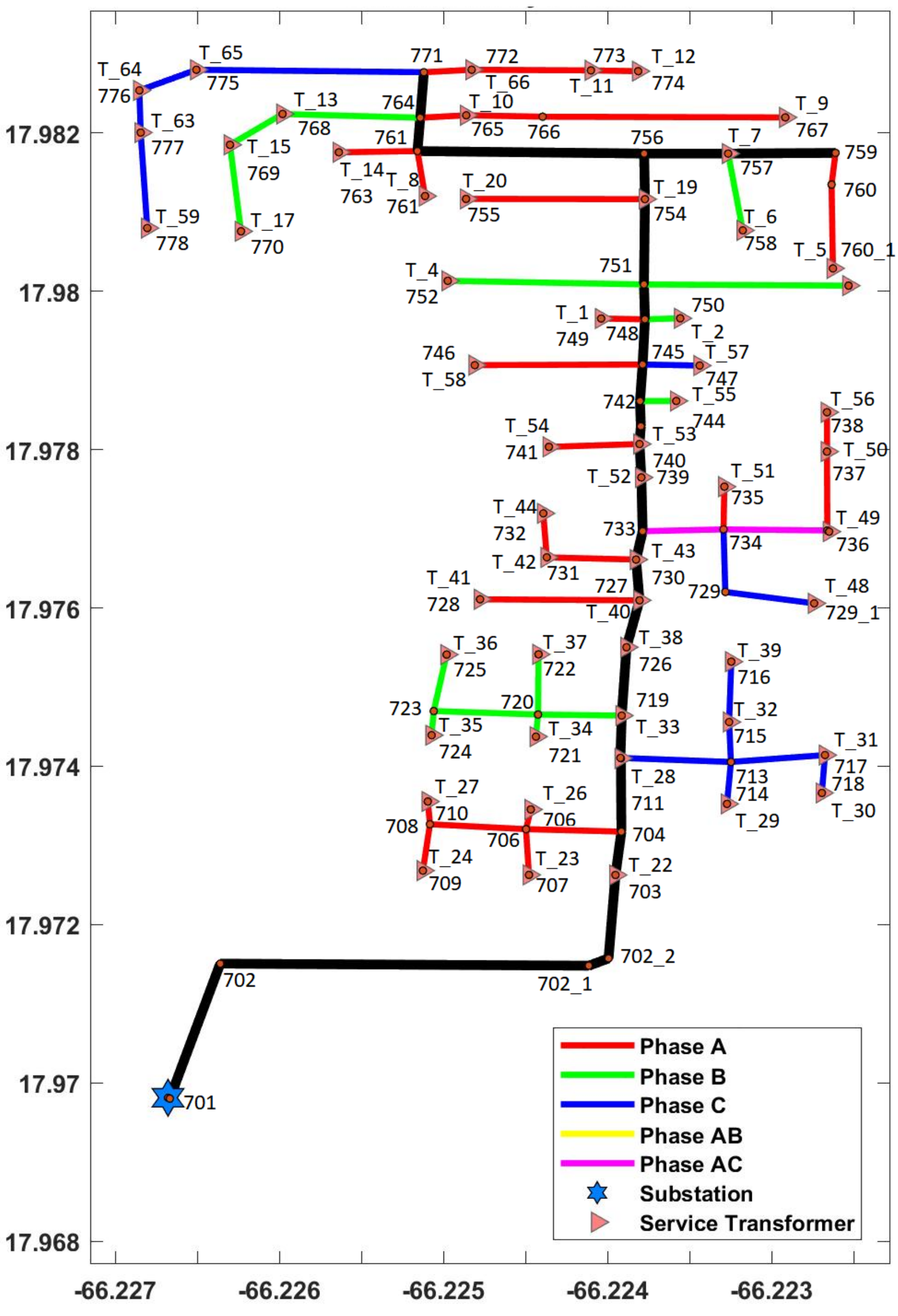

Figure 6.2: Location of transformers and nodes on feeder.

Table 6.1: Classification of households by type of demand profile at each distribution transformer

Node	Trans.	Rating (kVA)	P1 33kW	P2 22kW	P3 15kW	P4 10kW	P5 5.75kW	Number of HH	Demand Total (kWh)	Demand Total (kVA)
749	T_1	50	1	4	5	1	3	14	223.3	9.30
750	T_2	50	1	6	5	3	1	16	275.8	11.49
753	T_3	50	1	3	3	1	3	11	171.3	7.14
752	T_4	25	0	2	3	2	3	10	126.3	5.26
760_1	T_5	75	2	7	6	2	5	22	358.8	14.95
758	T_6	75	1	5	4	2	4	16	246.0	10.25
757	T_7	50	1	3	2	1	1	8	144.8	6.03
761	T_8	75	1	5	3	1	2	12	209.5	8.73
767	T_9	50	0	4	7	2	4	17	236.0	9.83
765	T_10	50	1	2	2	0	0	5	107.0	4.46
773	T_11	75	1	4	3	1	2	11	187.5	7.81
774	T_12	75	1	1	1	1	3	7	97.3	4.05
768	T_13	75	3	3	2	1	4	13	228.0	9.50
762	T_14	50	0	5	6	1	8	20	256.0	10.67
769	T_15	75	1	2	1	1	3	8	119.3	4.97
770	T_17	75	2	3	4	2	3	14	229.3	9.55
754	T_19	75	2	4	2	1	0	9	194.0	8.08
755	T_20	75	2	4	4	1	5	16	252.8	10.53
703	T_22	75	1	4	3	1	3	12	193.3	8.05
707	T_23	75	1	4	5	1	3	14	223.3	9.30
709	T_24	75	1	4	5	1	3	14	223.3	9.30
706	T_26	50	1	3	3	1	2	10	165.5	6.90
710	T_27	75	1	3	3	1	2	10	165.5	6.90
711	T_28	50	1	3	2	1	2	9	150.5	6.27
714	T_29	75	1	5	4	2	4	16	246.0	10.25
718	T_30	75	1	4	4	2	4	15	224.0	9.33
717	T_31	50	1	2	2	1	2	8	128.5	5.35
715	T_32	75	1	3	3	1	3	11	171.3	7.14
719	T_33	75	1	3	3	1	3	11	171.3	7.14
721	T_34	50	1	3	3	1	2	10	165.5	6.90
724	T_35	50	1	3	3	1	3	11	171.3	7.14
725	T_36	75	1	4	4	2	4	15	224.0	9.33
722	T_37	75	1	5	4	2	4	16	246.0	10.25
726	T_38	50	1	4	4	1	3	13	208.3	8.68
716	T_39	50	1	2	2	1	2	8	128.5	5.35
727	T_40	50	1	4	4	1	3	13	208.3	8.68
728	T_41	50	1	4	3	1	3	12	193.3	8.05
731	T_42	50	1	4	4	1	3	13	208.3	8.68
730	T_43	50	1	2	2	1	2	8	128.5	5.35
732	T_44	50	1	4	5	1	3	14	223.3	9.30

Node	Trans.	Rating (kVA)	P1 33kW	P2 22kW	P3 15kW	P4 10kW	P5 5.75kW	Number of HH	Demand Total (kWh)	Total (kVA)
729_1	T_48	50	1	4	5	1	3	14	223.3	9.30
736	T_49	50	1	3	3	1	3	11	171.3	7.14
737	T_50	50	2	7	7	2	5	23	373.8	15.57
735	T_51	50	2	7	7	2	6	24	379.5	15.81
739	T_52	50	1	4	4	1	3	13	208.3	8.68
740	T_53	50	1	4	3	1	3	12	193.3	8.05
741	T_54	50	1	3	3	1	3	11	171.3	7.14
744	T_55	50	1	5	5	2	4	17	261.0	10.88
738	T_56	50	1	4	4	1	3	13	208.3	8.68
747	T_57	50	1	5	4	2	4	16	246.0	10.25
746	T_58	50	1	4	3	1	3	12	193.3	8.05
778	T_59	75	1	4	5	1	3	14	223.3	9.30
777	T_63	75	1	3	3	1	3	11	171.3	7.14
776	T_64	75	1	2	1	1	1	6	107.8	4.49
775	T_65	75	1	3	3	1	2	10	165.5	6.90
772	T_66	75	1	3	2	1	2	9	150.5	6.27

Table 6.2: Number of households with PV systems by PV penetration level

Trans.	Number of HH	Number of Households by PV Penetration Level														
		10%	20%	30%	40%	50%	60%	70%	80%	90%	100%	110%	120%	130%	140%	150%
T_1	14	2	3	4	6	7	8	9	11	12	13	14	13.0	14.0	14.0	13.0
T_2	16	2	4	5	7	8	10	11	13	14	16	15	16.0	16.0	15.0	16.0
T_3	11	1	2	3	4	5	6	7	8	9	10	11	10.0	11.0	11.0	11.0
T_4	10	1	2	3	3	4	5	5	6	7	8	8	9.0	10.0	10.0	10.0
T_5	22	3	5	7	9	11	13	15	17	19	21	19	21.0	20.0	22.0	21.0
T_6	16	2	3	5	6	7	9	10	12	13	14	16	15.0	16.0	15.0	16.0
T_7	8	1	2	3	4	5	5	6	7	8	7	8	8.0	8.0	8.0	8.0
T_8	12	2	3	4	5	6	8	9	10	11	12	12	11.0	12.0	11.0	12.0
T_9	17	2	3	4	6	7	8	10	11	12	14	15	16.0	15.0	16.0	15.0
T_10	5	1	2	2	3	4	4	5	5	5	5	5	5.0	5.0	5.0	5.0
T_11	11	2	3	4	5	6	7	8	9	10	11	10	11.0	11.0	10.0	11.0
T_12	7	1	2	2	3	3	4	4	5	5	6	7	7.0	7.0	7.0	7.0
T_13	13	2	3	4	6	7	8	9	11	12	13	13	12.0	13.0	12.0	13.0
T_14	20	2	3	5	6	8	9	11	12	13	15	16	18.0	19.0	18.0	19.0
T_15	8	1	2	3	3	4	5	5	6	7	7	8	7.0	8.0	8.0	8.0
T_17	14	2	3	4	6	7	8	10	11	12	13	13	14.0	13.0	14.0	13.0
T_19	9	2	3	4	5	6	7	8	9	9	9	9	9.0	9.0	9.0	9.0
T_20	16	2	3	5	6	8	9	10	12	13	15	16	15.0	16.0	15.0	16.0
T_22	12	2	3	4	5	6	7	8	9	10	11	12	12.0	11.0	12.0	11.0
T_23	14	2	3	4	6	7	8	9	11	12	13	14	13.0	14.0	14.0	13.0
T_24	14	2	3	4	6	7	8	9	11	12	13	14	13.0	14.0	14.0	13.0
T_26	10	1	2	3	4	5	6	7	8	9	10	9	10.0	10.0	10.0	10.0
T_27	10	1	2	3	4	5	6	7	8	9	10	9	10.0	10.0	10.0	10.0
T_28	9	1	2	3	4	5	6	6	7	8	9	8	9.0	9.0	9.0	9.0
T_29	16	2	3	5	6	7	9	10	12	13	14	16	15.0	16.0	15.0	16.0
T_30	15	2	3	4	6	7	8	9	11	12	13	14	13.0	15.0	14.0	15.0
T_31	8	1	2	3	3	4	5	6	6	7	8	8	8.0	8.0	8.0	8.0
T_32	11	1	2	3	4	5	6	7	8	9	10	11	10.0	11.0	11.0	11.0
T_33	11	1	2	3	4	5	6	7	8	9	10	11	10.0	11.0	11.0	11.0
T_34	10	1	2	3	4	5	6	7	8	9	10	9	10.0	10.0	10.0	10.0

Trans.	Number of HH	Number of Households by PV Penetration Level														
		10%	20%	30%	40%	50%	60%	70%	80%	90%	100%	110%	120%	130%	140%	150%
T_35	11	1	2	3	4	5	6	7	8	9	10	11	10.0	11.0	11.0	11.0
T_36	15	2	3	4	6	7	8	9	11	12	13	14	13.0	15.0	14.0	15.0
T_37	16	2	3	5	6	7	9	10	12	13	14	16	15.0	16.0	15.0	16.0
T_38	13	2	3	4	5	6	8	9	10	11	12	13	13.0	12.0	13.0	12.0
T_39	8	1	2	3	3	4	5	6	6	7	8	8	8.0	8.0	8.0	8.0
T_40	13	2	3	4	5	6	8	9	10	11	12	13	13.0	12.0	13.0	12.0
T_41	12	2	3	4	5	6	7	8	9	10	11	12	12.0	11.0	12.0	11.0
T_42	13	2	3	4	5	6	8	9	10	11	12	13	13.0	12.0	13.0	12.0
T_43	8	1	2	3	3	4	5	6	6	7	8	8	8.0	8.0	8.0	8.0
T_44	14	2	3	4	6	7	8	9	11	12	13	14	13.0	14.0	14.0	13.0
T_48	14	2	3	4	6	7	8	9	11	12	13	14	13.0	14.0	14.0	13.0
T_49	11	1	2	3	4	5	6	7	8	9	10	11	10.0	11.0	11.0	11.0
T_50	23	3	5	7	9	11	13	15	17	19	21	20	22.0	21.0	23.0	21.0
T_51	24	3	5	7	9	11	13	15	18	20	22	24	22.0	24.0	23.0	24.0
T_52	13	2	3	4	5	6	8	9	10	11	12	13	13.0	12.0	13.0	12.0
T_53	12	2	3	4	5	6	7	8	9	10	11	12	12.0	11.0	12.0	11.0
T_54	11	1	2	3	4	5	6	7	8	9	10	11	10.0	11.0	11.0	11.0
T_55	17	2	3	5	6	8	9	11	12	14	15	17	16.0	17.0	16.0	17.0
T_56	13	2	3	4	5	6	8	9	10	11	12	13	13.0	12.0	13.0	12.0
T_57	16	2	3	5	6	7	9	10	12	13	14	16	15.0	16.0	15.0	16.0
T_58	12	2	3	4	5	6	7	8	9	10	11	12	12.0	11.0	12.0	11.0
T_59	14	2	3	4	6	7	8	9	11	12	13	14	13.0	14.0	14.0	13.0
T_63	11	1	2	3	4	5	6	7	8	9	10	11	10.0	11.0	11.0	11.0
T_64	6	1	2	2	3	4	4	5	5	6	6	6	6.0	6.0	6.0	6.0
T_65	10	1	2	3	4	5	6	7	8	9	10	9	10.0	10.0	10.0	10.0
T_66	9	1	2	3	4	5	6	6	7	8	9	8	9.0	9.0	9.0	9.0

Table 6.3: Types of photovoltaic arrays

Color	Number of Panels	PV System Power (kW)
	12	3.96
	14	4.62
	16	5.28
	18	5.94
	20	6.6
	22	7.26

Table 6.4: Line segment data

Node A	Node B	Length(ft)	Phase Sequence
701	702	6487.3	ABC
702	702_1	244.1	ABC
702_1	702_2	19.7	ABC
702_2	703	112.9	ABC
703	704	33.2	ABC
704	705	57.6	A
705	706	30.2	A
705	707	80.5	A
705	708	66.9	A
708	709	60.6	A
708	710	31.5	A
704	711	71.1	ABC
711	712	28.6	ABC
712	713	70.8	C
713	714	57.8	C
713	715	57.0	C
713	717	62.0	C
715	716	83.3	C
717	718	54.7	C
712	719	60.3	ABC
719	720	54.1	B
720	721	31.5	B
720	722	84.6	B
720	723	68.5	B
723	724	31.7	B
723	725	79.9	B
719	726	116.9	ABC
726	727	45.8	BAC
727	728	100.6	A
727	730	56.3	ABC
730	731	56.4	A
731	732	63.4	A
730	733	38.1	ABC
733	734	48.7	AC
734	735	59.7	A
734	729	61.7	C
729	729_1	89.3	C
734	736	69.2	AC
736	737	62.5	A
736	736_1	8.0	A
737	738	102.5	A
733	739	76.8	ABC
739	740	49.1	ABC
740	741	58.2	A
740	742_1	24.8	BAC
742_1	742	36.4	ABC
742	744	24.4	B
742	745	45.1	ABC
745	746	107.0	A
745	747	38.2	C
745	748	68.5	ABC
748	749	25.2	A
748	750	21.2	B
748	751	46.4	ABC
751	752	126.5	B
751	753	130.0	B
751	754	120.7	ABC
754	755	111.6	A
754	756	61.5	ABC
756	757	51.0	CBA
757	758	110.9	B
757	759	93.5	CBA
759	760	46.8	A
760	760_1	120.7	A
756	761	152.2	ABC
761	761_1	62.1	A
761	762	46.9	A
761	764	48.1	CBA
764	765	28.9	A
765	766	79.0	A
766	767	125.0	A
764	768	88.6	B
768	769	73.1	B
769	770	122.5	B
764	771	69.0	CBA
771	772	31.6	A
772	773	27.4	A
773	774	81.7	A
771	775	141.9	C
775	776	81.2	C
776	777	89.5	C
777	778	91.4	C

Appendix B: OpenDSS Code

In this appendix the code used in OpenDSS is described.

Script 1: Main_Compiler.dss

In this scrip all the components of the feeder are joined together.

```
//....................Anny Huaman Rivera...............................//
//Main Compiler

Clear

Redirect Subestacion.dss
Redirect Linecodes.dss
Redirect Lineas.dss
Redirect Lineas_casas.dss
Redirect Perfilcargas.dss
Redirect Carga_parte1.dss
Redirect Carga_parte2.dss
Redirect Trasformador_Sub.dss
Redirect Transformer.dss

//.........PV.............//
!It is activated according to the case study from Matlab.
!Redirect PVV_60.dss

//.....Storage...........//
!It is activated according to the case study from Matlab
!Redirect Storage_80.dss

Redirect Tension_base.dss

//......... Solution Method.......//
Redirect solve_daily_storage.dss

!Activated from MATLAB
!solve

```

Script 2: Subestacion.dss

This scrip declares the creation of a new circuit called "Coqui".

```

//........Subestacion.dss.............//

new circuit.Coqui
~ basekv=38 pu=1.0001 phases=3 bus1=701
~ Angle=30
~ MVAsc3=20000 MVASC1=21000
//..............................//
```

Script 3: Linecodes.dss

In this scrip the characteristic impedance matrices for lines and cables are declared. These matrices can be defined directly or generated by specifying the symmetrical component data. For this work they were generated from scrip 4.

```
//----------------------------Linecode.dss---------------------------------------//
New Linecode.603 nphases=3  Units=mi
~ Rmatrix=[0.556245  |0.167167  0.549802  |0.167167  0.164007  0.549802  ]
~ Xmatrix=[1.0885  |0.499873  1.10719  |0.499873  0.424985  1.10719  ]
~ Cmatrix=[15.7089  |-3.93538  14.6854  |-3.93538  -1.88691  14.6854  ]
~ Normamps= 455 Emergamps=600 Ratings=455

New Linecode.602 nphases=2  Units=mi
~ Rmatrix=[0.887891  |0.207939  0.887891  ]
~ Xmatrix=[1.32211  |0.483909  1.32211  ]
~ Cmatrix=[13.1634  |-2.68714  13.1634  ]
~ Normamps= 319 Emergamps=500 Ratings=319

New Linecode.601 nphases=1  Units=mi
~ Rmatrix=[0.896457  ]
~ Xmatrix=[1.30715  ]
~ Cmatrix=[12.7871  ]
~ Normamps= 319 Emergamps=500 Ratings=319

New Linecode.604 nphases=2  Units=mi
~ Rmatrix=[1.41793  |0.297654  1.41793  ]
~ Xmatrix=[1.2059  |0.465016  1.2059  ]
~ Cmatrix=[15.5342  |-3.15305  15.5342  ]
~ Normamps= 230 Emergamps=400 Ratings=230
//---------------------------------------------------------------------//
```

Script 4: LineGeometry.dss

In this scrip the data of the characteristics of the conductors are declared in addition to the coordinates of the aerial distribution, using the data described in sections 3.4.3, 3.4.4, and 3.4.5.

```
Clear

New circuit.impedancia

new WireData.ACSR_266_8  Diam=0.642  GMRac=0.2604  Rdc=0.072916667
~ Runits=kft Radunits=in gmrunits=in
new WireData.ACSR_3/0    Diam=0.502  GMRac=0.072  Rdc=0.12869318
~ Runits=kft Radunits=in gmrunits=in
new WireData.ACSR_1/0    Diam=0.398  GMRac=0.05352  Rdc=0.212121212
~ Runits=kft Radunits=in gmrunits=in

! Coqui

//..........CONDUCTORES LADO PRIMARIO.................................................................//

new LineGeometry.603 nconds=4 nphases=3 reduce=y     ! three-phase lines
~ cond=1 wire=ACSR_266_8 x=0     h=20.5  units=ft
~ cond=2 wire=ACSR_266_8 x=3 h=20.5 units=ft
~ cond=3 wire=ACSR_266_8 x=-3 h=20.5 units=ft
~ cond=4 wire=ACSR_3/0     x=0 h=16 units=ft


new LineGeometry.602  nconds=3 nphases=2 reduce=y    !two-phase lines
~ cond=1 wire=ACSR_3/0 x=3  h=20.5 units=ft
~ cond=2 wire=ACSR_3/0 x=-3 h=20.5 units=ft
~ cond=3 wire=ACSR_1/0    x=0 h=16 units=ft

new LineGeometry.601 nconds=2 nphases=1 reduce=y     !single-phase lines
~ cond=1 wire=ACSR_3/0 x=0 h=20.5 units=ft
~ cond=2 wire=ACSR_1/0     x=0 h=16 units=ft


//......CONDUCTORES LADO SECUNDARIO.................................................//

new LineGeometry.604 nconds=3 nphases=2 reduce=y      !two-phase load lines
~ cond=1 wire=ACSR_1/0   x=1 h=18.0 units=ft
~ cond=2 wire=ACSR_1/0   x=-1 h=18.0 units=ft
~ cond=3 wire=ACSR_1/0   x=0 h=18.0 units=ft


show lineconstants freq=60 units=mile
```

Script 5: Lineas.dss

In this scrip we continue defining the characteristics of the lines, in order to know the connection nodes, the type of conductor used and the distance they have. These data were extracted from table 6.4. Only an extract of the scrip is shown.

```
//------------------------------------------------------------------------------------------------//
!LINE DEFINITIONS
New Line.702702_1    Phases=3 Bus1=702.1.2.3    Bus2=702_1.1.2.3  LineCode=603 Length=6487.25 units=ft
New Line.702_1702_2    Phases=3 Bus1=702_1.1.2.3    Bus2=702_2.1.2.3  LineCode=603 Length=244.14 units=ft
New Line.702_2702_3    Phases=3 Bus1=702_2.1.2.3    Bus2=702_3.1.2.3  LineCode=603 Length=19.69 units=ft
New Line.702_3703    Phases=3 Bus1=702_3.1.2.3    Bus2=703.1.2.3  LineCode=603 Length=112.92 units=ft
New Line.703704    Phases=3 Bus1=703.1.2.3    Bus2=704.1.2.3  LineCode=603 Length=33.2   units=ft
New Line.704705    phases=1 Bus1=704.1          Bus2=705.1      LineCode=601  Length=57.6   units=ft
New Line.705706    phases=1 Bus1=705.1          Bus2=706.1      LineCode=601  Length=30.2   units=ft
New Line.705707    phases=1 Bus1=705.1          Bus2=707.1      LineCode=601  Length=80.5   units=ft
New Line.705708    phases=1 Bus1=705.1          Bus2=708.1      LineCode=601  Length=66.9   units=ft
New Line.708709    phases=1 Bus1=708.1          Bus2=709.1      LineCode=601   Length=60.6    units=ft
New Line.708710    phases=1 Bus1=708.1          Bus2=710.1      LineCode=601   Length=31.5   units=ft
New Line.704711    phases=3 Bus1=704.1.2.3    Bus2=711.1.2.3  LineCode=603  Length=71.1    units=ft
New Line.711712    phases=3 Bus1=711.1.2.3    Bus2=712.1.2.3  LineCode=603 Length=28.6   units=ft
New Line.712713    phases=1 Bus1=712.3         Bus2=713.3      LineCode=601  Length=70.8    units=ft
New Line.713714    phases=1 Bus1=713.3        Bus2=714.3      LineCode=601 Length=57.8    units=ft
New Line.713715    phases=1 Bus1=713.3        Bus2=715.3      LineCode=601 Length=57.0   units=ft
New Line.713717    phases=1 Bus1=713.3        Bus2=717.3      LineCode=601  Length=62.0   units=ft
New Line.715716    phases=1 Bus1=715.3        Bus2=716.3      LineCode=601  Length=83.3    units=ft
New Line.717718    phases=1 Bus1=717.3        Bus2=718.3      LineCode=601  Length=54.7    units=ft
```

Script 6: Lineas_casas.dss

In this scrip we continue defining the characteristics of the lines that go to the houses, in order to know the connection nodes, the type of conductor used and the distance they have. These data were extracted from section 3.4.5. Only an extract of the scrip is shown.

```
//---------------------------Lineas_casas.dss---------------------------------------//
New Line.749_1749_1_1 phases=1 bus1=749_1.1.2 bus2=749_1_1.1.2      LineCode=604 length=32.8 units=ft
New Line.749_1749_1_2 phases=1 bus1=749_1.1.2 bus2=749_1_2.1.2      LineCode=604 length=32.8 units=ft
New Line.749_1749_1_3 phases=1 bus1=749_1.1.2 bus2=749_1_3.1.2      LineCode=604 length=32.8 units=ft
New Line.749_1749_1_4 phases=1 bus1=749_1.1.2 bus2=749_1_4.1.2      LineCode=604 length=32.8 units=ft
New Line.749_1749_1_5 phases=1 bus1=749_1.1.2 bus2=749_1_5.1.2      LineCode=604 length=32.8 units=ft
New Line.749_1749_1_6 phases=1 bus1=749_1.1.2 bus2=749_1_6.1.2      LineCode=604 length=32.8 units=ft
New Line.749_1749_1_7 phases=1 bus1=749_1.1.2 bus2=749_1_7.1.2      LineCode=604 length=32.8 units=ft
New Line.749_1749_1_8 phases=1 bus1=749_1.1.2 bus2=749_1_8.1.2      LineCode=604 length=32.8 units=ft
New Line.749_1749_1_9 phases=1 bus1=749_1.1.2 bus2=749_1_9.1.2      LineCode=604 length=32.8 units=ft
New Line.749_1749_1_10 phases=1 bus1=749_1.1.2 bus2=749_1_10.1.2      LineCode=604 length=32.8 units=ft
New Line.749_1749_1_11 phases=1 bus1=749_1.1.2 bus2=749_1_11.1.2      LineCode=604 length=32.8 units=ft
New Line.749_1749_1_12 phases=1 bus1=749_1.1.2 bus2=749_1_12.1.2      LineCode=604 length=32.8 units=ft
New Line.749_1749_1_13 phases=1 bus1=749_1.1.2 bus2=749_1_13.1.2      LineCode=604 length=32.8 units=ft
New Line.749_1749_1_14 phases=1 bus1=749_1.1.2 bus2=749_1_14.1.2      LineCode=604 length=32.8 units=ft
New Line.750_1750_1_1 phases=1 bus1=750_1.1.2 bus2=750_1_1.1.2      LineCode=604 length=32.8 units=ft
New Line.750_1750_1_2 phases=1 bus1=750_1.1.2 bus2=750_1_2.1.2      LineCode=604 length=32.8 units=ft
New Line.750_1750_1_3 phases=1 bus1=750_1.1.2 bus2=750_1_3.1.2      LineCode=604 length=32.8 units=ft
New Line.750_1750_1_4 phases=1 bus1=750_1.1.2 bus2=750_1_4.1.2      LineCode=604 length=32.8 units=ft
New Line.750_1750_1_5 phases=1 bus1=750_1.1.2 bus2=750_1_5.1.2      LineCode=604 length=32.8 units=ft
New Line.750_1750_1_6 phases=1 bus1=750_1.1.2 bus2=750_1_6.1.2      LineCode=604 length=32.8 units=ft
New Line.750_1750_1_7 phases=1 bus1=750_1.1.2 bus2=750_1_7.1.2      LineCode=604 length=32.8 units=ft
New Line.750_1750_1_8 phases=1 bus1=750_1.1.2 bus2=750_1_8.1.2      LineCode=604 length=32.8 units=ft
New Line.750_1750_1_9 phases=1 bus1=750_1.1.2 bus2=750_1_9.1.2      LineCode=604 length=32.8 units=ft
New Line.750_1750_1_10 phases=1 bus1=750_1.1.2 bus2=750_1_10.1.2      LineCode=604 length=32.8 units=ft
New Line.750_1750_1_11 phases=1 bus1=750_1.1.2 bus2=750_1_11.1.2      LineCode=604 length=32.8 units=ft
New Line.750_1750_1_12 phases=1 bus1=750_1.1.2 bus2=750_1_12.1.2      LineCode=604 length=32.8 units=ft
```

Script 7: Perfilcargas.dss

In this scrip the load profiles, described in section 3.3, are defined.

```
//.................................................................................................//
!PERFIL DE CARGA
New Loadshape.perfil_1 npts=24 interval=1 mult=[0.72 0.73 0.735 0.8 1.3 1.95 1.930 1.95 1.41 0.89 0.89 0.89 0.89 0.89 1.41 1.41 1.41 1.42 1.96 2.48 2.63 2.46 1.42 0.72]
New Loadshape.perfil_2 npts=24 interval=1 mult=[0.7 0.71 0.71 0.7 0.86 0.9 0.85 0.8 0.7 0.7 0.8 0.8 0.9 1.0 1.05 1.1 1.1 1.14 1.2 1.3 1.2 1.10 0.9 0.8]
New Loadshape.perfil_3 npts=24 interval=1 mult=[0.55 0.5 0.5 0.5 0.5 0.6 0.61 0.7 0.7 0.6 0.5 0.46 0.465 0.465 0.47 0.56 0.6 0.8 1.0 1.04 0.9 0.8 0.7 0.5]
New Loadshape.perfil_4 npts=24 interval=1 mult=[0.35 0.35 0.35 0.35 0.36 0.375 0.400 0.425 0.46 0.45 0.425 0.41 0.42 0.41 0.46 0.5 0.55 0.55 0.48 0.46 0.4 0.355 0.36 0.36]
New Loadshape.perfil_5 npts=24 interval=1 mult=[0.2 0.2 0.2 0.2 0.2 0.2 0.2 0.25 0.35 0.3 0.25 0.15 0.15 0.15 0.15 0.15 0.15 0.15 0.2 0.4 0.5 0.4 0.35 0.3]

//.................................................................................................//
```

Script 8: Trasformador_sub.dss

In this scrip describes the feeder substation transformer, the parameters used in this scrip were described in section 3.4.1.

```
//.................................................................//
!SUB TRANSFORMER DEFINITION
New Transformer.T_1 Phases=3 Windings=2   XHL=(8 1000 /)
~ wdg=1 bus=701     conn=delta  kv=38    kva=3000   %r=(.5 1000 /)  XHT=4
~ wdg=2 bus=702     conn=wye   kv=4.16  kva=3000   %r=(.5 1000 /)  XLT=4

//.....................................................................//
```

Script 9: Perfilcargas.dss

In this scrip the feeder loads are defined, the parameters that are defined were extracted from table 6.1. only the first sheet of the scrip is shown.

```
//---------------------------Carga_parte1.dss---------------------------------------//
New Load.Carga__749_1_1   bus1=749_1_1.1.2    phases=2   kv=0.208   kw=1 pf=0.98 model=1 daily=perfil_1  conn=Wye
New Load.Carga__749_1_2   bus1=749_1_2.1.2    phases=2   kv=0.208   kw=1 pf=0.98 model=1 daily=perfil_2  conn=Wye
New Load.Carga__749_1_3   bus1=749_1_3.1.2    phases=2   kv=0.208   kw=1 pf=0.98 model=1 daily=perfil_2  conn=Wye
New Load.Carga__749_1_4   bus1=749_1_4.1.2    phases=2   kv=0.208   kw=1 pf=0.98 model=1 daily=perfil_2  conn=Wye
New Load.Carga__749_1_5   bus1=749_1_5.1.2    phases=2   kv=0.208   kw=1 pf=0.98 model=1 daily=perfil_2  conn=Wye
New Load.Carga__749_1_6   bus1=749_1_6.1.2    phases=2   kv=0.208   kw=1 pf=0.98 model=1 daily=perfil_3  conn=Wye
New Load.Carga__749_1_7   bus1=749_1_7.1.2    phases=2   kv=0.208   kw=1 pf=0.98 model=1 daily=perfil_3  conn=Wye
New Load.Carga__749_1_8   bus1=749_1_8.1.2    phases=2   kv=0.208   kw=1 pf=0.98 model=1 daily=perfil_3  conn=Wye
New Load.Carga__749_1_9   bus1=749_1_9.1.2    phases=2   kv=0.208   kw=1 pf=0.98 model=1 daily=perfil_3  conn=Wye
New Load.Carga__749_1_10   bus1=749_1_10.1.2    phases=2   kv=0.208   kw=1 pf=0.98 model=1 daily=perfil_3  conn=Wye
New Load.Carga__749_1_11   bus1=749_1_11.1.2    phases=2   kv=0.208   kw=1 pf=0.98 model=1 daily=perfil_4  conn=Wye
New Load.Carga__749_1_12   bus1=749_1_12.1.2    phases=2   kv=0.208   kw=1 pf=0.98 model=1 daily=perfil_5  conn=Wye
New Load.Carga__749_1_13   bus1=749_1_13.1.2    phases=2   kv=0.208   kw=1 pf=0.98 model=1 daily=perfil_5  conn=Wye
New Load.Carga__749_1_14   bus1=749_1_14.1.2    phases=2   kv=0.208   kw=1 pf=0.98 model=1 daily=perfil_5  conn=Wye
New Load.Carga__750_1_1   bus1=750_1_1.1.2    phases=2   kv=0.208   kw=1 pf=0.98 model=1 daily=perfil_1  conn=Wye
New Load.Carga__750_1_2   bus1=750_1_2.1.2    phases=2   kv=0.208   kw=1 pf=0.98 model=1 daily=perfil_2  conn=Wye
New Load.Carga__750_1_3   bus1=750_1_3.1.2    phases=2   kv=0.208   kw=1 pf=0.98 model=1 daily=perfil_2  conn=Wye
New Load.Carga__750_1_4   bus1=750_1_4.1.2    phases=2   kv=0.208   kw=1 pf=0.98 model=1 daily=perfil_2  conn=Wye
New Load.Carga__750_1_5   bus1=750_1_5.1.2    phases=2   kv=0.208   kw=1 pf=0.98 model=1 daily=perfil_2  conn=Wye
New Load.Carga__750_1_6   bus1=750_1_6.1.2    phases=2   kv=0.208   kw=1 pf=0.98 model=1 daily=perfil_2  conn=Wye
New Load.Carga__750_1_7   bus1=750_1_7.1.2    phases=2   kv=0.208   kw=1 pf=0.98 model=1 daily=perfil_2  conn=Wye
New Load.Carga__750_1_8   bus1=750_1_8.1.2    phases=2   kv=0.208   kw=1 pf=0.98 model=1 daily=perfil_3  conn=Wye
New Load.Carga__750_1_9   bus1=750_1_9.1.2    phases=2   kv=0.208   kw=1 pf=0.98 model=1 daily=perfil_3  conn=Wye
New Load.Carga__750_1_10   bus1=750_1_10.1.2    phases=2   kv=0.208   kw=1 pf=0.98 model=1 daily=perfil_3  conn=Wye
New Load.Carga__750_1_11   bus1=750_1_11.1.2    phases=2   kv=0.208   kw=1 pf=0.98 model=1 daily=perfil_3  conn=Wye
New Load.Carga__750_1_12   bus1=750_1_12.1.2    phases=2   kv=0.208   kw=1 pf=0.98 model=1 daily=perfil_3  conn=Wye
```

Script 10: Trasformer.dss

In this scrip the feeder distribution transformers are defined, the parameters were defined in section 3.4.2. Only the first sheet of the scrip is shown.

```
!TRANSFORMER DEFINITION
New Transformer.T1  Phases=1     Windings=3  XHL=2.04   XHT=2.04   XLT=1.36 %loadloss=0.15 %noloadloss=.015
~ buses=[749.1  749_1.1.0  749_1.0.2]     kVs=[2.4 0.120 0.120]     kVAs=[50 50 50]   %Rs=[0.6 1.2 1.2]   conns=[wye wye wye]

New Transformer.T2  Phases=1    Windings=3  XHL=2.04   XHT=2.04   XLT=1.36 %loadloss=0.15 %noloadloss=.015
~ buses=[750.2  750_1.1.0  750_1.0.2]     kVs=[2.4 0.120 0.120]     kVAs=[50 50 50]   %Rs=[0.6 1.2 1.2]   conns=[wye wye wye]

New Transformer.T3  Phases=1     Windings=3  XHL=2.04   XHT=2.04   XLT=1.36 %loadloss=0.15 %noloadloss=.015
~ buses=[753.2  753_1.1.0  753_1.0.2]     kVs=[2.4 0.120 0.120]     kVAs=[50 50 50]   %Rs=[0.6 1.2 1.2]   conns=[wye wye wye]

New Transformer.T4  Phases=1   Windings=3  XHL=2.04   XHT=2.04   XLT=1.36 %loadloss=0.15 %noloadloss=.015
~ buses=[752.2  752_1.1.0  752_1.0.2]     kVs=[2.4 0.120 0.120]     kVAs=[25 25 25]   %Rs=[0.6 1.2 1.2]   conns=[wye wye wye]

New Transformer.T5  Phases=1  Windings=3  XHL=2.04   XHT=2.04   XLT=1.36 %loadloss=0.15 %noloadloss=.015
~ buses=[760_1.1  760_2.1.0  760_2.0.2]     kVs=[2.4 0.120 0.120]     kVAs=[75 75 75]   %Rs=[0.6 1.2 1.2]   conns=[wye wye wye]

New Transformer.T6  Phases=1   Windings=3  XHL=2.04   XHT=2.04   XLT=1.36 %loadloss=0.15 %noloadloss=.015
~ buses=[758.2  758_1.1.0  758_1.0.2]     kVs=[2.4 0.120 0.120]     kVAs=[75 75 75]   %Rs=[0.6 1.2 1.2]   conns=[wye wye wye]

New Transformer.T7  Phases=1   Windings=3  XHL=2.04   XHT=2.04   XLT=1.36 %loadloss=0.15 %noloadloss=.015
~ buses=[757.2  757_1.1.0  757_1.0.2]     kVs=[2.4 0.120 0.120]     kVAs=[50 50 50]   %Rs=[0.6 1.2 1.2]   conns=[wye
```

Script 11: Tension_base.dss

In this script the feeder voltage base is defined, the feeder coordinates are also declared and an energy meter is created on the line leaving the substation to check the energy flow in each feeder branch.

```
//----------------------------------------Tension_base.dss----------------------------------------//
! tension base

set VoltageBases=[38, 4.16, 0.208]

CalcVoltageBases

!BusCoords CoordenadasCoqui_111.txt
!BusCoords CoordenadasCoquiCasas.txt
BusCoords CoordenadasCoquimismopunto.txt


!New energymeter.meter element=Transformer.T_1 terminal=1
New energymeter.meter element=Line.702702_1 terminal=1

!ejemplo de medidor en linea: New energymeter.meter line.702702_1 1

//----------------------------------------------------------------------------------------------------
```

Script 12: solve_daily_storage.dss

In this script the solution mode is defined to be daily with hourly steps as discussed throughout the document.

```

//............ solve_daily_storage.dss.....................//
!se puede modificar en number= a la hora que deseamos hacer el analisis (1 2 .....  23)

!set controlmode=static
Set mode=daily
Set number=1
!Set hour=13
Set stepsize=1h
```

Script 13: PPV_10.dss

In this script, the parameters of the photovoltaic systems are defined, and the values of these parameters are described in section 4.2.2 and table 6.2. This script is used for case studies one, two, and three Only the first sheet of the script is shown.

```
New XYCurve.MyPvsT npts=4 xarray=[0 25 75 100] yarray=[1.2 1.0 0.8 0.6]
New XYCurve.MyEff npts=4 xarray=[.25 .5 .75 1.0] yarray=[.88 .93 .945 .9]
New Loadshape.MyIrrad npts=24 interval=1 mult=[0 0 0 0 0 0 .2 .4 .6 .8 .9 .9 .9 .8 .6 .4 .2 0 0 0 0 0 0 0]
New Tshape.MyTemp npts=24 interval=1 temp=[24 24 24 24 24 24 25 26 27 28 28 29 29 29 28 28 27 26 25 25 25 25 24 24]

New PVSystem.PV749_1_1    phases=2   bus1=749_1_1.1.2    kv=0.208  Kva=3.96    irrad=1  Pmpp=3.96    temperature=25  pf
=1
~ effcurve=Myeff   P-TCurve=MyPvsT  Daily=MyIrrad  TDaily=MyTemp
New PVSystem.PV749_1_2    phases=2   bus1=749_1_2.1.2    kv=0.208  Kva=3.96    irrad=1  Pmpp=3.96    temperature=25  pf
=1
~ effcurve=Myeff   P-TCurve=MyPvsT  Daily=MyIrrad  TDaily=MyTemp
New PVSystem.PV750_1_1    phases=2   bus1=750_1_1.1.2    kv=0.208  Kva=3.96    irrad=1  Pmpp=3.96    temperature=25  pf
=1
~ effcurve=Myeff   P-TCurve=MyPvsT  Daily=MyIrrad  TDaily=MyTemp
New PVSystem.PV750_1_2    phases=2   bus1=750_1_2.1.2    kv=0.208  Kva=3.96    irrad=1  Pmpp=3.96    temperature=25  pf
=1
~ effcurve=Myeff   P-TCurve=MyPvsT  Daily=MyIrrad  TDaily=MyTemp
New PVSystem.PV753_1_1    phases=2   bus1=753_1_1.1.2    kv=0.208  Kva=3.96    irrad=1  Pmpp=3.96    temperature=25  pf
=1
~ effcurve=Myeff   P-TCurve=MyPvsT  Daily=MyIrrad  TDaily=MyTemp
New PVSystem.PV752_1_1    phases=2   bus1=752_1_1.1.2    kv=0.208  Kva=3.96    irrad=1  Pmpp=3.96    temperature=25  pf
=1
~ effcurve=Myeff   P-TCurve=MyPvsT  Daily=MyIrrad  TDaily=MyTemp
New PVSystem.PV760_1_1    phases=2   bus1=760_1_1.1.2    kv=0.208  Kva=3.96    irrad=1  Pmpp=3.96    temperature=25  pf
=1
~ effcurve=Myeff   P-TCurve=MyPvsT  Daily=MyIrrad  TDaily=MyTemp
New PVSystem.PV760_1_2    phases=2   bus1=760_1_2.1.2    kv=0.208  Kva=3.96    irrad=1  Pmpp=3.96    temperature=25  pf
```

Script 14: Storage_10.dss

In this script the parameters of the RESS systems are defined, the values of these parameters are described in section 4.2.3.

This script is used for case studies three and four. Only the first sheet of the script is shown.

```
New Storage.Battery749_1_1    phases=2 bus1=749_1_1.1.2    kv=0.208 pf=1  kWrated=3.8     %reserve=50
~ effcurve=MyEff kWhrated=20.35  %stored=60    state=idling DispMode=External
New Storage.Battery749_1_2    phases=2 bus1=749_1_2.1.2    kv=0.208 pf=1  kWrated=3.8     %reserve=50
~ effcurve=MyEff kWhrated=20.35  %stored=60    state=idling DispMode=External
New Storage.Battery750_1_1    phases=2 bus1=750_1_1.1.2    kv=0.208 pf=1  kWrated=3.8     %reserve=50
~ effcurve=MyEff kWhrated=20.35  %stored=60    state=idling DispMode=External
New Storage.Battery750_1_2    phases=2 bus1=750_1_2.1.2    kv=0.208 pf=1  kWrated=3.8     %reserve=50
~ effcurve=MyEff kWhrated=20.35  %stored=60    state=idling DispMode=External
New Storage.Battery753_1_1    phases=2 bus1=753_1_1.1.2    kv=0.208 pf=1  kWrated=3.8     %reserve=50
~ effcurve=MyEff kWhrated=20.35  %stored=60    state=idling DispMode=External
New Storage.Battery752_1_1    phases=2 bus1=752_1_1.1.2    kv=0.208 pf=1  kWrated=3.8     %reserve=50
~ effcurve=MyEff kWhrated=20.35  %stored=60    state=idling DispMode=External
New Storage.Battery760_1_1    phases=2 bus1=760_1_1.1.2    kv=0.208 pf=1  kWrated=3.8     %reserve=50
~ effcurve=MyEff kWhrated=20.35  %stored=60    state=idling DispMode=External
New Storage.Battery760_1_2    phases=2 bus1=760_1_2.1.2    kv=0.208 pf=1  kWrated=3.8     %reserve=50
~ effcurve=MyEff kWhrated=20.35  %stored=60    state=idling DispMode=External
New Storage.Battery760_1_3    phases=2 bus1=760_1_3.1.2    kv=0.208 pf=1  kWrated=3.8     %reserve=50
~ effcurve=MyEff kWhrated=20.35  %stored=60    state=idling DispMode=External
New Storage.Battery758_1_1    phases=2 bus1=758_1_1.1.2    kv=0.208 pf=1  kWrated=3.8     %reserve=50
~ effcurve=MyEff kWhrated=20.35  %stored=60    state=idling DispMode=External
New Storage.Battery758_1_2    phases=2 bus1=758_1_2.1.2    kv=0.208 pf=1  kWrated=3.8     %reserve=50
~ effcurve=MyEff kWhrated=20.35  %stored=60    state=idling DispMode=External
New Storage.Battery757_1_1    phases=2 bus1=757_1_1.1.2    kv=0.208 pf=1  kWrated=3.8     %reserve=50
~ effcurve=MyEff kWhrated=20.35  %stored=60    state=idling DispMode=External
```

Script 15: PVV_10_CASO4.dss

This script defines the parameters of the photovoltaic systems and the Volt-VAR function of the smart inverter. The values of these parameters are described in sections 4.2.2, 4.2.4, and table 6.2. This script is used for case study four. Only the first sheet of the script is shown.

```
New XYCurve.MyPvsT npts=4 xarray=[0 25 75 100] yarray=[1.2 1.0 0.8 0.6]
New XYCurve.MyEff npts=4 xarray=[.25 .5 .75 1.0] yarray=[.88 .93 .945 .9]
New Loadshape.MyIrrad npts=24 interval=1 mult=[0 0 0 0 0 0 .2 .4 .6 .8 .9 .9 .9 .8 .6 .4 .2 0 0 0 0 0 0 0]
New Tshape.MyTemp npts=24 interval=1 temp=[24 24 24 24 24 24 25 26 27 28 28 29 29 29 28 28 27 26 25 25 25 25 24 24]

New PVSystem.PV749_1_1    phases=2   bus1=749_1_1.1.2    kv=0.208  Kva=4.22    irrad=1  Pmpp=3.96    temperature=25 %Pmpp=96.15
~ effcurve=Myeff   P-TCurve=MyPvsT  Daily=MyIrrad  TDaily=MyTemp   wattpriority=no varfollowinverter=true %PminNoVars=5 %PminkvarMax=20
New PVSystem.PV749_1_2    phases=2   bus1=749_1_2.1.2    kv=0.208  Kva=4.22    irrad=1  Pmpp=3.96    temperature=25 %Pmpp=96.15
~ effcurve=Myeff   P-TCurve=MyPvsT  Daily=MyIrrad  TDaily=MyTemp   wattpriority=no varfollowinverter=true %PminNoVars=5 %PminkvarMax=20
New PVSystem.PV750_1_1    phases=2   bus1=750_1_1.1.2    kv=0.208  Kva=4.22    irrad=1  Pmpp=3.96    temperature=25 %Pmpp=96.15
~ effcurve=Myeff   P-TCurve=MyPvsT  Daily=MyIrrad  TDaily=MyTemp   wattpriority=no varfollowinverter=true %PminNoVars=5 %PminkvarMax=20
New PVSystem.PV750_1_2    phases=2   bus1=750_1_2.1.2    kv=0.208  Kva=4.22    irrad=1  Pmpp=3.96    temperature=25 %Pmpp=96.15
~ effcurve=Myeff   P-TCurve=MyPvsT  Daily=MyIrrad  TDaily=MyTemp   wattpriority=no varfollowinverter=true %PminNoVars=5 %PminkvarMax=20
New PVSystem.PV753_1_1    phases=2   bus1=753_1_1.1.2    kv=0.208  Kva=4.22    irrad=1  Pmpp=3.96    temperature=25 %Pmpp=96.15
~ effcurve=Myeff   P-TCurve=MyPvsT  Daily=MyIrrad  TDaily=MyTemp   wattpriority=no varfollowinverter=true %PminNoVars=5 %PminkvarMax=20
New PVSystem.PV752_1_1    phases=2   bus1=752_1_1.1.2    kv=0.208  Kva=4.22    irrad=1  Pmpp=3.96    temperature=25 %Pmpp=96.15
~ effcurve=Myeff   P-TCurve=MyPvsT  Daily=MyIrrad  TDaily=MyTemp   wattpriority=no varfollowinverter=true %PminNoVars=5 %PminkvarMax=20
New PVSystem.PV760_1_1    phases=2   bus1=760_1_1.1.2    kv=0.208  Kva=4.22    irrad=1  Pmpp=3.96    temperature=25 %Pmpp=96.15
```

Appendix C: MATLAB Code

This appendix shows the code used in MATLAB to extract the OpenDSS results, only the programming for case one of the study is shown since the code is repeated for the following case studies. Script 2 follows the methodology described in section 4.3.1.

Script 1: Feeder power flow

```
clc
clear all
[DSSCircObj, DSSText, gridpvPath] = DSSStartup;
    DSSCircuit=DSSCircObj.ActiveCircuit;
    DSSBus=DSSCircuit.ActiveBus;
    DSSSolution=DSSCircuit.Solution;
    DSSTransformers=DSSCircuit.Transformers;
    DSSText.command = ['Compile (C:\Users\annyh\Desktop\Simulacion\Simulaciones Tesis\caso 1\Simulacion OpenDSS\Cerebro_Coqui.dss)'];
    DSSText.command = 'solve';
    DSSText.command = ['Set mode=daily stepsize=1h hour=0'];
    DSSText.command = 'Set controlmode=static ';
    DSSText.command = 'solve';
    %DSSText.command = 'Show voltages LN Nodes'
    %DSSText.command = 'Show powers kVA elem'

    %{
    %Power flow caso base
    figure; plotMonitor(DSSCircObj,'sublinea')
    xticks([1:1:24])
    xlim([1 24])
    ylabel('Power');
    %}

    %{
    %Current flowing through the lines
    figure; plotAmpProfile(DSSCircObj, '778','AveragePhase','addition')
    xlim([1 2.6])
    %}

    %{
    %Active Power
    figure;
    plotKWProfile(DSSCircObj,'AveragePhase','addition','BusName','703','Downstream','on')
    xlim([1 2.6])
    ylim([0 400])
    %}

    %{
    %Voltage Profile
    figure; plotVoltageProfile(DSSCircObj,'SecondarySystem','off','VoltScale','pu')
    plot([0,2.6],[1.05,1.05],'red')
    plot([0,2.6],[0.95,0.95],'red')
    xlim([0 2.6])
    ylim([0.94 1.06])
    %}
```

Script 2: HC - Case 1

```
clc
clear all
Limite_PV=150
PV=0;
i=0;
while PV<Limite_PV   %cycle for each PV scenario
    PV=PV+10;
    i=i+1;
    [DSSCircObj, DSSText, gridpvPath] = DSSStartup;
    DSSCircuit=DSSCircObj.ActiveCircuit;
    DSSBus=DSSCircuit.ActiveBus;
    DSSSolution=DSSCircuit.Solution;
    DSSTransformers=DSSCircuit.Transformers;

    DSSText.command = ['Compile (C:\Users\annyh\Desktop\Simulacion\Simulaciones Tesis\caso 1\Simulacion OpenDSS\Cerebro_Coqui.dss)'];
    DSSText.command = 'solve';

    %increased PV scenario to the simulation
    DSSText.command = ['Compile (C:\Users\annyh\Desktop\Simulacion\Simulaciones Tesis\caso 1\Simulacion OpenDSS\PVV_' num2str(PV)  '.dss)'];
    DSSText.command = 'solve';

    [numRows,numCols] = size(DSSTransformers.AllName);
    figure; plotCircuitLines(DSSCircObj,'LoadMarker','off','PVMarker','off');


    w=zeros(1,numRows);
    z=w';

    hora=0;
    while hora<24  %collection of results at each hour of the day
        hora=hora+1
        DSSText.command = ['Set mode=daily stepsize=1h number=' num2str(hora)  ''];
        DSSText.command = 'Set controlmode=static ';
        DSSText.command = 'solve';


        Nombre_NodoA=DSSCircuit.AllNodeNamesByPhase(1); %all names of nodes in phase 1
        Nombre_NodoB=DSSCircuit.AllNodeNamesByPhase(2); %all names of nodes in phase 2
        Nombre_NodoC=DSSCircuit.AllNodeNamesByPhase(3); %all names of nodes in phase 3

        VA=DSSCircuit.AllNodeVmagPUByPhase(1);   %all phase 1 pu voltages
        VB=DSSCircuit.AllNodeVmagPUByPhase(2);
        VC=DSSCircuit.AllNodeVmagPUByPhase(3);

        Matriz_Voltaje_Nodos=[[Nombre_NodoA;Nombre_NodoB;Nombre_NodoC] string([VA';VB';VC'])];
        [numRowsV,numColsV] = size(Matriz_Voltaje_Nodos);

        l=0;
        while l<numRowsV    %cycle to evaluate voltage violations
            l=l+1;
            cV=Matriz_Voltaje_Nodos(l,1);
            if str2double(Matriz_Voltaje_Nodos(l,2))>1.05
                DSSCircuit.SetActiveBus(cV);
                latV(l) = [DSSBus.y];
                lonV(l) = [DSSBus.x];
                por_violacion=(str2double(Matriz_Voltaje_Nodos(l,2))*100/1.05)-100;
                Porciento_De_Violacion=[string(hora) cV por_violacion];
            else
                por_violacion=0;
                latV(l) = 0;
                lonV(l) = 0;


            end
            porV(l)=por_violacion;

```

```
        end
        poV=porV';
        VoltageNode=[VA';VB';VC'];
        zV(1:numRowsV,hora)=poV;
        zvv(1:numRowsV,hora)=VoltageNode;

        latV;
        lonV;
        latV(latV==0) = [];
        lonV(lonV==0) = [];
        plot (lonV, latV, 'sr', 'MarkerSize', 7,'MarkerEdgeColor',[0 0 0],
        'MarkerFaceColor','red','DisplayName','Voltage Violation')


    %extracting parameters in distribution transformers
        DSSCktElement=DSSCircuit.ActiveCktElement;
        DSSActiveClass=DSSCircuit.ActiveClass;
        DSSTransformers.First;
        k=0;
        while k<numRows    %cycle to evaluate thermal violations
            k=k+1;

            Nombre_transformador=DSSTransformers.Name;
            Rating_transformador=DSSTransformers.kva;
            Potencia_transformador=DSSCktElement.TotalPowers;
            PotenciaKva_transformador=sqrt((Potencia_transformador(1,1))^2+(
            Potencia_transformador(1,2))^2);
            if Rating_transformador<=PotenciaKva_transformador
                porcentaje=(PotenciaKva_transformador-Rating_transformador)*100/
                Rating_transformador;
                c=DSSCktElement.BusNames{1};
                DSSCircuit.SetActiveBus(c);
                latt = [DSSBus.y];
                lonn = [DSSBus.x];
                plot (lonn, latt, 'o','LineWidth',0.8, 'MarkerSize', 9,'MarkerEdgeColor',
                'k','MarkerFaceColor','g','DisplayName','Thermal Violation');

            else
                porcentaje=0;

            end
            por(k)=porcentaje;
            DSSTransformers.Next;

        end
        po=por';
        z(1:numRows,hora)=po;

    end
    Z=string(zV);
    POR_VIO=[[Nombre_NodoA;Nombre_NodoB;Nombre_NodoC] Z];
    hra=[0:24];
    Z_tablaV=[string(hra);POR_VIO];

    %Maximum voltage values for 24 hours
    %PU values
    max(zvv);
    zvv_max=max(zvv);
    %Maximum values for 24 hours in pu
    zvv_maxx(1:24,i)=zvv_max;

    %writematrix(zvv_maxx,'C:\Users\annyh\Desktop\Simulacion\Simulaciones Tesis\caso
    1\Simulacion Matlab\Voltaje PU.xlsx','Sheet',1)


    %Percentage values
    max(zV);

```

```
    %VALORES
    max(z);

    %Maximum values of thermal violations for each hour
    trasfo=[DSSTransformers.AllName string(z)];

    Z_tabla=[string(hra);trasfo];

    %writematrix(Z_tabla,'C:\Users\annyh\Desktop\Simulacion\Simulaciones Tesis\caso 1\Simulacion Matlab\Voltaje PU.xlsx','Sheet',2)

    %%%%%Summarizing the results to plot percentage of violations
    syms x
    x=1;
    while x<25
    porcentaje_max_horaV(x)=max(zV(:,x));
    porcentaje_max_hora(x)=max(z(:,x));
    x=x+1;
    %punto_max(x)=(hora_max+100)*1.05/100
    end
    porcentaje_max_pvV(i)=max(porcentaje_max_horaV);
    porcentaje_max_pv(i)=max(porcentaje_max_hora);
    %title([' PV ' num2str(PV)  ' %(Voltage Violations) '])
    xlabel('X(Longitudex)');
    ylabel('Y(Latitude)');
end

PORC_VOLT=porcentaje_max_pvV'
PORC_TRANS=porcentaje_max_pv'

i=1;
while PORC_VOLT(i,1)<=0&PORC_TRANS(i,1)<=0
    i=i+1;
end
PORC_VOLT(i,1)

%grafica https://www.youtube.com/watch?v=K2axX_nSmh4
X=0:(i-1)*100/(Limite_PV):(((i-1)*10));
Y=(zeros((Limite_PV+10)/10,1)+100)';

x=10:10:Limite_PV;
y1=PORC_VOLT';
y2=PORC_TRANS';

XX=[X,X(length(X):-1:1)];
YY=[zeros(1,length(X)),Y(length(X):-1:1)];
%
hold
xx=[x,x(length(x):-1:1)];
yy1=[zeros(1,length(x)),y1(length(x):-1:1)];
yy2=[zeros(1,length(x)),y2(length(x):-1:1)];

p=fill(xx,yy2,'b',xx,yy1,'r',XX,YY,'g')
p(1).LineWidth = 2;
p(2).LineWidth = 2;
p(3).LineWidth = 2;
p(1).EdgeColor = [0 0.4470 0.7410];
p(2).EdgeColor = [0.6350 0.0780 0.1840];
p(3).EdgeColor = [0.4660 0.6740 0.1880];  %p(1).LineStyle = '-';
xticks([0:10:150])
yticks([0:10:100])
xlim([0 150])
ylim([0 100])
%title('Hosting Capacity');
xlabel('%PV');
ylabel('Scenarios at Each PV Size Violations (%)');
legend('Thermal Violations','Voltage Violations','Below Hosting Capacity/No Violations');
```

Script 3: Power flow of HC results - Case 1

```
clc
clear all
[DSSCircObj, DSSText, gridpvPath] = DSSStartup;
    DSSCircuit=DSSCircObj.ActiveCircuit;
    DSSBus=DSSCircuit.ActiveBus;
    DSSSolution=DSSCircuit.Solution;
    DSSTransformers=DSSCircuit.Transformers;
    DSSMonitors=DSSCircuit.Monitors
    Limite_PV=150
    PV=50
    hora=12
    %while PV<Limite_PV
    PV=PV+10;
    DSSText.command = ['Compile (C:\Users\annyh\Desktop\Simulacion\Simulaciones Tesis\caso 1\Simulacion OpenDSS\Cerebro_Coqui.dss)'];
    DSSText.command = 'solve';
    DSSText.command = ['Compile (C:\Users\annyh\Desktop\Simulacion\Simulaciones Tesis\caso 1\Simulacion OpenDSS\PVV_' num2str(PV)  '.dss)'];
    DSSText.command = 'solve';
    DSSText.command = ['Set mode=daily stepsize=1h number=' num2str(hora)  ''];
    DSSText.command = 'Set controlmode=static ';
    DSSText.command = 'solve'
    figure; plotCircuitLines(DSSCircObj,'Coloring','powerFlowDirection','ContourScale',[-100 100])

    %{
   %transformer profile
    [numRows,numCols] = size(DSSTransformers.AllName);
    DSSCktElement=DSSCircuit.ActiveCktElement;
        DSSActiveClass=DSSCircuit.ActiveClass;
        DSSTransformers.First;
        k=0;
        while k<numRows
            k=k+1;
        Nombre_transformador=DSSTransformers.Name
        Rating_transformador(k)=DSSTransformers.kva;
        Potencia_transformador=DSSCktElement.TotalPowers;
        PotenciaKva_transformador(k)=sqrt((Potencia_transformador(1,1))^2+(Potencia_transformador(1,2))^2);
        DSSTransformers.Next;
        end
    Rating=Rating_transformador'
    PotenciaKva=PotenciaKva_transformador'
x=[4]
y=PotenciaKva(5,1)
a=[2    3   4   8   10  11  15  23  25  28  31  32  35  36  37  38  39  40  41  42  43  44  45  46  47  48  49  50  51  52]
xx=[1   2   3   7   9   10  14  26  28  31  34  35  38  39  40  41  42  43  44  48  49  50  51  52  53  54  55  56  57  58]
yy=PotenciaKva(a,1)
b=[6    7   9   12  13  14  16  17  18  19  20  21  22  24  26  27  29  30  33  34  53  54  55  56  57]
xxx=[5  6   8   11  12  13  15  17  19  20  22  23  24  27  29  30  32  33  36  37  59  63  64  65  66]
yyy=PotenciaKva(b,1)
hold on
plot(x,y,'o','MarkerEdgeColor','b','MarkerFaceColor','b')
plot(xx,yy,'o','MarkerEdgeColor','r','MarkerFaceColor','r')
plot(xxx,yyy,'o','MarkerEdgeColor','g','MarkerFaceColor','g')
plot([0,66],[25,25],'b')
plot([0,66],[50,50],'r')
plot([0,66],[75,75],'g')

xticks([1:1:66])
xlim([1 66])
yticks([0:5:80])
ylim([0 80])
xlabel('Transformer Name');
```

```
ylabel('Power at Transformer Node(kVA)');
legend('Trans. 25kVA','Trans. 50kVA','Trans. 75kVA','Rating(25kVA)','Rating(50kVA)','Rating(75kVA)');
hold off
%}

 %{
    %Power flow base case
    figure; plotMonitor(DSSCircObj,'sublinea')
    xticks([1:1:24])
    xlim([1 24])
    ylim([-800 400])
    ylabel('Power');
    %}

%{
    %Voltage Profile
    figure; plotVoltageProfile(DSSCircObj,'SecondarySystem','on','VoltScale','pu')
    plot([0,2.6],[1.05,1.05],'red')
    plot([0,2.6],[0.95,0.95],'red')
    yticks([0.94:0.01:1.08])
    xlim([0 2.6])
    ylim([0.94 1.08])
%}

%{
    %Current passing through the lines
    figure; plotAmpProfile(DSSCircObj, '778','AveragePhase','addition')
    xlim([1 2.6])
%}
```